

AD-A121 485

DEVELOPMENT AND FLIGHT TEST OF AN ACTIVE FLUTTER
SUPPRESSION SYSTEM FOR T. (U) AIR FORCE WRIGHT
AERONAUTICAL LABS WRIGHT-PATTERSON AFB OH
H HONLINGER E AL. SEP 82

171

UNCLASSIFIED

F/G 28/4

NL

END

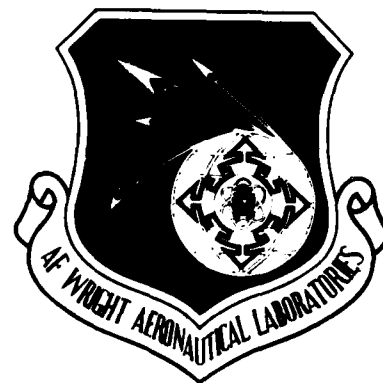
FILED

SEP

DTIC



MICROCOPY RESOLUTION TEST CHART
NATIONAL BUREAU OF STANDARDS-1963-A



DEVELOPMENT AND FLIGHT TEST OF AN ACTIVE
FLUTTER SUPPRESSION SYSTEM FOR THE F-4F
WITH STORES
PART I. DESIGN OF THE ACTIVE FLUTTER
SUPPRESSION SYSTEM

H. Honlinger
D. Mussman
R. Manser
Messerschmitt-Bolkow-Blohm GmbH
Ottobrunn, Federal Republic of Germany

and

L.J. Huttzell
Flight Dynamics Laboratory
Air Force Wright Aeronautical Laboratories
Wright-Patterson Air Force Base, Ohio 45433

September 1982

Final Report for Period April 1977 - March 1979

Approved for public release; distribution unlimited.

FLIGHT DYNAMICS LABORATORY
AIR FORCE WRIGHT AERONAUTICAL LABORATORIES
AIR FORCE SYSTEMS COMMAND
WRIGHT-PATTERSON AIR FORCE BASE, OHIO 45433

RECEIVED
SEP 15 1982

A

82 11 15 041

AD A121485

KEY

NOTICE

When Government drawings, specifications, or other data are used for any purpose other than in connection with a definitely related Government procurement operation, the United States Government thereby incurs no responsibility nor any obligation whatsoever; and the fact that the government may have formulated, furnished, or in any way supplied the said drawings, specifications, or other data, is not to be regarded by implication or otherwise as in any manner licensing the holder or any other person or corporation, or conveying any rights or permission to manufacture use, or sell any patented invention that may in any way be related thereto.

This report has been reviewed by the Office of Public Affairs (ASD/PA) and is releasable to the National Technical Information Service (NTIS). At NTIS, it will be available to the general public, including foreign nations.

This technical report has been reviewed and is approved for publication.



LAWRENCE J. HUTTSELL
Aerospace Engineer
Aeroelastic Group



FREDERICK A. PICCHIONI, Lt Col, USAF
Chief, Analysis & Optimization Branch
Structures & Dynamics Division

FOR THE COMMANDER



RALPH L. KUSTER, Lt. Col, USAF
Chief, Structures & Dynamics Division

"If your address has changed, if you wish to be removed from our mailing list, or if the addressee is no longer employed by your organization please notify AFWAL/FIBRC, W-PAFB, OH 45433 to help us maintain a current mailing list".

Copies of this report should not be returned unless return is required by security considerations, contractual obligations, or notice on a specific document.

UNCLASSIFIED

SECURITY CLASSIFICATION OF THIS PAGE (When Data Entered)

REPORT DOCUMENTATION PAGE		READ INSTRUCTIONS BEFORE COMPLETING FORM
1. REPORT NUMBER AFWAL-TR-82-3040, Part I	2. GOVT ACCESSION NO. <i>A121 486</i>	3. RECIPIENT'S CATALOG NUMBER
4. TITLE (and Subtitle) DEVELOPMENT AND FLIGHT TEST OF AN ACTIVE FLUTTER SUPPRESSION SYSTEM FOR THE F-4 WITH STORES, PART I. DESIGN OF THE ACTIVE FLUTTER SUPPRESSION SYSTEM	5. TYPE OF REPORT & PERIOD COVERED Final Report April 1977 - March 1979	
	6. PERFORMING ORG. REPORT NUMBER	
7. AUTHOR(s) H. Honlinger, D. Musmann, R. Manser, and L. Huttzell.	8. CONTRACT OR GRANT NUMBER(s) Memorandum of Understanding	
9. PERFORMING ORGANIZATION NAME AND ADDRESS Messerschmitt-Bolkow-Blohm GmbH (MBB) Ottobrunn, W. Germany	10. PROGRAM ELEMENT, PROJECT, TASK AREA & WORK UNIT NUMBERS PE 62201F 2401/02/23	
11. CONTROLLING OFFICE NAME AND ADDRESS Flight Dynamics Laboratory (AFWAL/FIBR) Air Force Wright Aeronautical Laboratories (AFSC) Wright-Patterson Air Force Base, Ohio 45433	12. REPORT DATE September 1982	
	13. NUMBER OF PAGES 91	
14. MONITORING AGENCY NAME & ADDRESS (if different from Controlling Office)	15. SECURITY CLASS. (of this report) Unclassified	
	15a. DECLASSIFICATION/DOWNGRADING SCHEDULE	
16. DISTRIBUTION STATEMENT (of this Report) Approved for public release; distribution unlimited		
17. DISTRIBUTION STATEMENT (of the abstract entered in Block 20, if different from Report)		
18. SUPPLEMENTARY NOTES		
19. KEY WORDS (Continue on reverse side if necessary and identify by block number) Active Controls Aeroservoelasticity Flutter Flutter Suppression Wing/Store Flutter		
20. ABSTRACT (Continue on reverse side if necessary and identify by block number) Extensive research programs have been conducted at MBB and at AFWAL to investigate the application of active controls for the suppression of wing/store flutter. A flutter suppression system was developed and flight tested on an F-4F aircraft. The control law was designed by MBB using optimal control theory to minimize the control surface motion and to provide the required stability margins. During the test it was found that the dynamic behavior of the wing-pylon-store changed considerably with excitation amplitude due to free play and preload. The active flutter suppression system worked well and		

DD FORM 1 JAN 73 1473

EDITION OF 1 NOV 65 IS OBSOLETE

UNCLASSIFIED

SECURITY CLASSIFICATION OF THIS PAGE (When Data Entered)

UNCLASSIFIED

SECURITY CLASSIFICATION OF THIS PAGE(When Data Entered)

20 Abstract (continued)

provided an increase in flutter speed.

UNCLASSIFIED

SECURITY CLASSIFICATION OF THIS PAGE(When Data Entered)

FOREWORD

The research described in this report was conducted by Messerschmitt-Bolkow-Blohm GmbH (MBB) under a joint U.S. Air Force/German Ministry of Defense Memorandum of Understanding. The Air Force Project engineers for this effort (work unit 24010223) were Thomas E. Noll and Lawrence J. Huttzell of the Structures and Dynamics Division, Flight Dynamics Laboratory, Air Force Wright Aeronautical Laboratories. The project engineer for MBB was H. Honlinger.

The authors wish to acknowledge the cooperation and support of the OTC E-61 of the Federal Armed Forces in Manching and DFVLR, Institute for Aeroelastics, in Gottingen.

This report (Part I) documents the analysis and design phase of this active flutter suppression program. Part II will document the ground vibration tests, the ground tests on the flutter suppression system, and the initial subcritical flight tests. Part III will document the flight test demonstration of the active flutter suppression system.

This report (Part I) covers work conducted from April 1977 to March 1979.



Accession No.

NY 79 CP-41

100

1. *Journal of the American Medical Association*, 1997; 277: 1033-1038.

100

1.

11

#

11

TABLE OF CONTENTS

SECTION	PAGE
I INTRODUCTION	1
II THEORETICAL ANALYSES	3
1. Vibration Calculations	3
2. Flutter Calculations	4
3. Comparison of Flutter Calculations with Past Test Results	5
4. Design of Control Law for Flutter Suppression	6
5. Hydraulic Study	14
6. Fatigue Analysis of the Wing Structure in the Aileron Attachment Area	16
7. Flight-Mechanical Effect of the Bias Aileron Necessary for Flutter Suppression Tests	17
8. Aircraft Center of Gravity Position with a Critical External Store Configuration	17
III DESIGN AND ANALYSIS OF THE FLUTTER SUPPRESSION AND TEST SYSTEMS	18
1. Use of Available Equipment and Instrumentation	18
2. Additional Instrumentation of the LH Aileron for Measuring Unsteady Pressure Distribution	19
3. Design of the Control Electronics	21
4. Integration of the Flutter Suppression System into the Existing Flight Control System	23
5. Flutter Stopper Concept for the Flutter Critical External Stores	23
6. Operation of the Flutter Suppression System in the Aircraft	24
7. Data Recording and Telemetry	26
8. Safety Precautions	27
9. Installation of the Flutter Suppression System in the Aircraft	30
10. Impedance Test of the High Gain Aileron Power Actuators	30
IV CONCLUSIONS	32
REFERENCES	33

LIST OF ILLUSTRATIONS

FIGURE		PAGE
1	Store Configuration and Sign Convention	35
2	Wing Structure Idealization and Grid Points	36
3	Pylon and Store Arrangement	37
4	First Wing Bending Mode	38
5	Store Yaw Mode	39
6	Store Pitch Mode	40
7	Fourth Wing Mode	41
8	Fifth Wing Mode	42
9	Wing Torsion with Aileron Mode	43
10	Flutter Speeds of Various Stores vs. Store Radius of Gyration	44
11	V-g Plot for Critical Store Configuration at $Ma=0.9$ (Store Mass = 1500 kg)	45
12	V-g Plot of F-4F with Store (Store Mass = 1190 kg)	46
13	Measured Damping and Frequency Trends of the F-4F with Normal Store (Store Mass = 1190 kg)	47
14a	Mathematical Model of the Flutter Suppression System	48
14b	Block Diagram of the Flutter Suppression System with Complete State-Vector Feedback	48
15a	Vector Diagram for Control Law I, Design Speed $V = 500$ kts, ($V_{flutter} = 465$ kts, without Structural Damping)	49
15b	Response of the Aircraft with Flutter Suppression System at $V = 500$ kts, ($V_{flutter} = 465$ kts, Control Law I)	50
16	Vector Diagram for Control Law II, Design Speed $V = 600$ kts, ($V_{flutter} = 567$ kts with 1% Structural Damping)	51
17a	Nyquist Diagram for Control Law I at $V = 500$ kts	52
17b	Nyquist Diagram for Control Law II at $V = 600$ kts	53
18a	Hydraulic System	54

LIST OF ILLUSTRATIONS (Continued)

FIGURE		PAGE
18b	Flow Rate Necessary for the Flutter Suppression System	54
19	Pressure Decrease in the Tubes vs Flow Rate	55
20	Scheme of the F-4F Roll Channel	56
21	Transfer Function (Amplitude) of the Standard Power Actuator Compared with the NW High Gain Actuator	57
22	Comparison of the Phases of NW Standard and NW High Gain Actuator	58
23	F-4F with Normal Store (1190 kg), In-Flight Measured Accelerations and Deformations due to Aileron Excitation	59
24	Block Diagram of the Flutter Suppression System and Flight Test Equipment	60
25	Block Diagram of the System to Measure the Unsteady Pressure Distribution on the Aileron	61
26	Calibration of the Filter Used for the Measurement of the <u>Steady</u> Reference Pressure	62
27	Installation of the Pressure Transducers in the Left F-4F Aileron	63
28	Position of the Sensors Installed for the Flutter Suppression System	64
29	Block Diagram of the Control Electronics for One Wing	65
30	Integration of the Flutter Suppression System into the AFCS	66
31	Efficiency of the Flutter Stopper	67
32	Sketch of the Flutter Stopper	68
33	Sensor Installation in the Flutter Stopper	69
34	F-4F Flutter Suppression System, Switch-Off Modes of the Test Programs	70
35	Control Panels for the Active Flutter Suppression System	71
36	Block Diagram of Flight Data Processing	72

LIST OF ILLUSTRATIONS (Concluded)

FIGURE		PAGE
37	Safety Concept for Flight Tests with Flutter Suppression System	73
38	Block Diagram of Failure Mode Analysis for the Flutter Suppression System	74
39	Block Diagram of Failure Mode Analysis of the Flutter-Stopper	75
40	Additional Wiring in the F-4F for the Flutter Suppression System	76
41	Additional Installations for the Flutter Suppression System and Flight Test Equipment	77

LIST OF TABLES

TABLE	PAGE
1 Modal Sensitivity Study	78
2 Control Law Gains	78
3 Comparison of MDC and MBB Data for Fatigue Life Assessment	79

NOMENCLATURE

b_r	reference length
C_{qq}	generalized aerodynamic force matrix
F	reference surface
g, G	structural damping
k	reduced frequency ($\omega S_R/V$)
K	gain factor of the control law
K_{qq}	generalized stiffness matrix
K_{tot}	global gain
m	mass
M_{qq}	generalized mass matrix
Ma	Mach number
q	generalized coordinate
S_R	half-wing span
V	speed
β_0	angle of aileron deflection
φ	wing bending
θ	store pitch
$\dot{\varphi}$	wing bending velocity
$\dot{\theta}$	store pitch velocity
$\ddot{\varphi}$	wing bending acceleration
$\ddot{\theta}$	store pitch acceleration
ω	frequency
ρ	air density, radius of gyration

ABBREVIATIONS

c.g.	center of gravity
Hz	Hertz
LH	left hand
MAC	mean aerodynamic chord
RH	right hand
AFCS	Active Flight Control System
KEAS	Knots Equivalent Air Speed
kg	kilograms
kts	knots
MDC	McDonnell Douglas Corporation
NW	National Waterlift
m	meters
mm	millimeters

SECTION I

INTRODUCTION

During the last several years, considerable interest has emerged in the U.S. and European communities for the application of active control technology to suppress flutter. Both the U.S. Air Force and Messerschmitt-Bolkow-Blohm GmbH (MBB) have performed extensive research programs accompanied by wind tunnel tests in the field of active flutter and elastic mode suppression.

In 1975, MBB conducted a successful wind tunnel test which also led to a flight demonstration. This research demonstrated suppression of wing store flutter with store mounted vanes (Reference 1). On another program, flutter speed was increased on a fin-tailplane-aft fuselage with a hydraulically driven rudder (References 2 and 3). Miniature model actuators and new wind tunnel test techniques were developed to investigate Flutter Suppression Systems (FSS) with flutter models. Special computer programs - utilizing optimal control theory were adapted to find suitable control laws for flutter suppression (Reference 4). A very successful application of these programs is described in Reference 5. Analytical development of systems to reduce buffet induced pilot vibrations was presented in Reference 6. A system to improve ride comfort of a low wing loaded fighter was laid out recently (Reference 7).

Two full scale airplanes were equipped and flight tested to prove the feasibility of active flutter suppression. The first flight test was performed with a Fiat G 91/T3 which used additional control surfaces (vanes) to produce aerodynamic forces which counteract the store motion (Reference 8). In 1977, a much more challenging flight test program was launched in cooperation with the Bundesamt fur Wehrtechnik und Beschaffung (BWB) and the Flight Dynamics Laboratory (FDL). The objective of this program was to design and flight test a system for flutter suppression on an F-4F aircraft with stores. As a flying test bed for this program, an F-4F aircraft of the German Air Force test center at Manching (Erprobungsstelle 61 der Bundeswehr) was chosen. This airplane was already equipped to perform flight flutter tests with stores. To generate the necessary

unsteady aerodynamic control forces, existing control surfaces (ailerons) were used. Accelerometers located on the wing provided the signals which were fed back through the existing stability augmentation system of the airplane.

This report (Part I) documents the analysis and design of the active flutter suppression system for the F-4F aircraft with stores. Part II will document the ground vibration tests, the ground tests on the flutter suppression system, and the initial subcritical flight tests. Part III will document the flight test demonstration of the active flutter suppression system.

SECTION II

THEORETICAL ANALYSES

In the early 1970's, the FDL sponsored a feasibility study (Reference 9) and a preliminary design study (Reference 10) by the McDonnell Aircraft Company for the installation of an active flutter suppression system in a Phantom F-4C with external stores. These studies and the analyses and tests performed by MBB in this report confirm that the F-4F used by the German Air Force is a suitable flying test bed for an experimental system to suppress wing/store flutter using the available aircraft control surfaces. Furthermore, by establishing a certain external store configuration, it is possible to create flutter conditions on the F-4F, as well as on the F-4C, which is suitable for testing the flutter suppression system. Two external store dummies (LBFK) from another project were used to simulate the flutter-critical external store.

The following sections deal with the results of the flutter analyses, the design of the control laws, and the requirements for the flight system which are important in designing a flutter suppression system.

1. VIBRATION CALCULATIONS

To be able to design a control system, the dynamic behavior of the individual elements in the control system must be known as well as possible. In the case of flutter suppression, this applies particularly to the controlled system; i.e., the aircraft. Unlike normal control systems, the controlled system here becomes unstable at speeds above the critical air speed. For this reason, the aircraft with the flutter-critical external stores was first subjected to a detailed vibration analysis in which the mass data of the external stores were varied. As can be seen in Figure 1, the calculation model used consists of an elastic wing with an external store attached to the outboard wing pylon. The fuselage and tailplane are assumed rigid. References 11 and 12 show that these simplifications can be made.

The wing elasticity was introduced into the calculation in the form of an influence coefficient matrix. Figure 2 shows the location of the

57 influence points. The influence matrix and the associated mass matrix have been taken from Reference 13. The geometry of the external store and its flutter-critical mass data can be seen in Figure 3. The elasticity data of the pylon (MAU 12) have been taken from Reference 12. Six symmetrical vibration modes were calculated for the aircraft. Figures 4 through 9 show these modes; mode 2, wing bending, and mode 3, external store pitching, are the most significant vibration modes with respect to this flutter.

2. FLUTTER CALCULATIONS

To keep the test risk as low as possible, it was desirable to conduct the flight test on a mild flutter case with a low flutter speed. For this purpose, a trend study was first carried out to determine a low flutter case by varying the mass data of the external store. In Figure 10, the established flutter speeds for the different external store masses versus the radius of gyration of the external store have been plotted. This figure shows that the lowest flutter speed can only be obtained by increasing the mass and extending the radius of gyration of the attached external stores.

The unsteady aerodynamic forces used for these flutter trend calculations were determined by using unsteady subsonic theory for the symmetrical natural modes of the wing and for the rigid body modes at $Ma = 0.9$. Only symmetrical flutter calculations were carried out since antisymmetrical flutter speeds lie above the symmetrical ones (Reference 11).

With the aid of the trend study, Figure 10 and the document on the LBFK dummies (Reference 13), an external store configuration was selected which had a mass of 1500 kg (Figure 3) and a radius of gyration of 1.28 m. This external store configuration provided the most favorable flutter case for the planned tests. The configurations could be simulated using the existing store dummies without the extra trouble of attaching additional weights. Furthermore, an additional flutter calculation for this critical external store configuration was made, taking into account the influence of the aileron vibration modes at $Ma = 0.9$. In this case, the aerodynamic forces were calculated using the doublet-lattice procedure.

The flutter speed and the damping curve of the flutter mode versus air speed are shown in Figure 11. Without taking into account the structural damping, the flutter speed is 467 KEAS; furthermore, it can be seen from the curves of frequency versus speed (Figure 11) that the first 3 wing modes are responsible for the flutter. The flutter trend curves in Figure 10 show a higher flutter speed for the selected configuration than in Figure 11. The differences stem from the different methods of calculation and the more exact representation of the vibration modes shown in the flutter calculation in Figure 11.

3. COMPARISON OF FLUTTER CALCULATIONS WITH PAST TEST RESULTS

As mentioned above, MBB had the results of flight flutter tests carried out on the F-4F with LBFK dummies (Reference 14). The comparison between the results of the flutter calculations conducted here and the flight test results in Figures 12 and 13 show that this calculation model supplied realistic values. The much higher sub-critical damping values measured in the flight tests are due on the one hand to the structural damping of 2 to 5% g which was not accounted for in the calculation, and on the other hand to the damping effect of the fins on the external stores. Furthermore, the calculation can only supply exact damping values near the point of flutter.

The same proven calculation model (Reference 13) was used for the flutter calculations for the critical external store configuration selected for the flutter suppression tests. The greater mass (20%) and the larger the radius of gyration (10%) lowers the frequencies by approximately 0.5 Hz. However, the vibration modes essential for flutter remain to a great extent unchanged. Thus the flutter case calculated in Subsection 2 can also be regarded as a reliable result.

For the design of a flutter suppression system, not only the flutter point has to be well known but also the flutter mechanism, i.e., which vibration modes cause the flutter. Therefore, for the purpose of a more detailed analysis of this flutter mechanism the number of rigid body and natural modes in the flutter calculation were varied, and the respective flutter speed calculated. The results of these variations have been

Part I

compiled in the Table 1. It should be pointed out here that the original LBFK dummy was used in this analysis. This is also reflected in the high flutter speeds in variation 7. However, this result can also be used analogously for the modified dummies ($m = 1500$ kg).

Table 1 shows that the basic bending (mode 2) and external store pitch (mode 3) are the important modes for flutter. The external store yaw has an infinitely small vibratory influence. The introduction of further normal modes into the calculation has a damping effect only, thus increasing the flutter speed. Therefore, an effective flutter suppression system must influence the basic bending and the store pitch mode of the wing.

4. DESIGN OF CONTROL LAW FOR FLUTTER SUPPRESSION

The suppression system used on the G 91 suppressed flutter by means of control vanes at the tips of external stores. The control of the deflection of the vanes was in accordance with the principle of a speed-proportional damper covering one control quantity only, namely the pitch mode of the external store. The control action was optimized along classical lines by using Nyquist diagrams. The situation regarding the F-4F became more complicated since the ailerons were used as the damping surfaces. In cases like this, the optimum control theory can be used to obtain an optimum control law. The purpose of this optimization is to find a control law which enables effective flutter suppression to be achieved with a minimum of control surface deflections. A number of publications (References 15, 16, 17) contain detailed information on the initial use of the optimum control theory for developing control laws for flutter suppression systems; these methods have already proved suitable for the design of flight control systems. For this reason, only the design methods used on the F-4F will be dealt with in this report.

a. System Description and Calculation Methods for the Control Law Optimization

The equation of motion for a forced aeroelastic system can be described as follows:

$$m_r b_r^2 \begin{bmatrix} M_{qq} & M_{q\beta_0} \\ M_{\beta_0 q} & M_{\beta_0 \beta_0} \end{bmatrix} \begin{Bmatrix} \ddot{q} \\ \ddot{\beta}_0 \end{Bmatrix} + \frac{s_R}{k v} \begin{bmatrix} \omega_r^2 m_r b_r^2 & 0 \\ 0 & K_{\beta_0 \beta_0} \end{bmatrix} \begin{Bmatrix} \dot{q} \\ \dot{\beta}_0 \end{Bmatrix} + \frac{\rho}{2} v^2 F s_R \frac{b_r^2}{s_R^2} \begin{bmatrix} C_{qq}^* & C_{q\beta_0}^* \\ C_{\beta_0 q}^* & C_{\beta_0 \beta_0}^* \end{bmatrix} \begin{Bmatrix} \dot{q} \\ \dot{\beta}_0 \end{Bmatrix} \\ + \begin{bmatrix} \omega_r^2 m_r b_r^2 & 0 \\ 0 & K_{\beta_0 \beta_0} \end{bmatrix} \begin{Bmatrix} q \\ \beta_0 \end{Bmatrix} + \frac{\rho}{2} v^2 F s_R \frac{b_r^2}{s_R^2} \begin{bmatrix} C_{qq} & C_{q\beta_0} \\ C_{\beta_0 q} & C_{\beta_0 \beta_0} \end{bmatrix} \begin{Bmatrix} q \\ \beta_0 \end{Bmatrix} = \{Q(t)\}$$

(1)

where:

m_r	reference mass
b_r	reference length
ω_r	reference frequency
M_{qq}	generalized mass
K_{qq}	generalized stiffness
C_{qq}	generalized aerodynamic forces
v	speed
s_R	half-wing span
$k = \omega s_R / v$	reduced frequency
F	reference surface
g	structural damping
Q	generalized forces
q	generalized coordinates

The complex stiffness of the actuator is given by

$$K_{\beta_0 \beta_0}^* = K_{\beta_0 \beta_0}^* + i K_{\beta_0 \beta_0}^g$$

(2)

β_0 = angle of deflection of aileron which is rigidly attached to actuator.

Part I

For the controlled aircraft, a new quantity has to be introduced into the system matrix as a new degree of freedom, this bending $\Delta\beta$ which is the angle of deflection of the elastic aileron additionally induced by the control system.

The generalized forces, Q , created by the aileron deflection $\Delta\beta$, which is induced by the control system, can be described as the right side of Equation 1.

$$\{Q(t)\} = -m_r b_r^2 \begin{Bmatrix} M_{q\Delta\beta} \\ M_{\beta_0\Delta\beta} \end{Bmatrix} \Delta\ddot{\beta} - \frac{\rho}{2} v^2 F_{sR} \frac{b_r^2}{s_R^2} \frac{s_R}{k \cdot v} \begin{Bmatrix} C_{q\Delta\beta}^* \\ C_{\beta_0\Delta\beta}^* \end{Bmatrix} \Delta\dot{\beta} - \frac{\rho}{2} v^2 F_{sR} \frac{b_r^2}{s_R^2} \begin{Bmatrix} C_{q\Delta\beta} \\ C_{\beta_0\Delta\beta} \end{Bmatrix} \Delta\beta \quad (3)$$

Assuming normalized rigid aileron modes β_0 and $\Delta\beta$, the entire aileron deflection β can be described as:

$$\beta = \beta_0 + \Delta\beta \quad (4)$$

After Equation 1 has been divided by $m_r \cdot b_r^2 \omega_r^2$ and after an approximation of the unsteady aerodynamic forces using a polynomial in $s = i\omega$ for the reduced frequency k around the flutter point,

$$(C^* + iC^*) = a_0 + a_1 s + a_2 s^2 \quad (5)$$

and after introducing the actuator transfer function

$$\frac{\Delta\beta}{x_i} = F_{ACT} = \frac{1}{1 + b_1 s + b_2 s^2} \quad (6)$$

Equation 1 can be represented in the state space as follows:

$$\{\dot{x}\} = [A] \{x\} + [B] x_i \quad (7)$$

where $\{x\}$ is the state vector.

This equation is used as a system equation for developing a control law. Figure 14a shows the corresponding block diagram.

$$\{x\} = \begin{Bmatrix} q \\ \beta_0 \\ \Delta\beta \\ \dot{q} \\ \dot{\beta}_0 \\ \dot{\Delta\beta} \end{Bmatrix} = \text{STATE VECTOR} \quad (8)$$

$$[A] = \begin{bmatrix} 0 & 1 \\ [S_1]^{-1} \cdot [S_2] & [S_1]^{-1} \cdot [S_3] \end{bmatrix} \quad (9)$$

$$[S_1] = \begin{bmatrix} \frac{1}{\omega_f^2} \begin{vmatrix} M_{qq} & M_{q\beta_0} & M_{q\Delta\beta} \\ M_{\beta_0 q} & M_{\beta_0 \beta_0} & M_{\beta_0 \Delta\beta} \\ 0 & 0 & \omega_f^2 b_2 \end{vmatrix} \cdot \frac{D}{2} v^2 \frac{F}{s_R} \frac{1}{m_f \omega_f^2} \begin{vmatrix} a_{2qq} & a_{2q\beta_0} & a_{2q\Delta\beta} \\ a_{2\beta_0 q} & a_{2\beta_0 \beta_0} & a_{2\beta_0 \Delta\beta} \\ 0 & 0 & 0 \end{vmatrix} \end{bmatrix} \quad (10)$$

$$[S_2] = \begin{bmatrix} \begin{vmatrix} K_{qq} & 0 & 0 \\ 0 & K_{\beta_0 \beta_0} & 0 \\ 0 & 0 & 1 \end{vmatrix} \cdot \frac{D}{2} v^2 \frac{F}{s_R} \frac{1}{m_f \omega_f^2} \begin{vmatrix} a_{0qq} & a_{0q\beta_0} & a_{0q\Delta\beta} \\ a_{0\beta_0 q} & a_{0\beta_0 \beta_0} & a_{0\beta_0 \Delta\beta} \\ 0 & 0 & 0 \end{vmatrix} \end{bmatrix} \quad (11)$$

$$[S_3] = \begin{bmatrix} \frac{s_R}{v k} \left(\begin{vmatrix} s K_{qq} & 0 & 0 \\ 0 & K_{\beta_0 \beta_0} & 0 \\ 0 & 0 & \frac{v k}{s_R} b_1 \end{vmatrix} \cdot \frac{D}{2} v^2 \frac{F}{s_R} \frac{1}{m_f \omega_f^2} \begin{vmatrix} a_{1qq} & a_{1q\beta_0} & a_{1q\Delta\beta} \\ a_{1\beta_0 q} & a_{1\beta_0 \beta_0} & a_{1\beta_0 \Delta\beta} \\ 0 & 0 & 0 \end{vmatrix} \right) \end{bmatrix} \quad (12)$$

$$[B] = \begin{Bmatrix} 0 \\ 0 \\ 0 \\ [S_1]^{-1} \cdot \begin{Bmatrix} 0 \\ 0 \\ 1 \end{Bmatrix} \end{Bmatrix} \quad (13)$$

Part I,

In order to obtain an optimum control law, a performance criterion has to be found for the optimization process. In this case, the following quadratic performance criterion was selected:

$$J = \int_0^T (\{x\}^T [\bar{Q}] \{x\} + x_i R x_i) dt \quad (14)$$

Here, \bar{Q} is a weighting matrix for the individual state quantities and has to be estimated. R in this case is a scalar quantity since there is only one regulated quantity (aileron). An optimum control law is obtained by minimizing the performance criterion.

$$x_i = \{K_{opt}\}^T \{x\} \quad (15)$$

where

$$\{K_{opt}\}^T = -R^{-1} \{B\}^T [P] \quad (16)$$

and P represents the solution to the matrix Riccati equation.

$$[-P] + [P][A] + [A]^T [P] - [P][B] R^{-1} [B]^T [P] + [Q] \quad (17)$$

The procedure described here applies to the complete feedback of the state vector. This is the simplest solution when the state vector is small.

For measuring reasons, the state vector cannot be measured directly. However, the following holds true.

$$\{x\} = [C^*] \cdot \{y\} \quad (18)$$

where C^* is the measuring matrix and y is the individual measured quantities.

In practice, however, only reference values for the flutter modes can be measured, i.e., the bending angular acceleration \ddot{U} and the pitch angular acceleration $\ddot{\theta}$ of the wing with the aid of an accelerometer. These are integrated to obtain the state quantities U , \dot{U} and θ , $\dot{\theta}$ as shown in the block diagram (Figure 14b).

The elastic components of the aileron deflection β_0 can be easily determined using a strain gauge if the equation

$$\frac{m_\beta}{K_\beta} = \beta_0 \quad (19)$$

m_β = actuator moment
 K_β = actuator impedance

is taken into account as well as the simplification that K_β is a constant (valid for one frequency only, i.e., the flutter frequency). $\dot{\beta}_0$ is obtained by differentiation of the signal. $\Delta\beta$ and $\Delta\dot{\beta}$ are the only state quantities which can be measured directly by means of a potentiometer.

The modern control theory has already produced many methods for designing complicated control systems which work in the time or frequency domain. The method described here was expanded to form a program system with an interactive screen terminal (Reference 15). This terminal permits rapid dialogue with the computer, which greatly speeds up the process of solving the optimization problems. In the optimization process the engineer's difficulty lies in defining a weighting matrix as a performance criterion (Equation 14) to determine the influence of the individual state quantities in the optimum control law. Certain marginal conditions can be specified for the optimum control laws by means of the weighting matrix and the scalar R which weights the control energy of the active surface.

In our case, the results of the flutter calculation were used to define the weighting matrix. The solution vector of the flutter calculation indicates the proportion of the individual vibration modes in the flutter mode. These proportions are transferred to the weighting matrix as they represent the state quantities θ , u , $\dot{\theta}$, \dot{u} which are the main vibration modes found in this flutter. The weighting of the remaining state quantities is less than 5% in the control laws as shown in the trend studies; therefore, this weighting was chosen to be zero.

b. Discussion of the Optimum Control Laws

With the aid of the weighting method described previously, two types of control laws for the flutter suppression system have been optimized.

A design point for both control laws was an air speed of 35 kts above the flutter point. The outcome of the optimization, the vectors K of the control law (Equation 18), are compiled in Table 2. The signs and their ratios are important for assessing the vector elements. The absolute quantities are determined by the electrical data of the sensors and the actuator activation.

Table 2 shows that only the state quantities of the flutter mode are fed back. As previously mentioned, the state quantities of the aileron mode $\Delta\beta$ and β_0 are negligible and thus entered as zero. The overall gain K^* in Control Law I is $K^*_I = 1.7$, and in Control Law II $K^*_{II} = 2.4$.

The difference between the two control laws can be seen in the Figures 15a and 16 which show the phase location of the control vectors X_i versus the natural vibration vectors of the wing bending Q and the external store pitch mode θ . In Control Law I shown in Figure 15a, the vector X_i is turned by approximately 180° to the natural vibration vectors Q and θ .

Figure 15b shows the effect of the control law on the system response (wing bending and store pitch). These responses of the aircraft (Control Law I) while flying at 500 kts (35 kts above flutter point) are due to a Dirac pulse. The damping of the two response curves, the wing bending as well as external store pitch, is well damped (3.2% g). However, according to the flutter calculation, the aerodynamic damping of the wing bending for an uncontrolled aircraft flying at this speed is 6.5% g.

This kind of reduction in the aerodynamic damping of the bending mode by the control system can be explained by the fact that Control Law I causes an aerodynamic change in the coupling between the bending and

external store pitch modes by increasing the frequency separation. This in turn causes a decrease in the damping of the bending mode by the unsteady aerodynamic forces.

The increase in the aerodynamic damping and thus the stabilization of the external store pitch mode can be explained as follows: part of the damping is obtained in the form of speed-proportional damping across the damping surface. The other part of damping is produced by the fact that Control Law I increases the frequency separation between the wing bending and the external store pitch, thus stabilizing it. Control Law I offers particular advantages for the F-4F wing/aileron configuration since the wing bending, which can be easily influenced by the aileron, is an essential component of the control law (Figure 15a).

Figure 16 shows that in Control Law II the vector X_i is turned by approximately 90° to the natural vibration vector θ . This control law causes the flutter speed to be increased by introducing artificial damping in the external store pitch mode. This idea has already been demonstrated in tests of the G 91 (Reference 8).

Open-loop calculations were made for the stability analysis of the control system using Control Law I as well as the control system using Control Law II. The calculated Nyquist diagrams in Figures 17 a and b show that both control systems have sufficient stability (the -1 point is located on left-hand side for increasing frequency).

All calculations described here were made assuming the following:

- The aileron power actuator behaves like a real spring.
- The sensors measure quantities characteristic of pure natural modes.

The control laws should be revised once additional information is available, i.e., actuator impedance and experimental sensor test values.

c. Gust Behavior of the Control System

Gusts are defined by their duration and the distribution of the spectrum and amplitudes. Therefore, when the aircraft flies through

gusts, the gusts excite its natural frequencies and thus also its flutter frequencies. Thus, in the supercritical flight range, the gusts the vibratory effect of the unsteady aerodynamic forces, and so the flutter suppression system must be capable of damping these additional excitations, too. This is complicated by the fact that the amplitudes of the actuator of the damping surface have to be restricted to prevent the actuator from being driven into saturation.

For this reason, the optimum control laws have been designed so that only a small overall increase of $K_{tot} \leq 5.0$ of the control system is required to suppress this type of flutter.

Thus, the actuator still possesses enough reserves to suppress the additional excitation caused by medium-sized gusts without being driven into saturation.

5. HYDRAULIC STUDY

a. Use of Aileron Control System for Flutter Suppression

To be able to realize the concept, i.e., using the aileron to damp vibration and flutter, it first has to be determined if the aircraft has sufficient hydraulic reserves for this additional function. To check this, the assumption is made that at a flutter frequency of approximately 6 Hz, aileron deflections of $\pm 1.5^\circ$ are required for flutter suppression. The study in Reference 10 contains higher requirements, namely $\pm 1.5^\circ$ at 10 Hz.

Figures 18a and 18b (from Reference 10) show that the F-4F has four hydraulic pumps, each having a flow rate of 25 gal/min. For the lower requirements of this flutter suppression system, the hydraulic flow requirements per pump calculated in section 3.5.2.1 of Reference 10, Hydraulic Flow Requirements is reduced to 4.2 gal/min, which leaves 20.8 gal/min for other purposes. According to section 3.5.2.1 of Reference 10, the pressure drop in the aircraft's 3/8" wide pressure lines to the aileron power actuator is 63 psi/ft. This means that the expected line loss is so high that the aileron can no longer satisfy the specified performance.

For this reason, MDC recommended the installation of a new hydraulic line to the aileron power actuator. MBB feels that the pressure loss per foot estimated by MDC is too pessimistic. Figure 19 shows that for the reduced flow of 4.2 gal/min the line loss is low. Thus it is not necessary to change the pressure line system to the aileron power actuator as proposed in Reference 10.

Section 3.5.2.1 of Reference 10 deals with the danger of "water hammer", i.e., power surges in the line system caused by the quick opening and closing of the control valve in the actuator. MBB did not encounter a phenomenon of this kind in its flight vibration tests using aileron excitation in the 2-10 Hz frequency range. Therefore, no problems are expected in the tests using similar aileron deflections and aileron frequencies.

b. Actuation of Aileron Power Actuator

For roll control, the F-4F has ailerons and spoilers which are linked by control rods in such a way that the ailerons can only deflect from $+1^\circ$ to -30° ; Figure 20 shows this in a schematic diagram. However, for flutter suppression only the ailerons are to be used since the aerodynamic effect of the spoilers is predominantly non-linear. The power actuators of the ailerons and spoilers can only be actuated mechanically. Only the series servo controlling the aileron as well as the spoiler actuator can process electrical inputs. If only the aileron is to be actuated, the spoiler has to be separated. This can be done by trimming the aileron to -2° (BIAS), for example. If aileron deflections of -0.5° to -3.5° only are permitted, the spoiler will not move. The flight mechanical effects of this trimming will be described in Subsection 7. The flutter suppression effect of the aileron is, however, not influenced by this small trimming. The easiest way of electrically actuating the series servo is by means of a test input in the roll channel of the autopilot servo amplifier. The manufacturer of the F-4F and MBB have both used this method of actuating the aileron in flight flutter tests (flight flutter tests for LBFK, Reference 14).

c. High Gain Aileron Power Actuator

The F-4F is equipped with an aileron power actuator (standard actuator) made by National Waterlift (NW). The dynamic behavior of this standard actuator is not at all suitable for the flutter suppression test. As can be seen from the frequency response of the standard actuator shown in Figure 21, the amplitude drop at 6 Hz is already so large that the required aileron deflection of $\pm 1.5^\circ$ could not be reached without driving the actuator into the saturation region. The saturation region should be avoided at all cost since phase relations are incalculable here and can cause the flutter suppression system to become unstable. The frequency response of the aileron actuator can, as proposed in Section 3.5.4.1 of Reference 10, be improved considerably by increasing the degree of gain in the valve to 350%. Figures 21 and 22 show the amplitude response and phase response of the improved actuator. This indicates that an improved actuator should be used for flutter suppression. Tests using this kind of actuator have been carried out by McDonnell and MBB.

Figure 23 is a time history from a flight flutter test conducted by MBB on the F-4F with LBFK external stores and aileron excitation. In the test, a more advanced aileron power actuator made by the Weston Power Company was used, and for comparison its transfer function has been entered in Figure 21. Figure 23 clearly shows that the aileron can easily excite wing torsion and wing bending (aileron deflection $\pm 0.6^\circ$ and -3° BIAS). Since there is a phase difference of only 180° between damping and excitation by the aileron, the system can also be used effectively for damping purposes.

6. FATIGUE ANALYSIS OF THE WING STRUCTURE IN THE AILERON ATTACHMENT AREA

The service life of the aileron attachments and the back-up structure of the F-4F wing has not been designed for the high aileron frequencies necessary for flutter suppression. For this reason the FDL study (Section 3.7.2.1 of Reference 10) looked into the effects of a flutter suppression system on the service life of these structural areas. FDL based its study on far higher load assumptions than in this project and found out that certain structural areas need to be strengthened for fatigue reasons. The aileron mid position (BIAS) and the aileron oscillation

frequency were the most important parameters in the FDL analysis. The analysis also revealed that aileron deflections of $\pm 1.5^\circ$ at 0° BIAS (which is only possible theoretically) had no perceivable influence on the service life. Table 3 contains a comparison of the data assumed by MDC and the loads expected to occur in this project.

Table 3 shows that far lower preloads and few load cycles are to be expected in this test program. It must, however, be considered that maximum aileron amplitudes only occur in gusts. The normal aileron amplitudes are approximately 50% of the given value.

No signs of fatigue could be found after the eight MBB flights with aileron excitation and similar loads. However, to be on the safe side, the wing structure in the aileron attachment area will be checked for signs of fatigue during the flight test.

7. FLIGHT-MECHANICAL EFFECT OF THE BIAS AILERON NECESSARY FOR FLUTTER SUPPRESSION TESTS

As already mentioned the aileron has to be trimmed to -2° so that the spoilers can be separated for the flutter suppression test. This trimming causes a nose-heavy longitudinal moment which requires a stabilizing deflection of the elevator for balancing. Since the ailerons and spoilers are linked by connecting rods, once the aileron has been trimmed to -2° the spoiler cannot deflect within a certain range. The MBB flight flutter tests with aileron excitation were conducted using an aileron BIAS of approximately -3° . There were no effects of the BIAS on the aircraft's roll stability to be found in the 8 test flights.

8. AIRCRAFT CENTER OF GRAVITY POSITION WITH A CRITICAL EXTERNAL STORE CONFIGURATION

Tests were conducted with the critical external store configuration at the outboard wing pylons. To avoid exceeding the aircraft's maximum permissible rear c.g. position of 34% MAC during take-off with this configuration, fuselage tanks 5 and 6 can only be one third filled. The aircraft can fly for a maximum of 1 hour with this amount of fuel. This means that in each flight there are 20 minutes for completing each test point. However, it was found in the G 91 program that up to 6 test points can be obtained in this period of time.

SECTION III

DESIGN AND ANALYSIS OF THE FLUTTER SUPPRESSION AND TEST SYSTEM

1. USE OF AVAILABLE EQUIPMENT AND INSTRUMENTATION

As mentioned in Section I, OTC E-61 together with BWB supplied a test aircraft of the type F-4F as a flying test bed. The aircraft was equipped for flight flutter tests with an aileron excitation system which had already been tested by MBB; this system formed the basis of the flutter suppression system to be installed. Furthermore, the test system's spare wiring could largely be used for the additional wiring needed for the flutter suppression system.

In addition, external store dummies (LBFK) were available for this project so that critical external store configurations could be prepared. MBB also had available the flight test results for these store dummies and their flutter speed was known.

If simple mechanical and structural modifications are made to the dummies' mass data (max. 20%), their flutter speed can be brought into a speed range of between 500 and 600 KEAS, this being favorable for flutter tests. This low flutter case is very similar to that of the F-4F with normal LBFK's, which had already been tested; this means that detailed and valuable test results from the previous test could be used. This greatly simplified the test program and, of course, also the design of the flutter suppression system.

Bearing this in mind, the following systems were designed for the F-4F test aircraft:

- Flutter suppression system using the ailerons as damping surfaces.
- Test system in the LH aileron to measure unsteady pressure distribution on the aileron in a section with parallel flow.
- Flutter stopper in the external stores to keep test risk as low as possible.

. All important data of the flutter suppression system are monitored by telemetry.

Figure 24 shows a wiring diagram of all these systems.

The flutter suppression system is an automatic control unit which controls the aileron. It can be used for eight different flight test programs. They are operated by the pilot via a trigger in the forward cockpit and monitored on a control panel. The system can be switched off manually only by the pilot pressing the bomb release button. In addition, this system has an automatic threshold cut-off switch which switches off the flutter suppression system and operates the flutter stopper if the frequency amplitudes are so high that there is a risk of damaging the aircraft structure. The copilot sets the 8 test programs on a second control panel in the rear cockpit and monitors the system's functions as well.

Ten pressure transducers in the LH aileron measure the unsteady pressure distribution which, together with the aileron deflection, are recorded by an airborne recorder for later computer evaluation. The object of using this system is to gain information about the complicated aerodynamics in the transonic range.

By increasing the inertia moment of the external store about the pitch axis the flutter speed of the external store configuration can be raised. This effect can be obtained by movable trim weights in the external stores, thus obtaining an artificial flutter stopper.

2. ADDITIONAL INSTRUMENTATION ON THE LH AILERON FOR MEASURING UNSTEADY PRESSURE DISTRIBUTION

a. Function of Test System

Nine differential pressure transducers have been installed in a line parallel with flow which is located approximately in the center of the LH aileron. Six of these pressure transducers are located on the upper surface of the aileron and three on the lower surface. A tenth pressure transducer is a total pressure transducer which measures the reference pressure. Figure 25 illustrates the operating principle of this

test system. The differential pressure transducers require a constant reference pressure, the most suitable being dynamic pressure. As it is too expensive to install an additional dynamic pressure measuring device on the wing and on the aileron, the reference pressure is obtained by filtering the unsteady pressure measured on the aileron. The filter is a pressure hose 20 meters in length with an internal diameter of 1 mm, which has been wound onto a spool. Figure 26 illustrates the filter characteristics of this hose spool (calibration was performed by the Institute for Aeroelastics of the DFVLR in Gottingen). The aileron deflection responsible for creating the unsteady pressure distribution is measured with a potentiometer. Furthermore, the actuator force and the entire aileron moment can also be used as test data and for verifying the results. The test results will be evaluated by MBB and the DFVLR in Gottingen.

b. Transducers and Data Recording

As part of the cooperation program, FDL furnished 10 pressure transducers with a filter of the type KULITE X CQH 152-10. They have a measuring range of 0 - 10 psi. The measured pressure data, aileron position and aileron moment are amplified and filtered by a single conditioner and simultaneously recorded on the aircraft's recorder.

c. Changes to the Aileron Design

The LH aileron had to be modified so that the pressure transducer and filter could be installed. As can be seen in Figure 27, an opening with a screw lid had to be made. The individual pressure transducers were bonded into aluminum blocks and then screwed from the inside to the upper or lower aileron skin. To ensure the reading is as accurate as possible, pressure holes in the aileron skin of 1 mm were chosen and the paths from the upper edge of the skin to the center of the transducer kept as short as possible. Additional soldered strips were also installed in the aileron for transducer wiring.

3. DESIGN OF THE CONTROL ELECTRONICS

a. Location of Sensors

Theoretically, in order to be able to realize the optimum control law calculated in Section II, a complete feedback of the state vector is required (Equation 8). However, as mentioned previously, the state vector cannot be measured directly in all cases, which means that the vector has to be produced by additional electronic means. Figure 28 shows the position of the individual sensors used for the automatic control. The wing bending angles (α , $\dot{\alpha}$) and wing torsion angle (θ , $\dot{\theta}$) are measured by combining and subtracting the four accelerometers FBL 1-4 and FBR 1-4, respectively. Accelerometers of the Kulite GAD 813-10 type are used as transducers. The aileron deflection (ASL, ASR) is measured by means of a linear emulsion film potentiometer, and the angular velocity of the aileron by means of a speed transducer connected in parallel. Three main strain gauges have been attached to the aileron actuator housing to measure the actuator forces.

b. Description of Circuitry for the Control Electronics

The control electronics for this flutter suppression system is of a universal design, similar to that used in the G 91 program so that on the one hand the various sensor signals can be processed, and on the other hand a flutter test can be conducted economically. The main elements of the control electronics are shown in the block diagram in Figure 29. They are:

- signal conditioner to produce state quantities which cannot be measured directly
- control amplifier with 8 inputs for feedback of the entire state vector
 - switching logic to adjust the various functions
 - phase shifter for additional corrections
 - adapter unit for the servo amplifier of the F-4F's autopilot
 - cut-off switch for the control signal as a safety device

The signal conditioner processes four acceleration signals from the wings by first filtering out of the entire measured spectrum the

bending and pitch velocities of the wing by subtracting two signals each. The state quantities ϕ , $\dot{\phi}$, θ , $\dot{\theta}$ are then obtained by integrating these differential signals.

The additional phase shifter downstream of the servo amplifier permits subsequent manual phase corrections to be made in the control law. The main reason for its installation is to enable easy adjustments to be made to the control concept used on the F-4F - the control concept that has proved useful on the G 91.

The built-in switching logic enables the flutter suppression system to be operated from the cockpit which is particularly important for the flight test to be effective. Furthermore, it serves to select the eight test programs in the flutter suppression system which were described in detail in Section II. The switching logic is activated by means of a combination of three control signals.

Two of the control signals are initiated by means of a program selector switch on the control panel number 2 in the rear cockpit. The third control voltage is produced by pressing the trigger button on the forward control stick. All the test functions of the flutter suppression system, except for the flutter suppression itself, are activated for as long as the pilot depresses the trigger button thus producing the third control voltage.

The adaptor unit had to be incorporated in the control electronics to enable the flutter suppression system to be integrated in the existing flight control system of the F-4F. The unit modulates the output signal from the control electronics for the servo amplifier of the F-4F autopilot to be able to process it. The cut-off switch at the output of the control electronics serves as a safety switch. In the case of a current drop or an automatic or emergency cut-off, the safety switch disconnects the output of the flutter control electronics from the input into the servo amplifier of the autopilot. This prevents the voltage peaks produced by the capacitors discharging when the electronics are switched off from causing uncontrolled aileron deflections.

The electronic unit described here was installed separately for each wing so that there are two independent control circuits, each of which is capable of suppressing flutter up to a certain critical speed.

4. INTEGRATION OF THE FLUTTER SUPPRESSION SYSTEM INTO THE EXISTING FLIGHT CONTROL SYSTEM

The integration of the flutter suppression system into the existing flutter control unit is relatively easy in the F-4F since only two electric inputs into the roll damping channel are necessary. When the flying test bed was modified as a flight test aircraft, the aileron excitation was channelled by a test input into the servo amplifier in the roll channel of the flight control unit (Figure 30). The control signal from the LH and RH control electronics is fed into the flutter suppression system via these proven test inputs. The ailerons are then operated quite normally via the two servo amplifiers. To prevent the flutter damping from being affected by the roll damping of the autopilot in case of an autopilot error, the roll sensor signal has to be separated from the servo amplifier input. The block diagram (Figure 29) shows that this can be easily done at the summing point upstream of the attenuator.

5. FLUTTER STOPPER CONCEPT IN THE FLUTTER CRITICAL EXTERNAL STORES

a. Design of the Flutter Stopper

A flutter stopper for each external store has been included in the general concept as an additional safety measure for the flutter suppression tests. Figure 31 illustrates the operating principle of this flutter stopper. The flutter speed of the chosen critical external store mass of 1500 kg exhibits the normal parabolic curve when plotted versus the radius of gyration of the external store. The concept of the flutter stopper is based on the fact that the most effective increase in the flutter speed, i.e., "stopping" the flutter, is achieved by increasing the radius of gyration of the external store. This is technically possible by using movable trim weights in the external stores to increase the gyration moment, if all the other mass data of the external stores, such as the c.g. position, remain unchanged as illustrated in Figures 32 and 33.

b. Testing of the Flutter Stopper

Since the use of a flutter stopper as a safety measure plays an important role in the flight test, the increase in the flutter speed by 10% and the initiation of the flutter stopper must be ensured. In addition to the ground tests on the external store itself, the testing of the flutter stopper constitutes an important part of the flight test program. The aircraft must not fly in the critical speed range until after these test have been completed.

6. OPERATION OF THE FLUTTER SUPPRESSION SYSTEM IN THE AIRCRAFT

a. Circuits in the Control Electronics for the Functional Testing of the Flutter Suppression System

As these flight tests using the flutter suppression system are also of a basic nature, the control electronics were designed in a way that three possible basic functions of the flutter suppression system can be connected by means of switching logic; they are:

- flutter suppression system in an open-loop circuit
- flutter suppression system in a closed-loop circuit
- unstable flutter suppression system.

In addition, for test purposes, a frequency shift signal which is used as an electrical disturbance variable can be fed into the open-loop as well as closed-loop control circuit. The possibility of being able to switch these basic functions separately for each wing has yielded eight different functions or test programs for the entire flutter suppression system. The eight test programs which can be turned on in the aircraft during the flight test are listed on Figure 34.

Programs 1 to 7 are test programs which enable the behavior of the flutter suppression system to be studied in the subcritical range. They are used to study the control system in flight according to the classical methods using Nyquist and Nichols diagrams.

On the other hand, programs 2, 3, 5, and 6 can be used to study to what extent the aircraft exhibits symmetrical flutter behavior. They also enable investigations to be made in the subcritical, and thus safe, flight range, as to what extent a control system and an aileron are capable of suppressing forced vibration (programs 2 and 3) and an induced instability (programs 5 and 6). These investigations are of particular importance for checking the safety concept.

In addition, program 4 offers the possibility of quickly determining suppression capability using a measuring procedure first tested on the G 91.

Program 8 which concerns flutter suppression in the critical flight range is not carried out until programs 1 to 7 have been successfully completed.

Figure 34 shows the eight test programs and also the various ways of switching off the entire system. The switching will be discussed in the following paragraph.

b. Switch-On and Switch-Off Devices for the Flutter Suppression System

Since the flutter suppression system has been integrated in both the measuring system and the flight control system, it cannot be centrally switched on by means of a master switch. When the power is switched on for the measuring system, both the sensors and the cut-off system and the frequency shift generator are turned on. The flutter stopper is switched on at the same time as the aircraft power supply. Only the power supply for the control electronics is switched on separately for the LH and RH wing at the control panel in the rear cockpit. This allows each part of the system to be tested separately.

In test programs 1 to 7, the flutter suppression system is not activated until the pilot presses the trigger button. In test program 8, i.e., active flutter suppression, the program is switched on directly and the pilot can cancel the flutter suppression by pressing the trigger button. This switching possibility is necessary in tests where the sup-

pression or excitation in the close vicinity of the flutter point is measured directly.

The normal method of switching off the system in programs 1 to 7 is, as was mentioned above, by releasing the trigger button. However, if, in the tests using programs 1 to 7, flutter amplitudes occur on the wing which exceed a given safety value (below the maximum permissible value for the structure) and the pilot does not switch off the program himself, the automatic cut-off system discontinues the program. This is brought to the pilot's attention by the red indicator light which illuminates on the control panel. The program cannot be restarted until "Press to Reset" is depressed and the trigger button is pressed again (Figure 35).

Besides the automatic cut-off system, the pilot can switch off all the programs by using the emergency cut-off switch if defects arise in the system or excessive flutter amplitudes occur on the aircraft. The bomb release button in the forward cockpit functions as the emergency cut-off switch in the aircraft. Actuation of the emergency cut-off switch always activates the flutter stopper. Test program 8 concerning flutter suppression is the only one in which the automatic cut-off system also activates the flutter stopper. In the G 91 program, a modified method of switching the flutter suppression system on and off has already proved itself to be effective and safe for flight tests.

7. DATA RECORDING AND TELEMETRY

a. Onboard Tape Recording

So that the flight test results can be evaluated, all the sensor signals entered in block diagram (Figure 24) are recorded on tape by the aircraft recorder. In addition, the control unit signals, the cut-off system pulse, and all the important flight parameters are recorded.

b. Telemetry

A flight test, such as the one planned here, can only be conducted with the aid of telemetry since the flutter suppression system has to be monitored for safety reasons and each test point has to be evalu-

ated before the next test point can be explored. Thus it is only by using telemetry that several test points can be handled during one flight. The block diagram in Figure 36 shows that the most important parameters can be checked during the flight by means of three recorders each with eight channels.

c. Quick-Look Evaluation

The most important data to the person in charge of the flight tests for evaluating the test results are the flutter amplitudes, damping, and phase relationship of the flutter mode. The amplitudes of the flutter mode and of the aileron can be monitored directly by means of the telemetric time signals, whereas the damping of the critical mode can only be estimated from the decrement of the amplitudes. So that the damping and phase relations in the control unit can be quickly evaluated during the test a Fourier analyzer (HP 5451 B) is connected to the telemetry station, which processes the selected telemetric signals in real time.

Thus, besides the evaluation of damping in almost real time, the control laws can be directly checked in flight by using calculated Nyquist diagrams of the open-loop circuit and Nichols diagrams of the closed-loop control circuit.

8. SAFETY PRECAUTIONS

a. General Safety Concept

Flight in the critical and supercritical speed ranges can only be carried out with an active flutter suppression system. Thus, a failure of the suppression system is extremely dangerous for the pilot and the aircraft. To keep the risk during testing of the flutter suppression system to a minimum, the redundancy of the flutter suppression system must be especially high. This is usually achieved by means of redundant systems. However, since in this case no changes in the control system of the flying test bed could be made for financial reasons, it was impossible for us to follow the classical redundancy concept in which all the systems of the flutter suppression system have a triple or quadruple redundancy.

Using the results from the G 91 program, the flutter suppression system was designed in such a way that it comprises two independent control circuits, one for the LH and one for the RH wing. Each control circuit is capable on its own of suppressing flutter with a sufficient safety margin, up to a defined and permissible air speed. If both suppressing circuits fail, a safe flight condition can be recovered by operating the flutter stopper. If the flutter stopper fails, a safe flight condition can still be recovered by an emergency jettison of the external stores. This concept is illustrated in a block diagram in Figure 37.

Thus, based on these redundancy considerations, a flutter suppression system was constructed to cope with the first failure. Figure 38 shows this in detail. As previously mentioned, only a second failure needs to be countered by the flutter stopper.

b. Failure Behavior of Flutter Stopper

The mathematically determined increase in the flutter speed due to the flutter stopper must, of course, first be proved in a flight test at the beginning of the test program. The electromechanical system of the flutter stopper was also designed in such a way that the system can still cope with the first failure. A schematic diagram on the flutter stopper's failure behavior is shown in Figure 39.

c. Switch-Off Modes

The switch-off devices installed in the aircraft were already described and this section will only deal with the safety aspects. In the flight tests in the sub-critical speed range, flight vibration modes were excited with approximately 6 Hz so that their damping could be determined from their decay behavior. Since it is a known fact that in the case of resonance very small excitation forces can quickly produce very high amplitudes, damage can be caused to the aircraft structure. In order to avoid this, the cut-off system described previously has been installed.

With the aid of the accelerometers FBR 1/2 and FBL 1/2, this unit monitors the flutter amplitudes, integrating the largest signal to occur within a given time. If the preset value is exceeded within this time, the unit switches off the control electronics. The electronic elements of this unit are not redundant. However, the pilot still has two ways of manually switching off the flutter suppression system using the trigger or emergency-off buttons. The switching-off pulse of the automatic cut-off system is transmitted via a switching unit in panel 2 which switches off the control electronics. This unit comprises two circuits of identical design and thus the flutter suppression system can still be safely switched off if one circuit fails.

d. Test Specifications for the Flutter Suppression System

Based on the facts and findings from the G 91 program, the following test specifications for the flutter suppression system operation were drawn up in order to increase the safety factor during supercritical flight:

Pre-Flight Check

- Functional test of flutter suppression system using test programs 1 to 7
- Check of all sensors
- Check of automatic cut-off system by means of test signal
- Test of emergency cut-off
- Test of flutter stopper prior to critical flights

In-Flight Check (prior to entering supercritical flight range)

- Check that flutter suppression system is in perfect working order by means of test program 7 and simultaneous evaluation of test data in the telemetric station.

Furthermore, it must be stated that all the tests are monitored by telemetry, thus ensuring that all the sensors and electrical equipment necessary for the system to operate satisfactorily are monitored continuously.

9. INSTALLATION OF THE FLUTTER SUPPRESSION SYSTEM IN THE AIRCRAFT

Since the flying test bed had already been equipped as a universal test aircraft, only a few additional mechanical installations were needed for the incorporation of the flutter suppression system. The major mechanical operation was installing the pressure transducers in the LH aileron. Figure 27 shows that an opening and a cover had to be made. Four new fittings had to be screwed down into the wing to secure the sensors of the flutter suppression system. Four of these fittings were already installed in the aircraft. To a large extent the existing cables could be used for wiring the system which meant that no large openings had to be made in the aircraft structure to lay the few extra cables. Except for installing the control panels in the cockpit all the other mechanical work was performed during refit overhaul.

In order to save costs, additional cables were laid during refit overhaul when various zones of the aircraft were accessible. A wiring diagram of the new harnesses is given in Figure 40.

A set of drawings was prepared to cover the entire mechanical work and the additional wiring. An amended TOP drawing was made which includes all the items of equipment which were added during the installation of the flutter suppression system. In this report, only a sketch (Figure 41) of the installed equipment belonging to the flutter suppression system has been included for clarity. The sensors which have been newly installed are shown in Figures 28 and 33.

10. IMPEDANCE TEST OF THE HIGH GAIN AILERON POWER ACTUATORS

In designing the control law for the flutter suppression system, as described in Section II, the actuator stiffness was at first assumed to be a real spring. However, the actuator stiffness is actually dependent on frequency and is thus a complex stiffness. This complex stiffness, or impedance of the actuator, cannot be satisfactorily determined mathematically.

AFWAL-TR-82-3040
Part I

As part of the cooperation with DFVLR in Gottingen, the impedance of the actuator was determined in experiments carried out by the Institute for Aeroelastics (Reference 18). The tests were performed in April 1978 so that the results were available in time for the final calculation of the control system data.

SECTION IV

CONCLUSIONS

A flutter suppression system was designed for the F-4F aircraft with external stores. The existing control surfaces (ailerons) were used as the active control surfaces. Accelerometers located on the wing provided the feedback signals which were compensated and fed back through the existing stability augmentation system.

The control law was obtained from an optimal theory program which minimized the control surface deflections due to disturbances and provided the required stability margins. It was found that the two important states that must be measured were the first wing bending and the first wing torsion/store pitch modes. The contribution of the states related to the aileron (β_0 , $\Delta\beta$) is small and were not necessary to use them in the control law mechanization.

The ground testing and the initial subcritical flight tests will be presented in Part II of this report. Part III will cover the flight test demonstration of the active flutter suppression system.

REFERENCES

1. G. Haidl, A. Lotze, O. Sensburg, "Active Flutter Suppression on Wings with External Stores," AGARDograph No. 175, July 1975.
2. O. Sensburg, H. Honlinger, M. Kuhn, "Active Control of Empennage Flutter," AGARD-SMP Brussels, 13-18 April 1975.
3. H. Honlinger, O. Sensburg, "Dynamic Simulation in Wind Tunnels," AGARD Conference Proceedings, No. 187.
4. G. Oesterheld, W. Kubbat, "Entwurf von Regelungssystemen mit Hilfe von Computer Aided Design and ihre Anwendung," MBB-Report GD 8-74.
5. H. Honlinger, O. Sensburg, M. Kuhn, "Definition of the German Flutter Suppression Control Law for the YF-17 International Wind Tunnel Program," Paper presented at the 51st SMP of AGARD, Athens 13-18 April 1980.
6. O. Sensburg, J. Becker, H. Honlinger, "Active Control of Flutter and Vibration of an Aircraft," IUTAM Symposium, Waterloo/Canada June 4-7, 1979, MBB-Report No. S/PUB/8.
7. J. Becker, W. Schmidts, "TKF-Boenbelastung," International MBR-Report TKF.
8. H. Honlinger, and A. Lotze, "Active Flutter Suppression of Aircraft Flutter," 11th ICAS-Congress, Lisbon/Portugal, 10-16 Sept. 1978.
9. W.E. Triplett, Hans Peter Kappus, and R.J. Landy, "Active Flutter Suppression System for Military Aircraft, A Feasibility Study," AFFDL-TR-72-116, Feb 1973.
10. W.E. Triplett, R.J. Landy, and D.W. Irwin, "Preliminary Design of Active/Wing Store Flutter Suppression Systems for Military Aircraft," AFFDL-TR-74-67, August 1974.
11. H.R. Gongloff, and J.W. Walker, "Model F-4E (Slat) Aircraft Wing Flutter Analysis with External Stores," MDC-Report A 2560; Nov. 30, 1973.
12. J.W. Walker, and C.J. Moore, "Model F-4E (Slat) Thick Skin Wing Flutter Analysis with and without External Stores," MDC-Report A 2770; June 15, 1974.
13. G. Schneider, "Flatteruntersuchungen am Flugel der MDC-F-4F mit LBFK Tragflugkorpern an auBeren Flugelpylon," MBB-Bericht Nr. UFE1280; Sept 1976.
14. M. Steininger, "Flugversuche zur Untersuchung der Flatterstabilitat F-4F mit AuBenlast LBFK," MBB-Report Nr. GTR-F-4007.

REFERENCES (Concluded)

15. W. Dressler, "Control of an Elastic Aircraft Using Optical Control Laws," paper presented at the Joint Symposium of the Flight Mechanics Panel and Guidance and Control Panel in Paris, France, 14-17 Oct 1974. (AGARD-CP-157, June 1975).
16. M. Turner, "Active Flutter Suppression," AGARD-CP-175, July 1975.
17. O. Sensburg, and H. Zimmerman, "Impact of Active Control on Structures," AGARD Multi-Panel Symposium Florence/Italy, Oct 1977.
18. R. Freymann, and H. Giese, "Experimentell-rechnerische Ermittlung der dynamischen Übertragungsfunktionen des in einer F-4F Phantom zur Flatterunterdrückung eingesetzten Querruderaktuator," DFVLE-interner Bericht Nr. IB 253-78 J 05, October 1978.

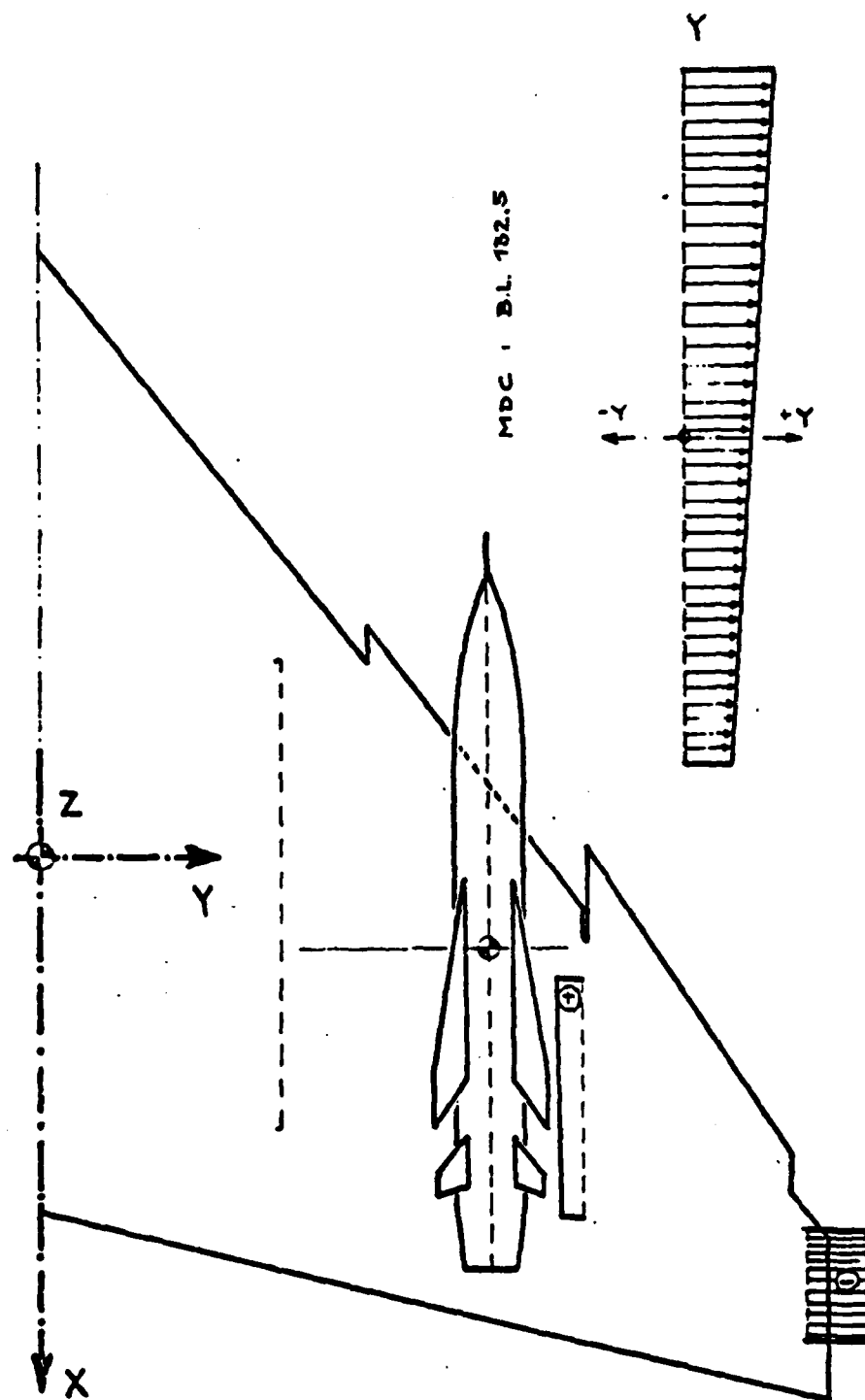


Figure 1. Store Configuration and Sign Convention

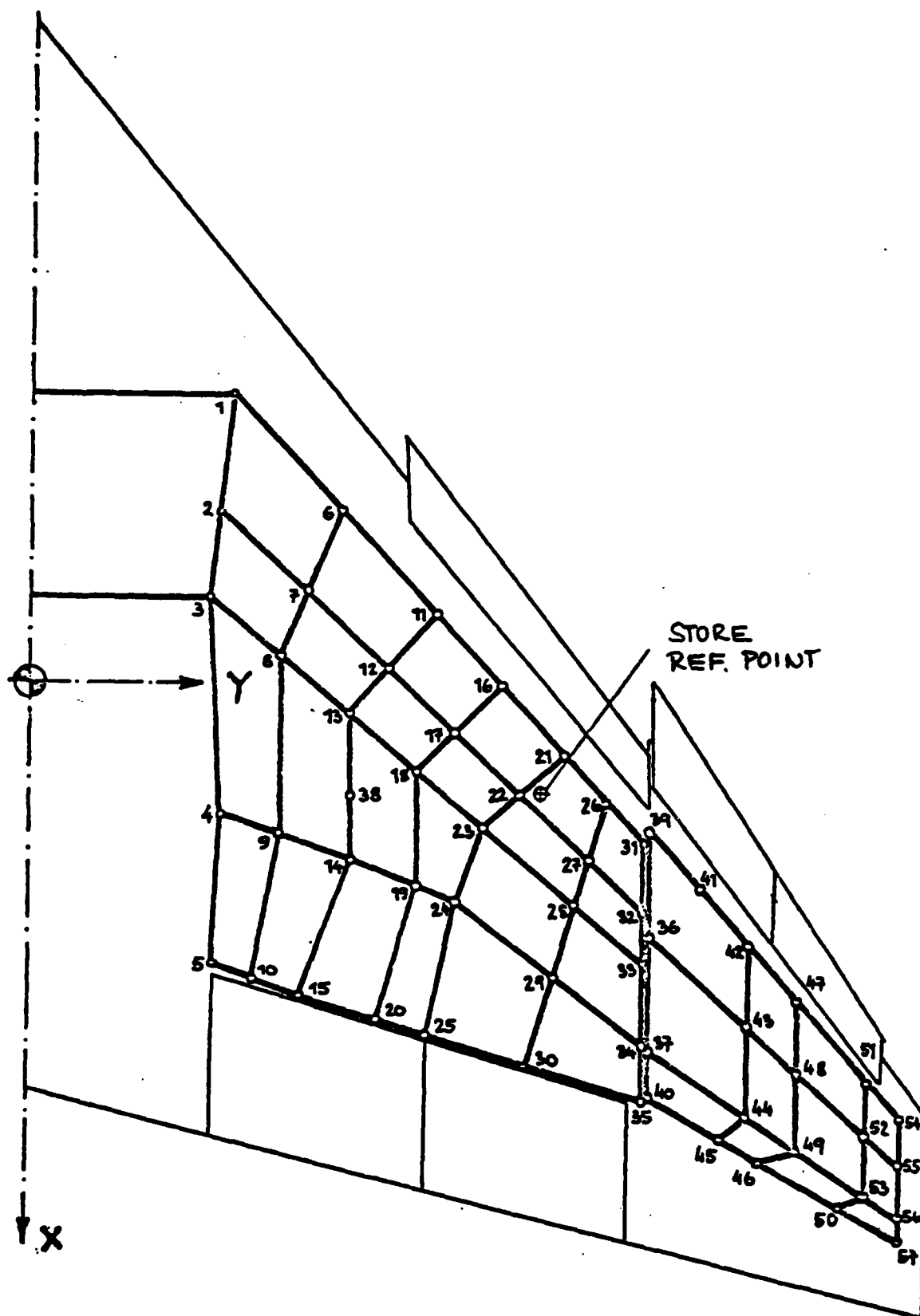
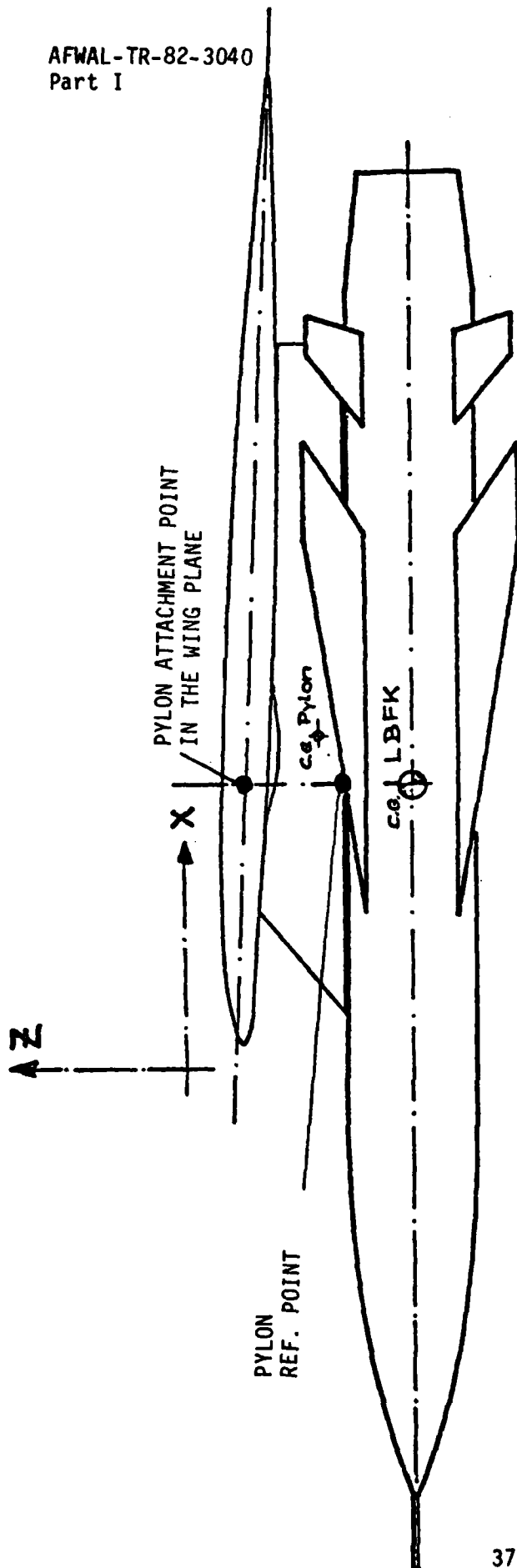


Figure 2. Wing Structure Idealization and Grid Points



MASS	MASS MOMENT OF INERTIA	X	Y	Z
[kg]	[kg cm ²]		[cm]	
PYLON MAU 12	2.45 · 10 ⁷	924.05	336.55	+ 6.10
LBFK STORE C.G. FROM PYLON REF. POINT		901.95	343.82	- 22.49
PYLON ATTACHMENT STORE REF. POINT		901.95	336.55	19.05
		901.95	336.55	- 17.65

Figure 3. Pylon and Store Arrangement

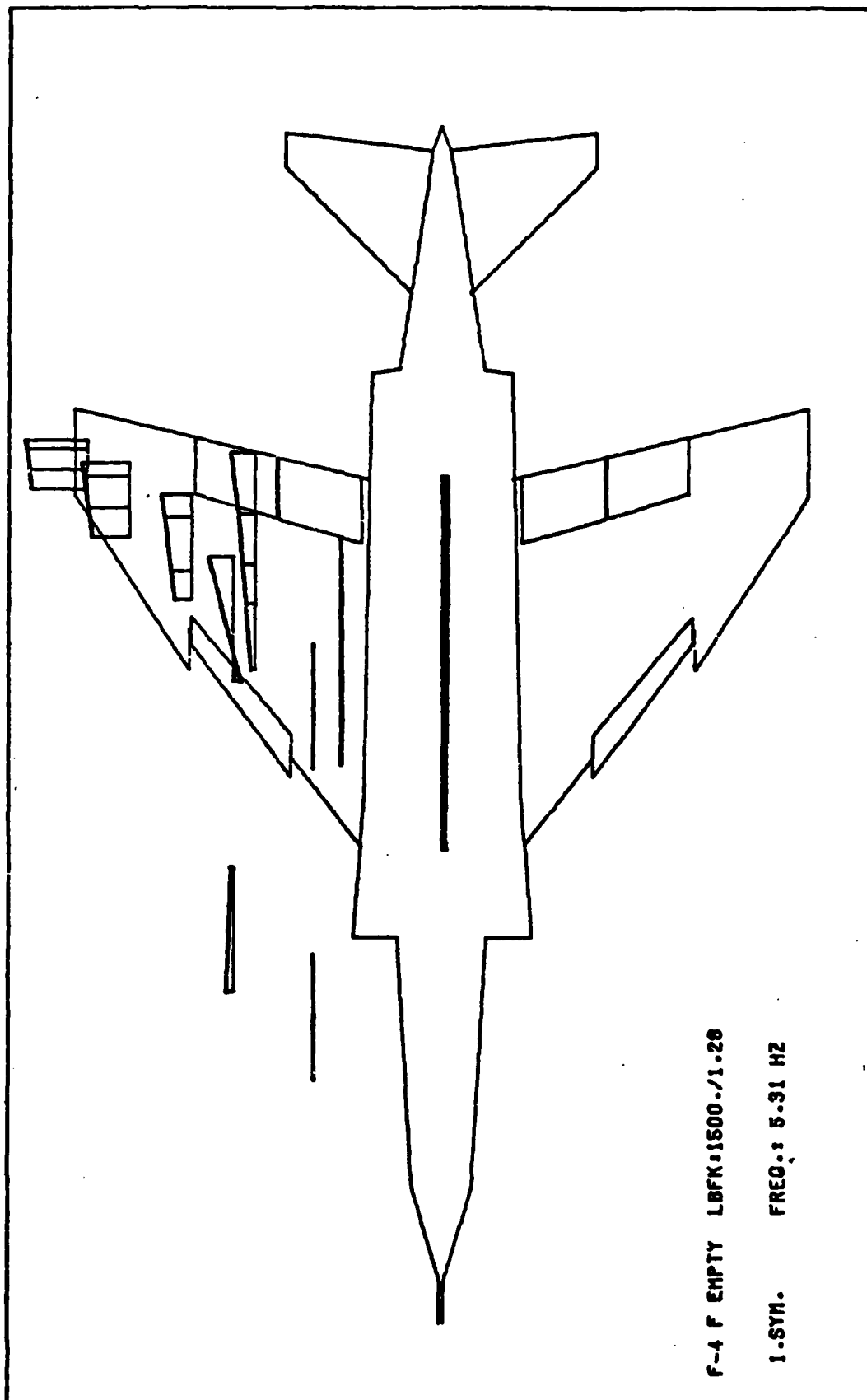


Figure 4. First Wing Bending Mode

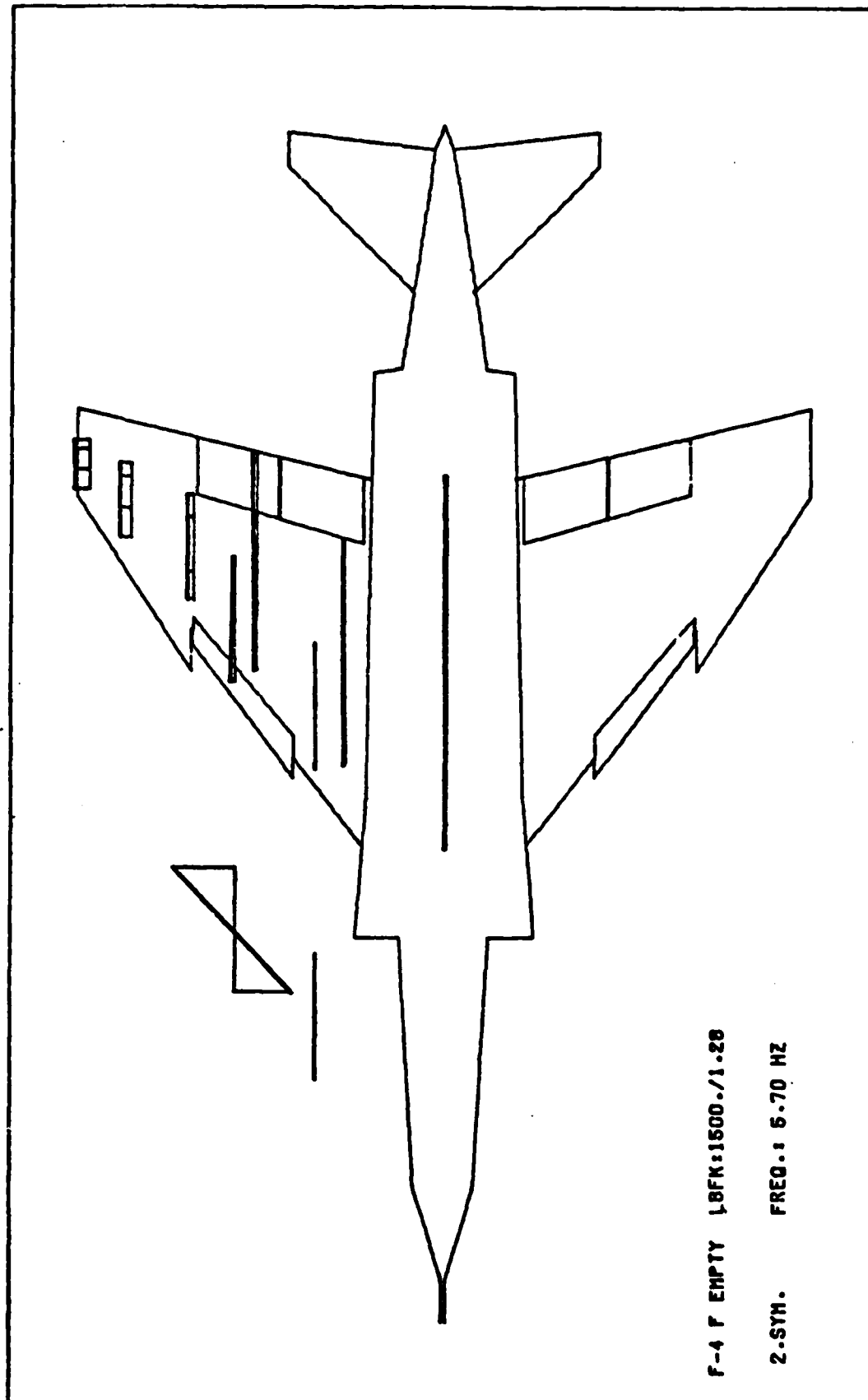


Figure 5. Store Yaw Mode

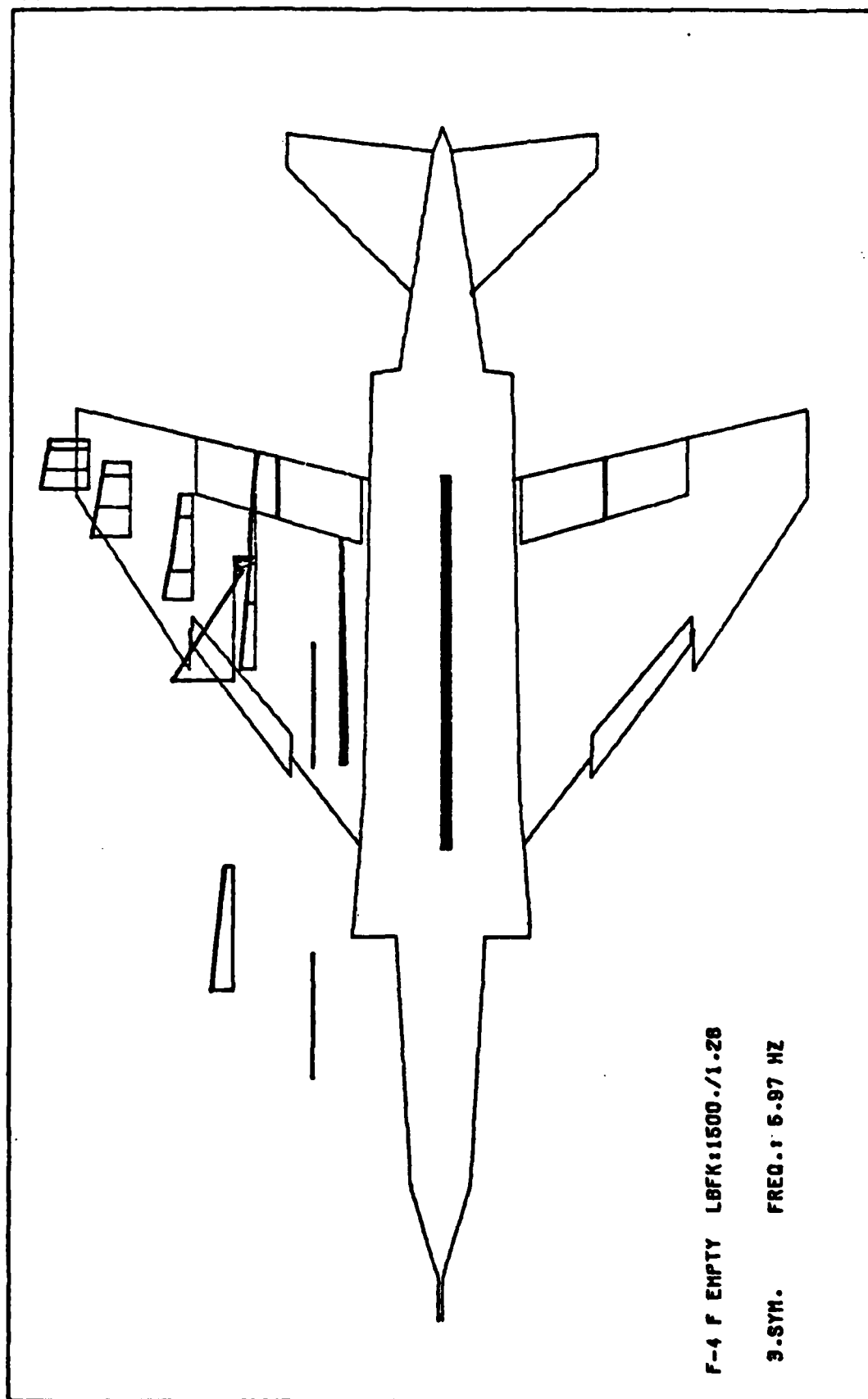


Figure 6. Store Pitch Mode

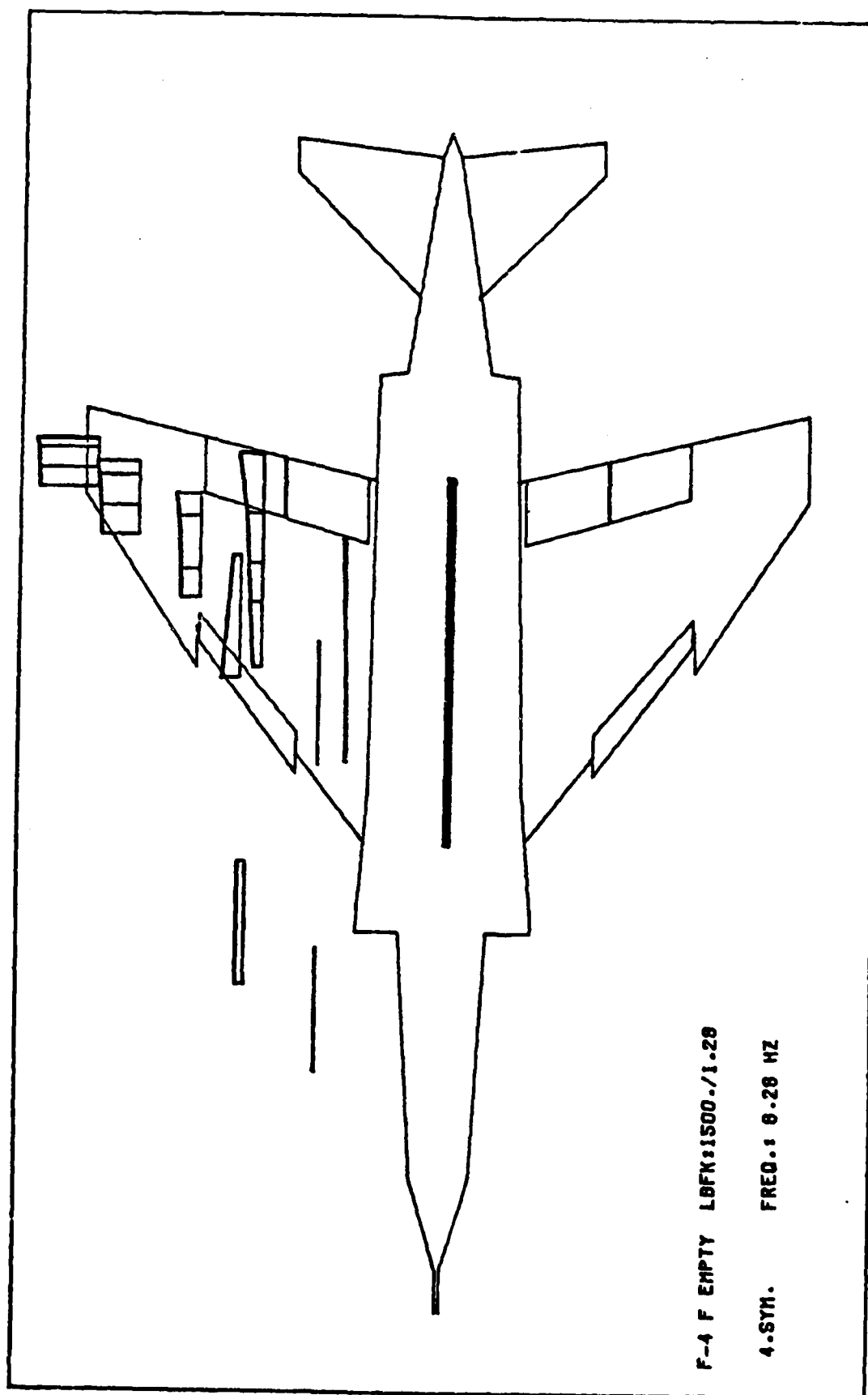


Figure 7. Fourth Wing Mode

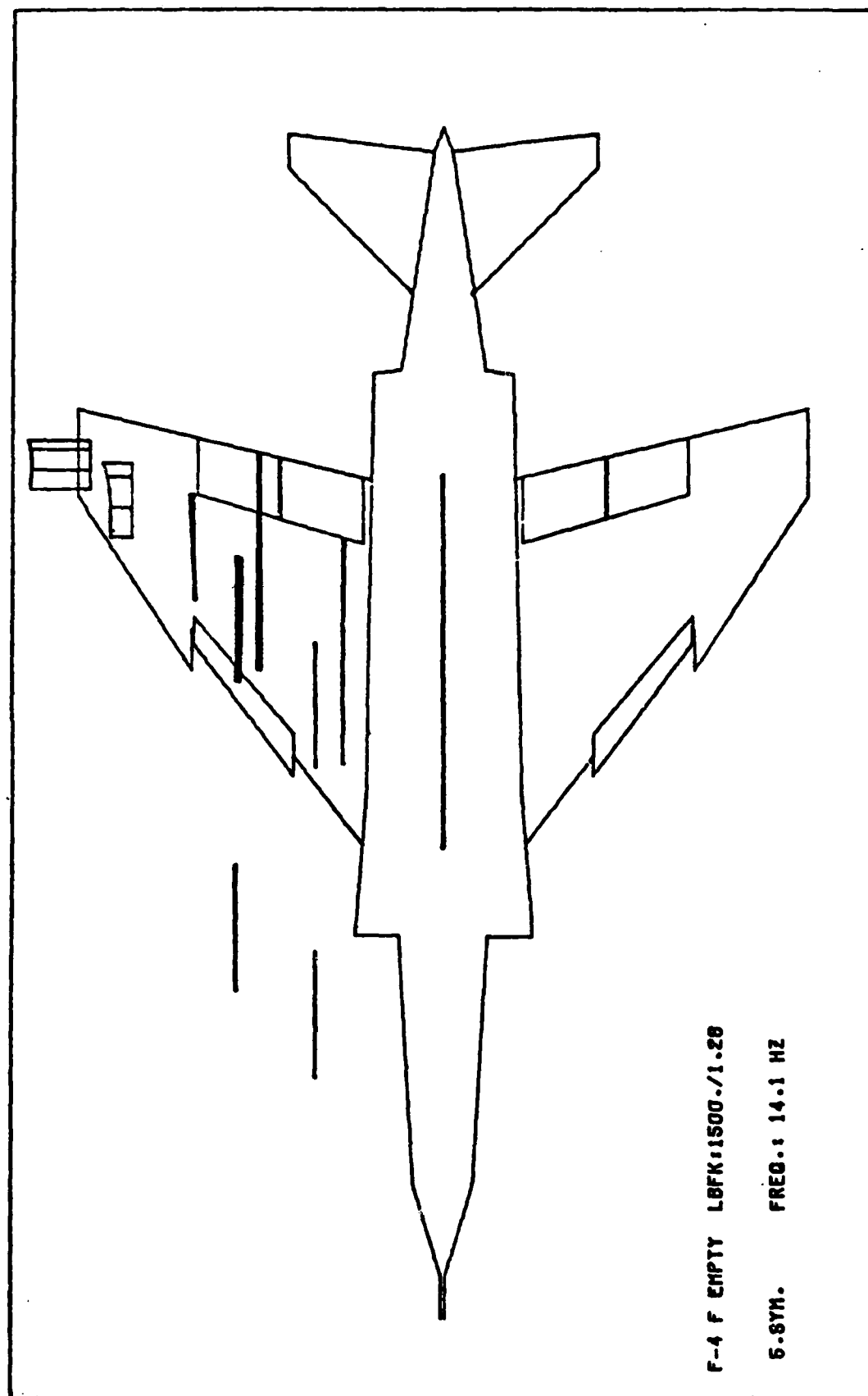


Figure 8. Fifth Wing Mode

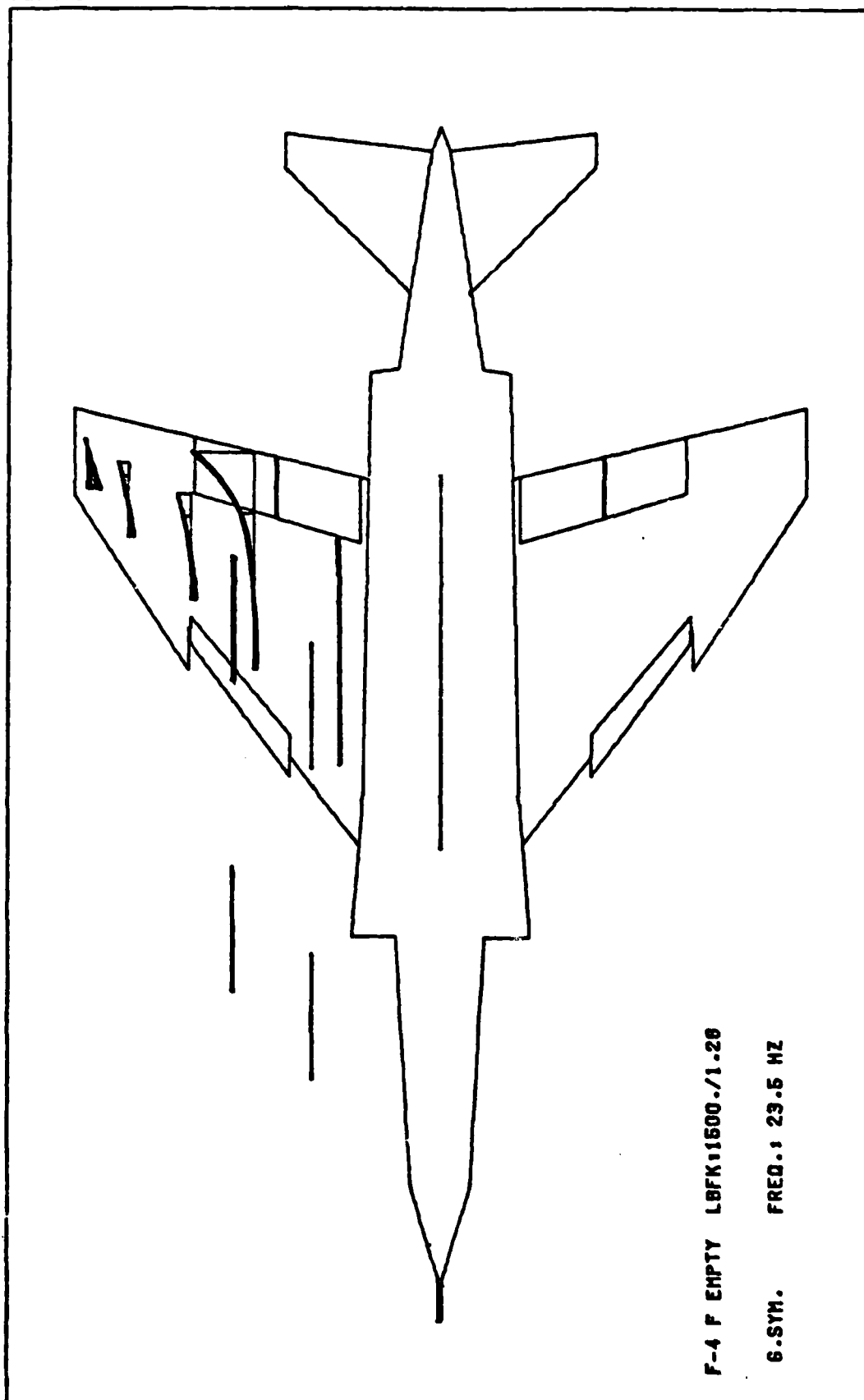


Figure 9. Wing Torsion with Aileron Mode

\triangle $m = 1190$ Kg
 ∇ $m = 1328$ Kg
 \circ $m = 1500$ Kg

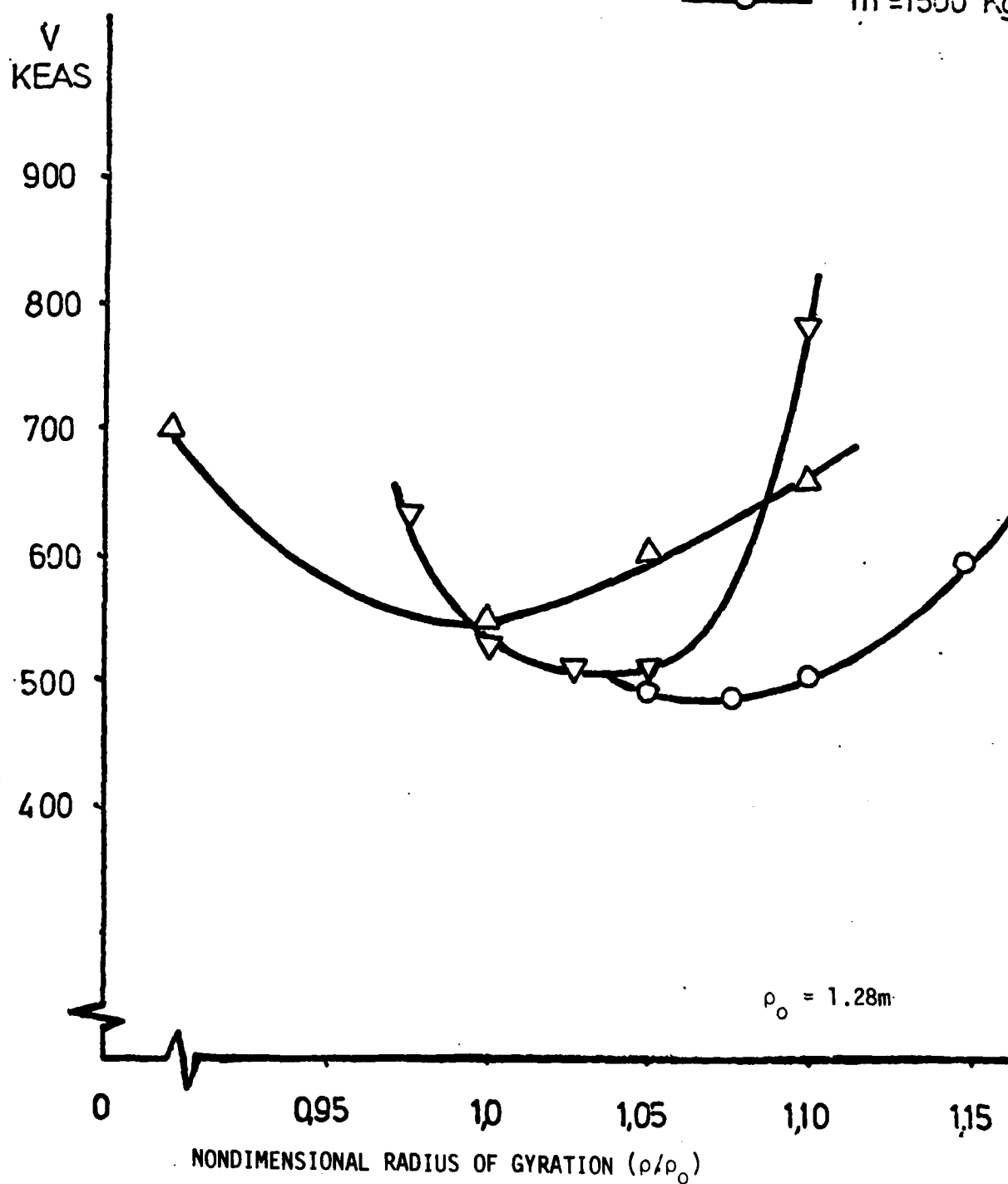


Figure 10. Flutter Speeds of Various Stores vs Store Radius of Gyration

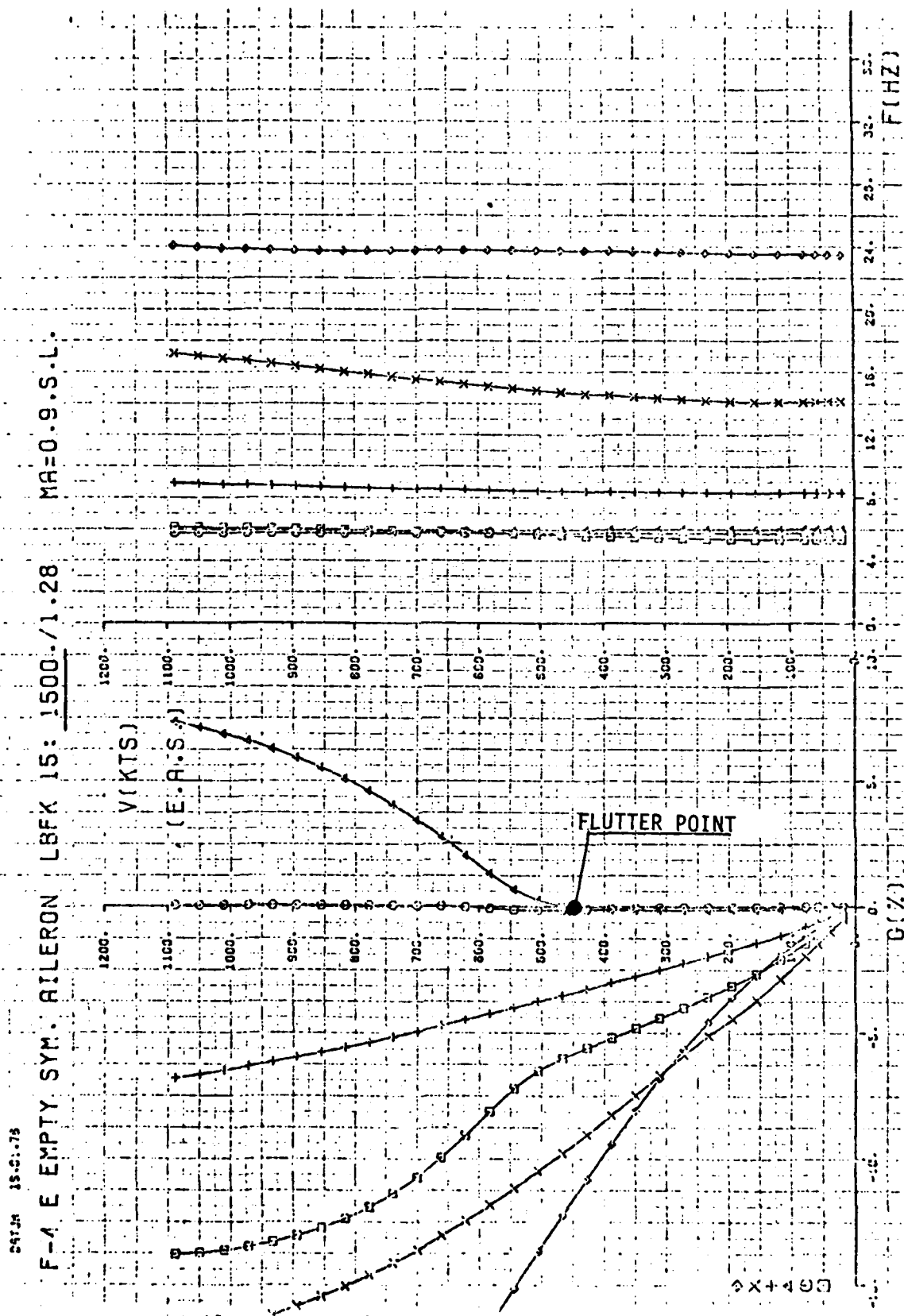


Figure 11. V-g Plot for Critical Store Configuration at $Ma = 0.9$ (Store Mass = 1500 kg)

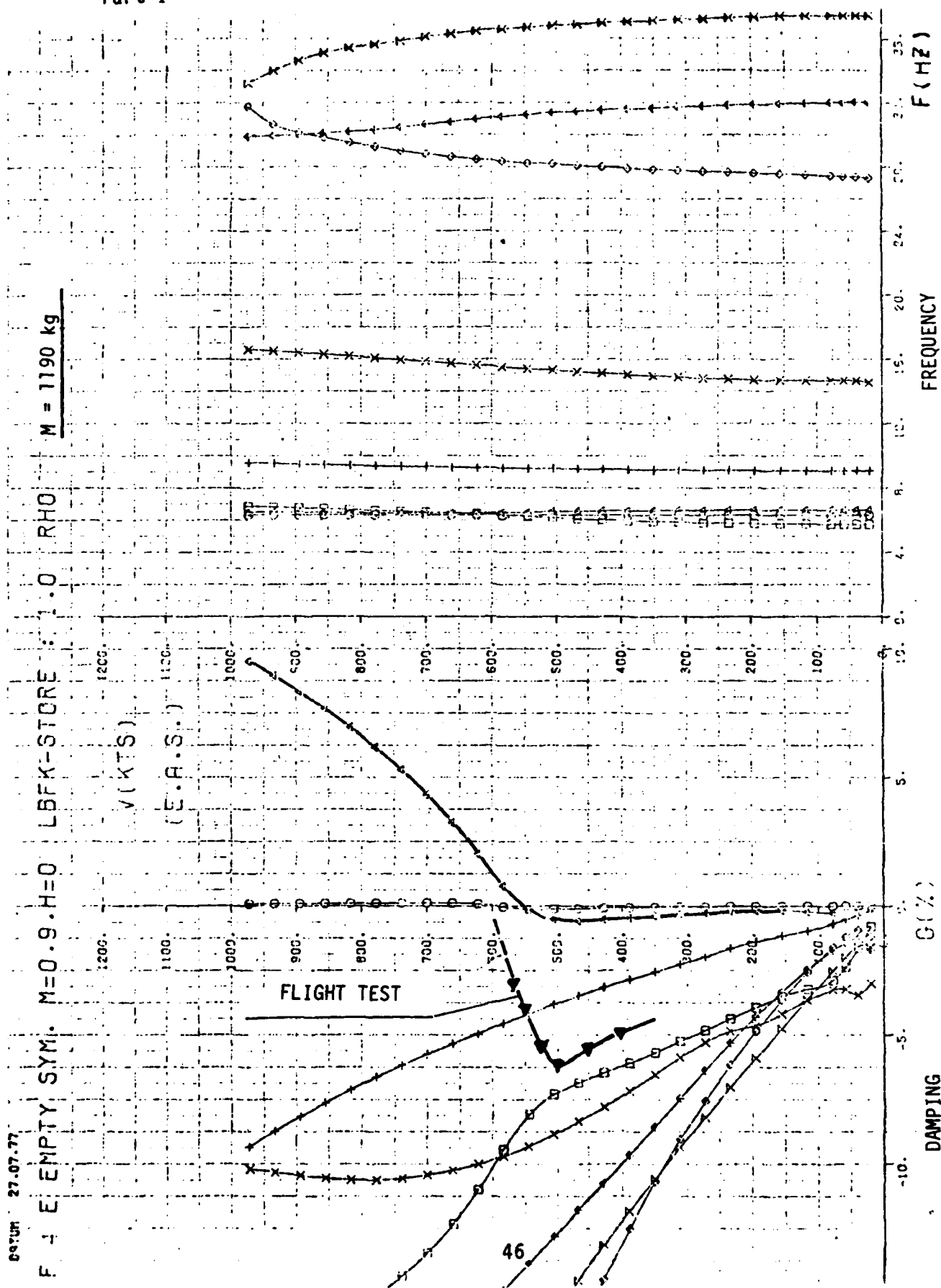


Figure 12. V-g Plot of F-4F with Store (Store Mass = 1190 kg)

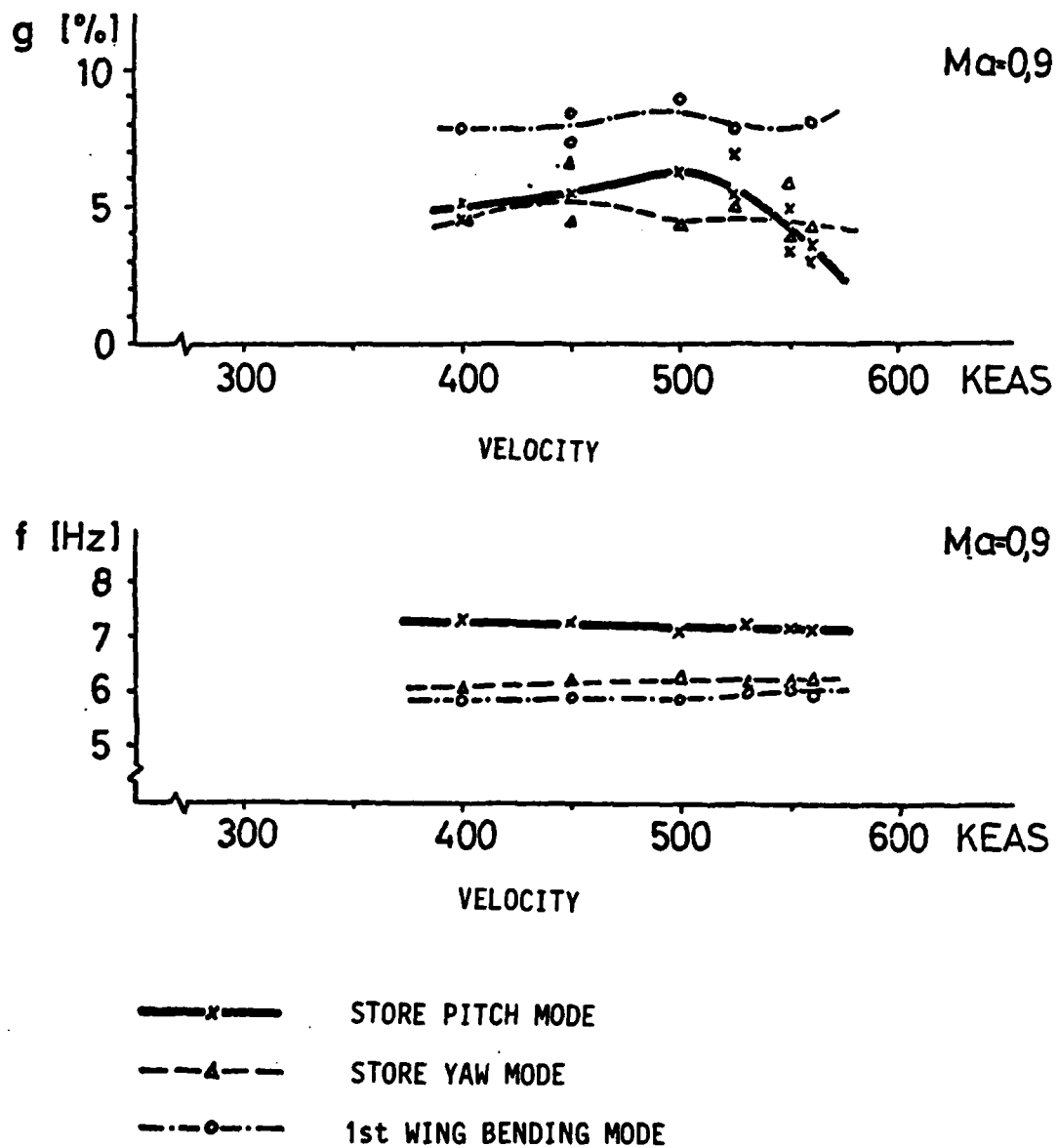


Figure 13. Measured Damping and Frequency Trends of the F-4F with Normal Store (Store Mass = 1190 kg)

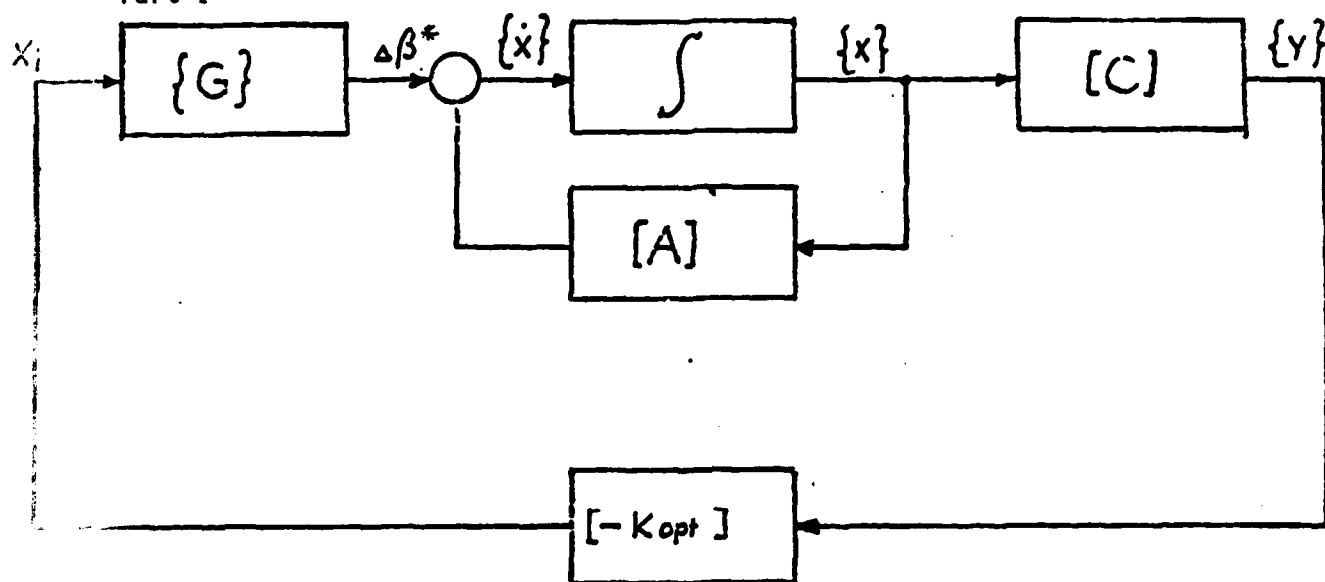


Figure 14a. Mathematical Model of the Flutter Suppression System

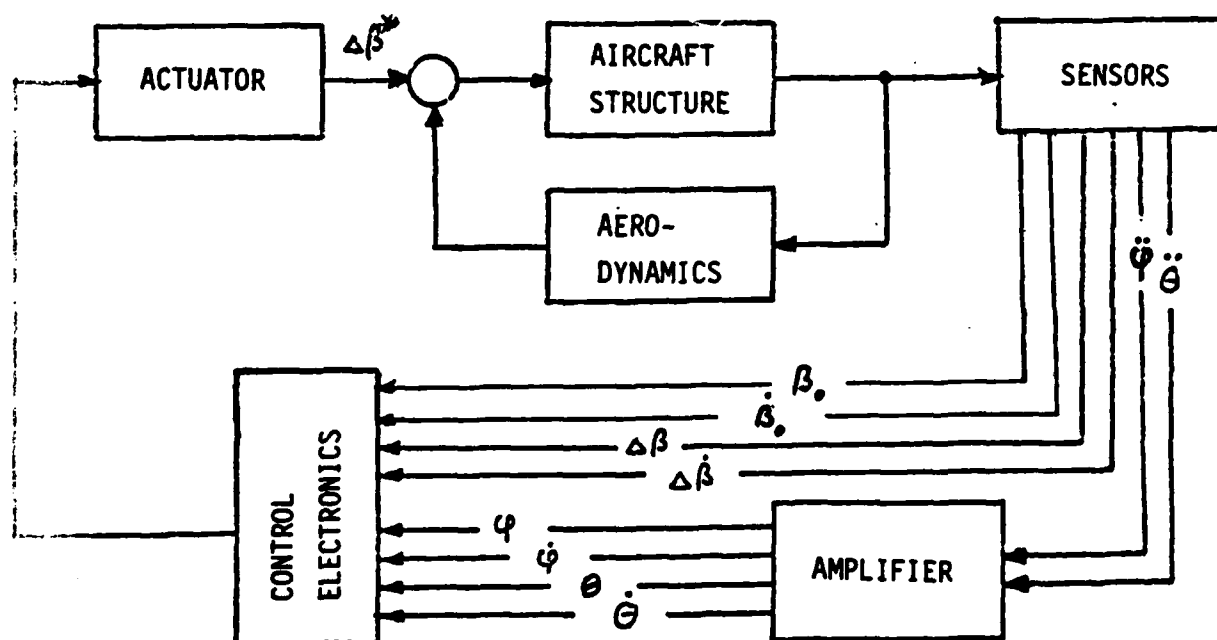


Figure 14b. Block Diagram of the Flutter Suppression System with Complete State-Vector Feedback

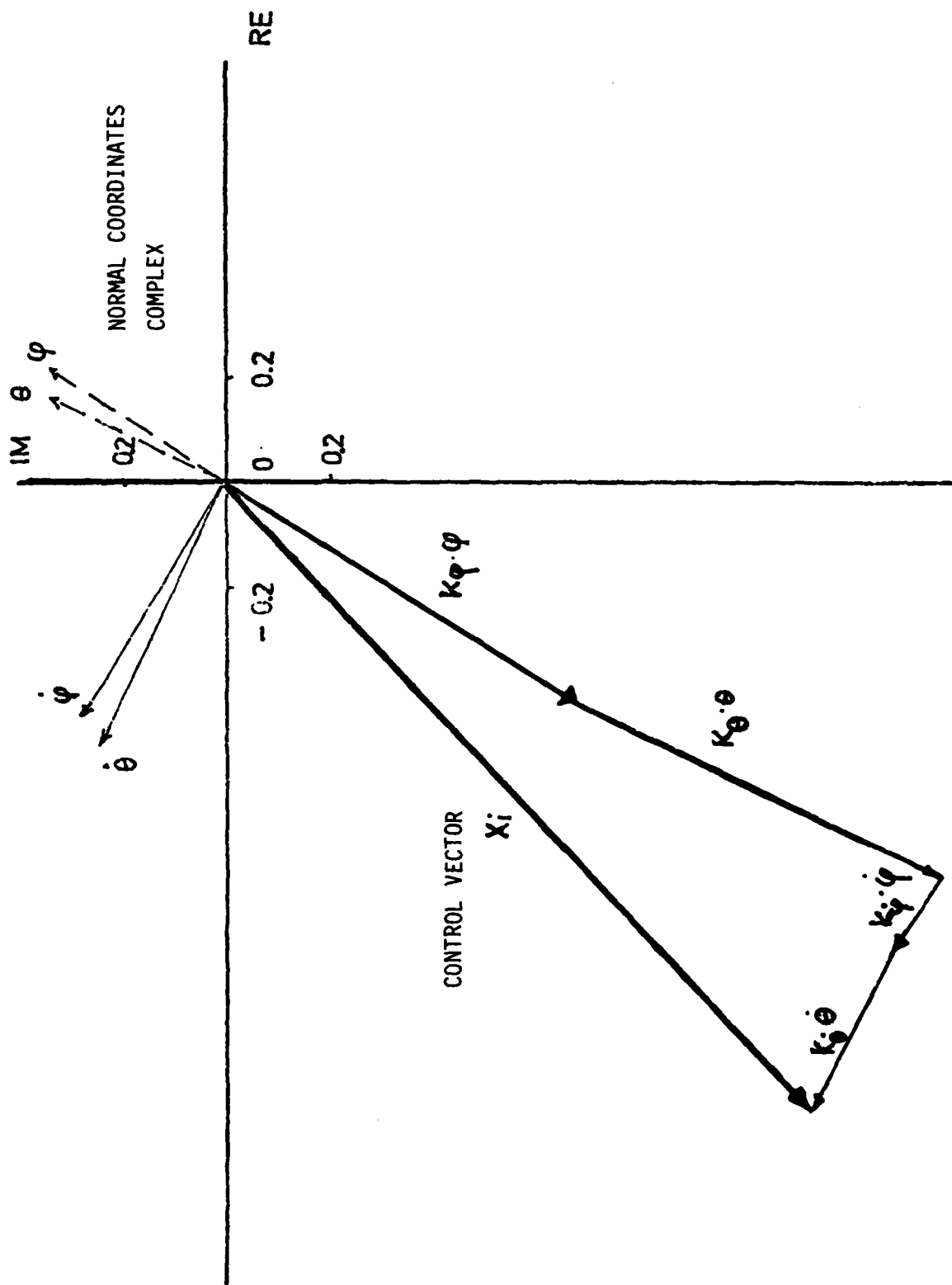
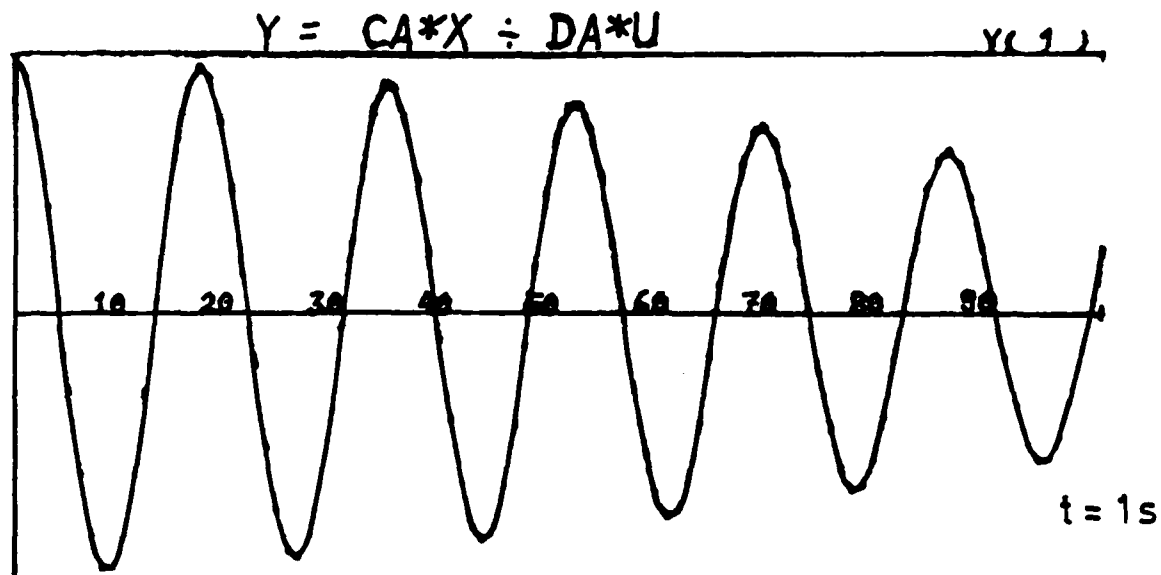
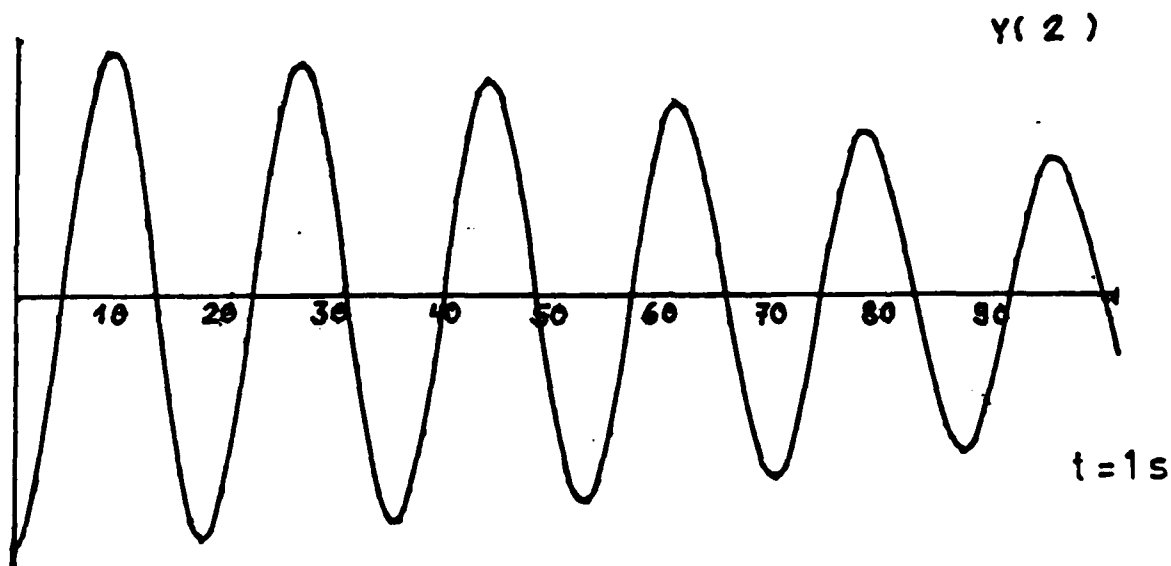


Figure 15a. Vector Diagram for Control Law I, Design Speed $V = 500$ kts,
($V_{\text{flutter}} = 465$ kts, without Structural Damping)

1st WING BENDING



STORE PITCH



EXCITATION DIRAC IMPULSE

Figure 15b. Response of the Aircraft with Flutter Suppression at
 $V = 500$ kts ($V_{Flutter} = 465$ kts, Control Law I)

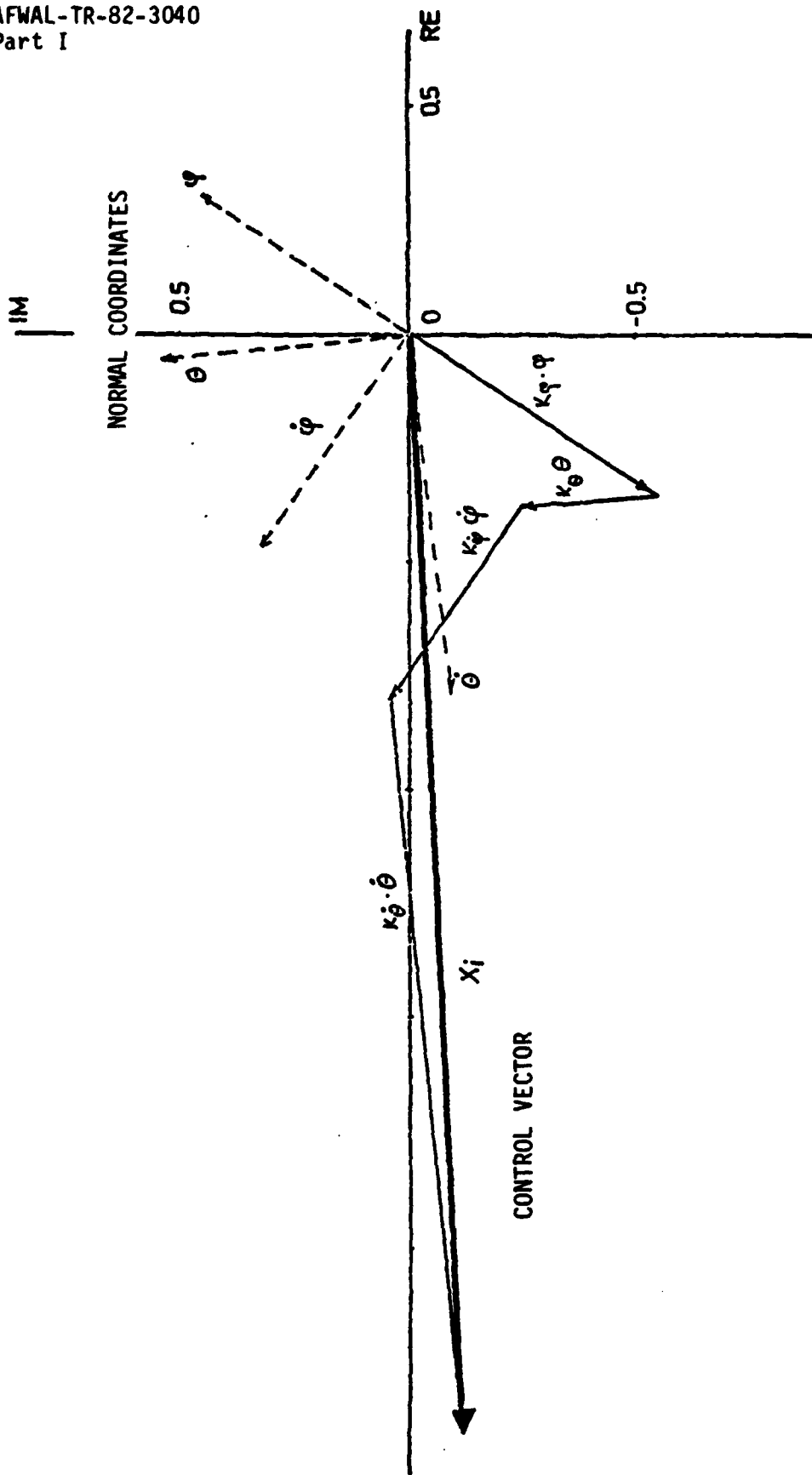


Figure 16. Vector Diagram for Control Law II, Design Speed $V = 600$ kts, ($V_{flutter} = 567$ kts with 1% Structural Damping)

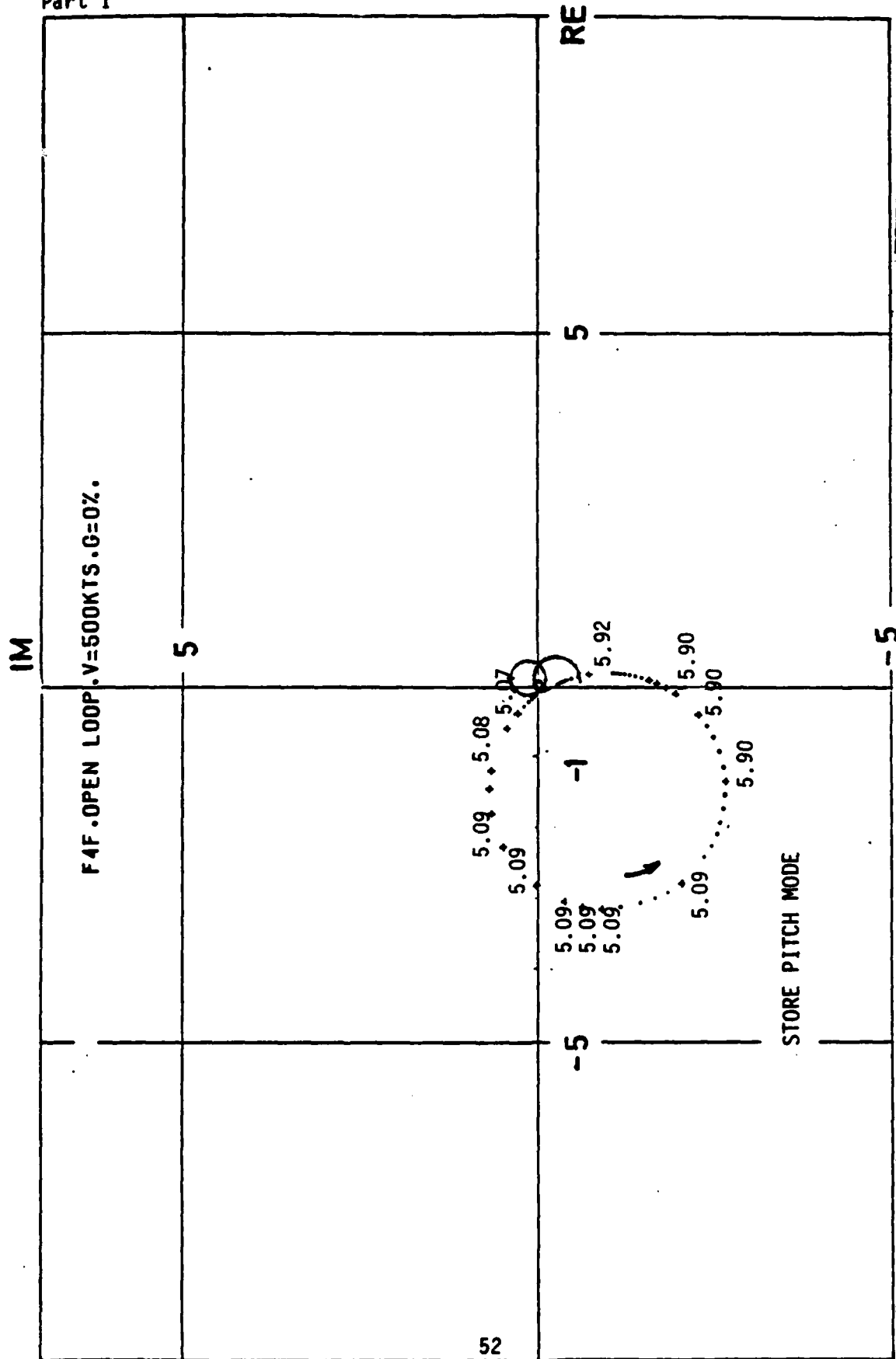


Figure 17a. Nyquist Diagram for Control Law I at V = 500 kts

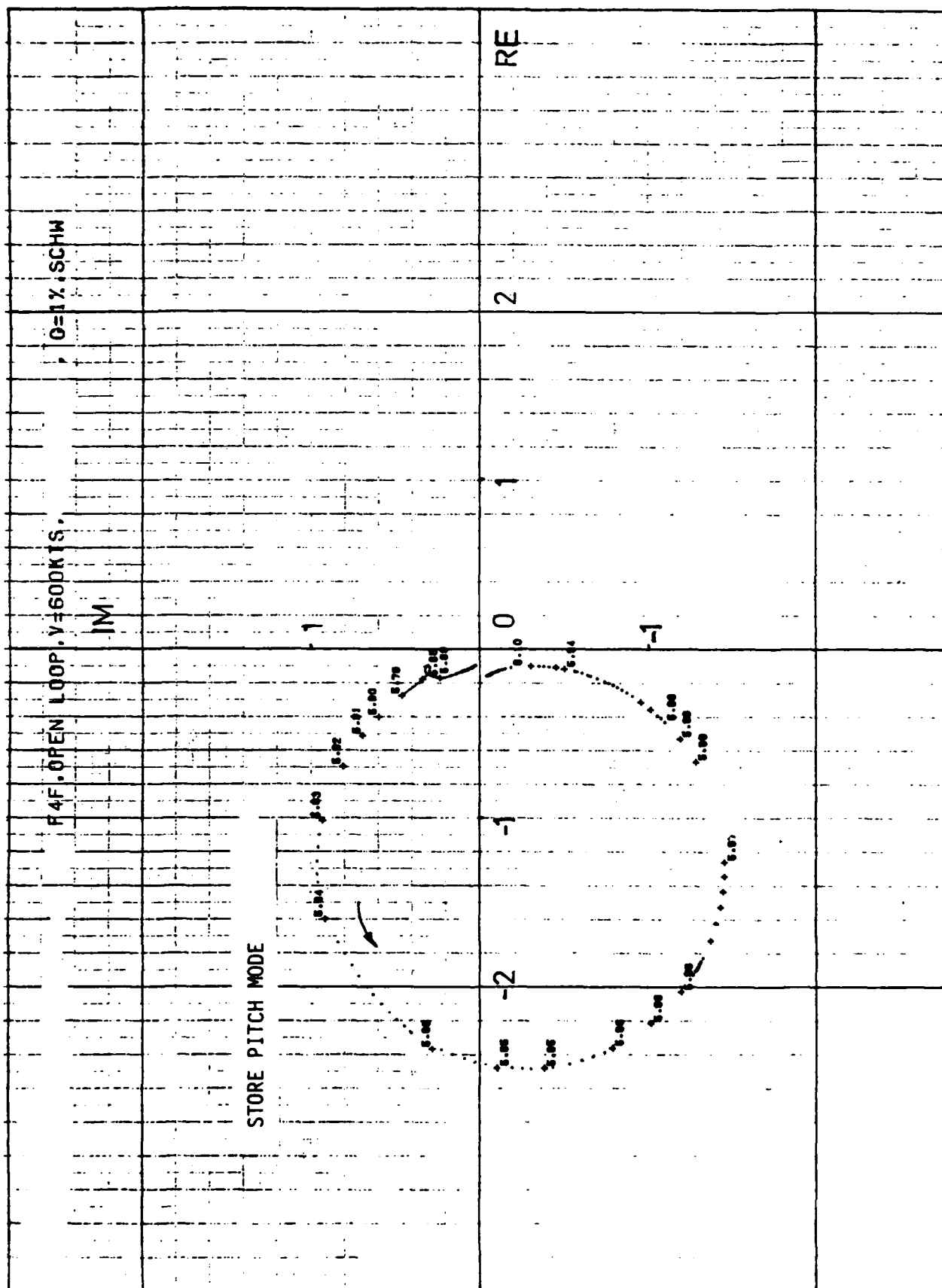


Figure 17b. Nyquist Diagram for Control Law II at $V = 600$ kts

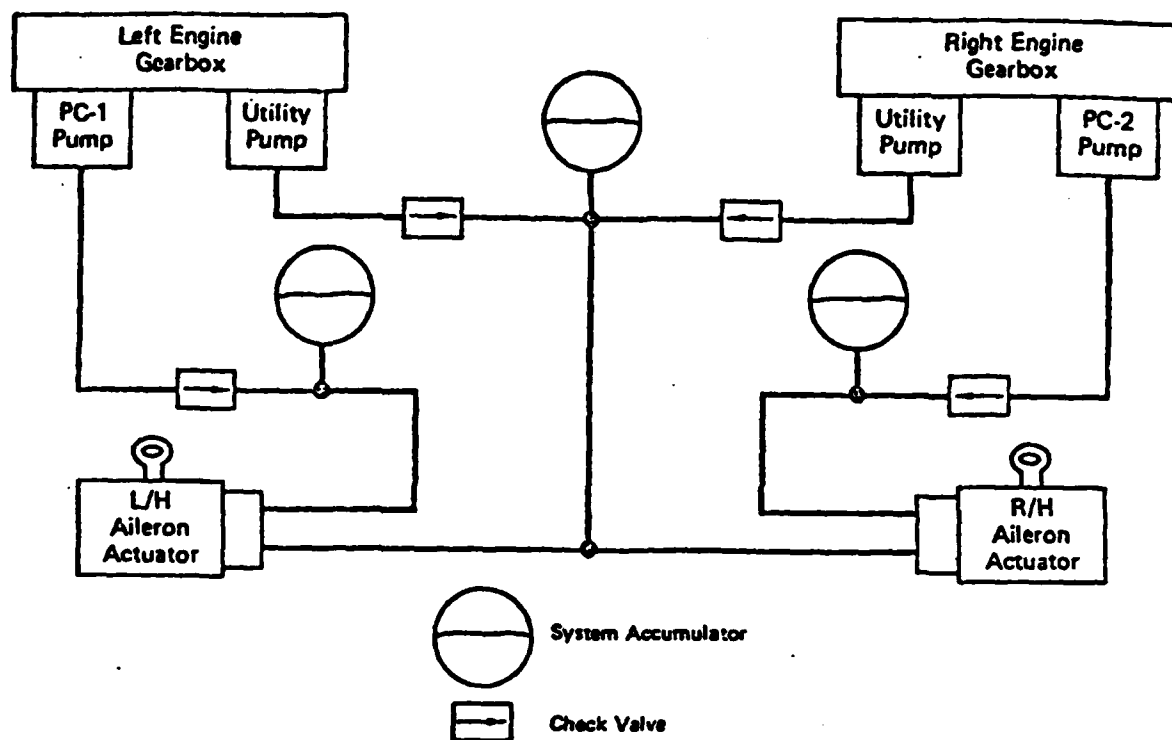


Figure 18a. Hydraulic System

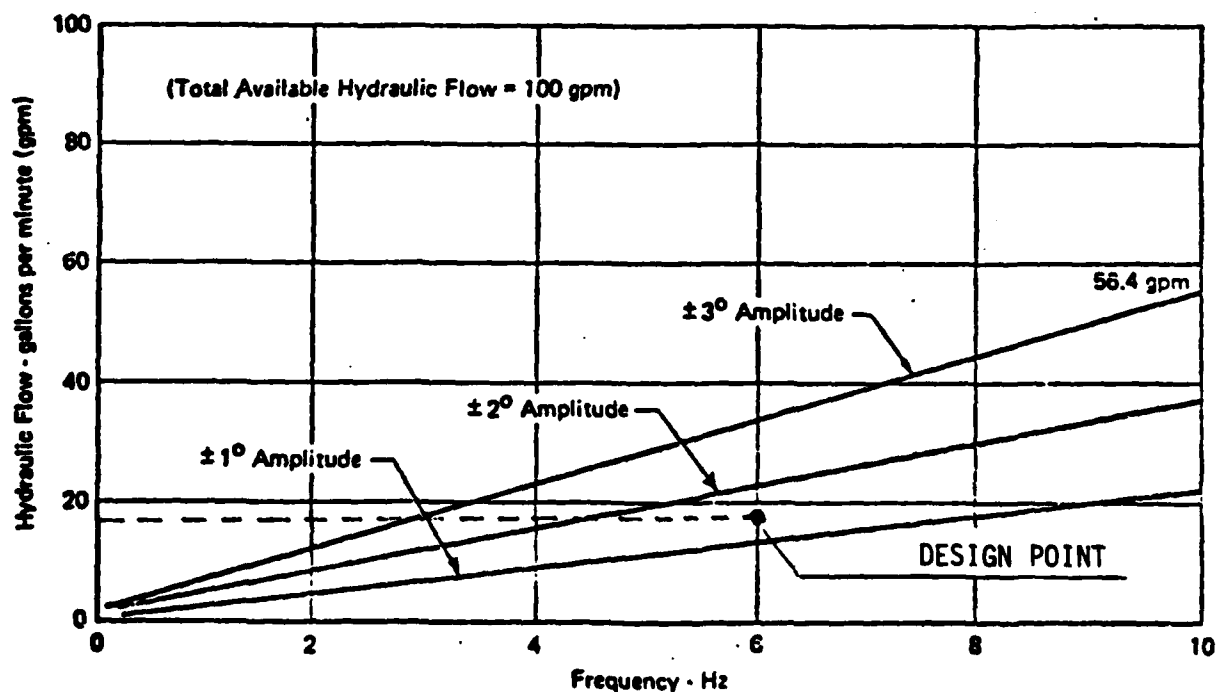


Figure 18b. Flow Rate Necessary for the Flutter Suppression System

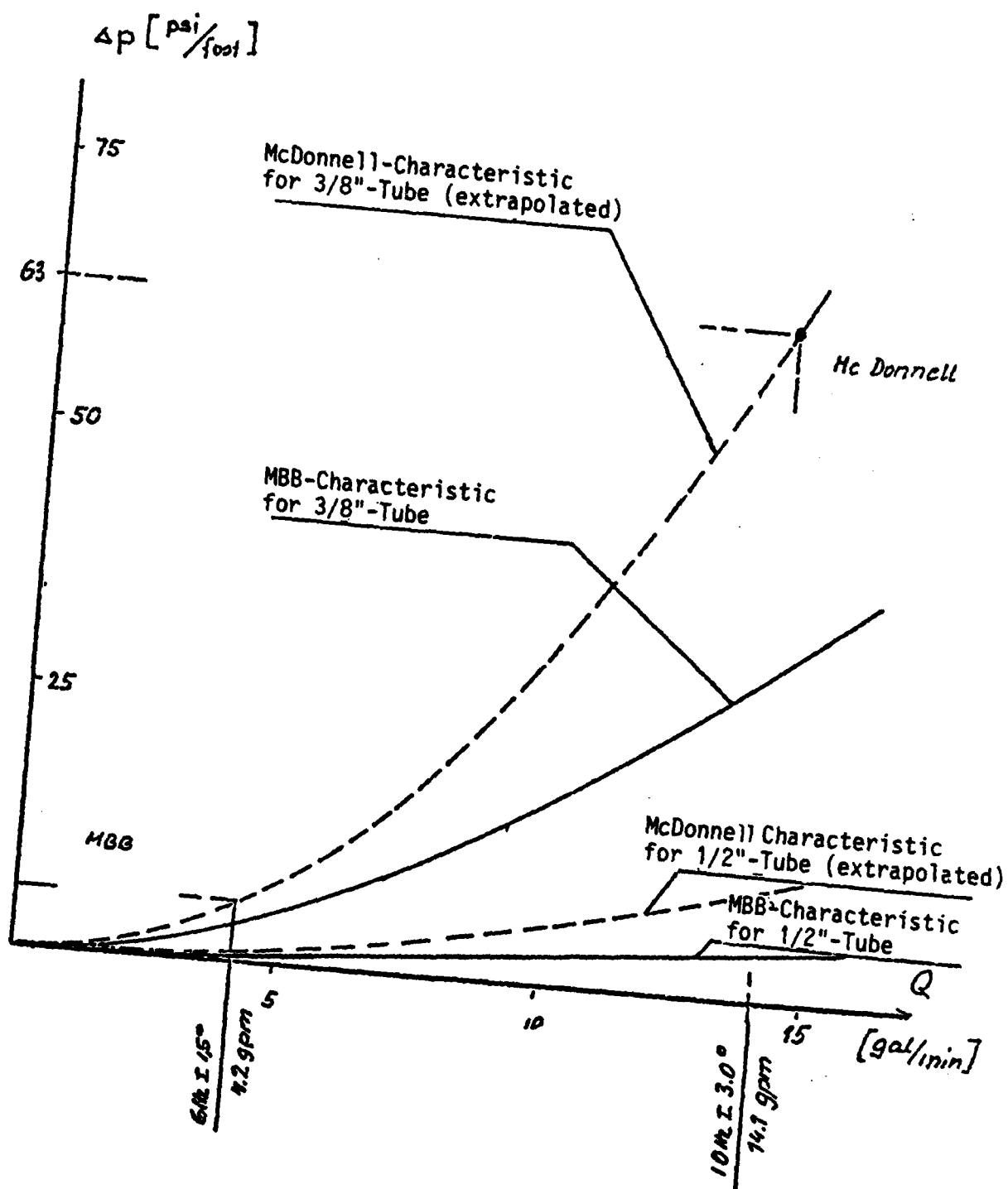


Figure 19. Pressure Decrease in the Tubes vs Flow Rate

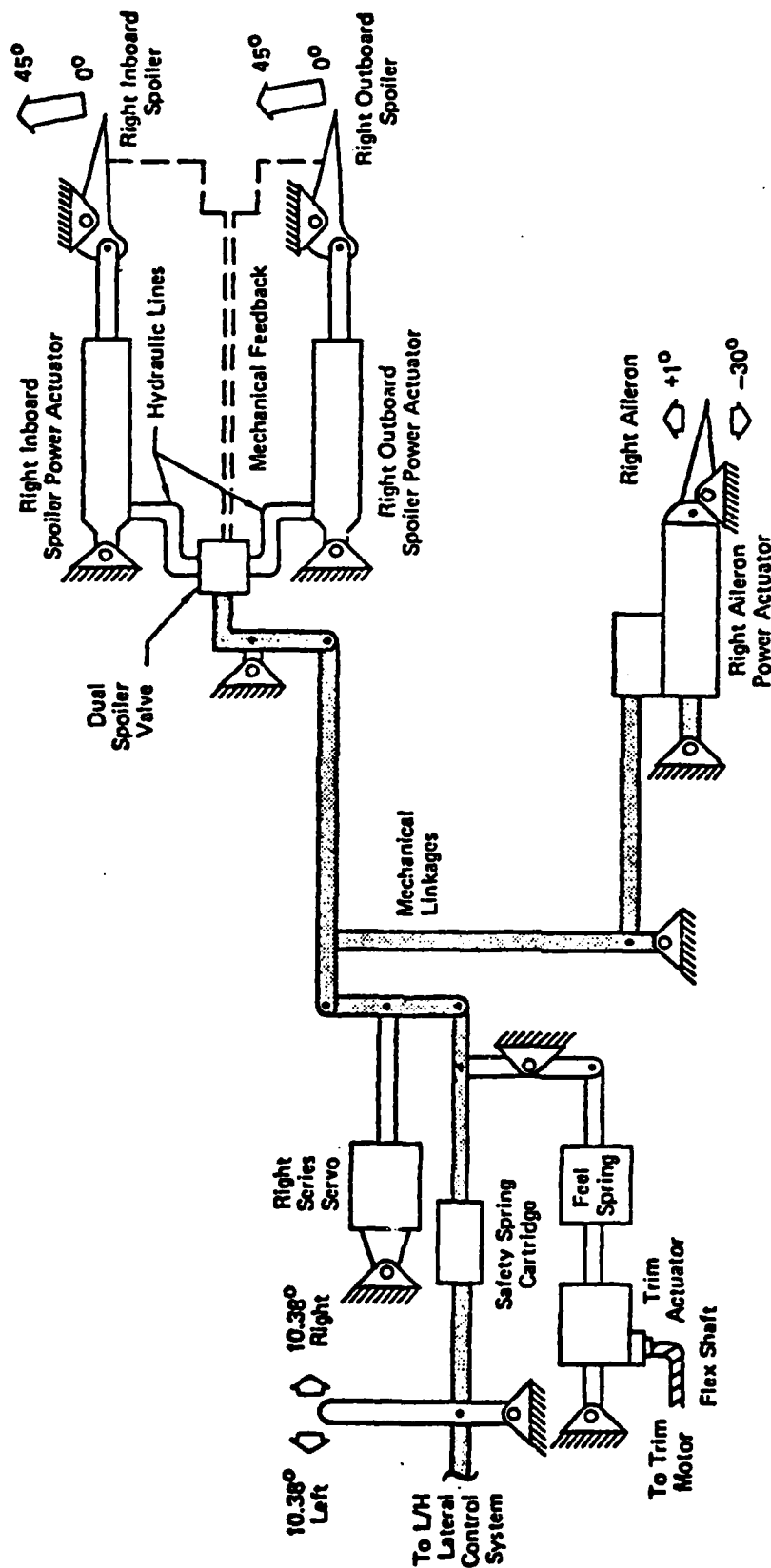


Figure 20. Scheme of the F-4F Roll Channel

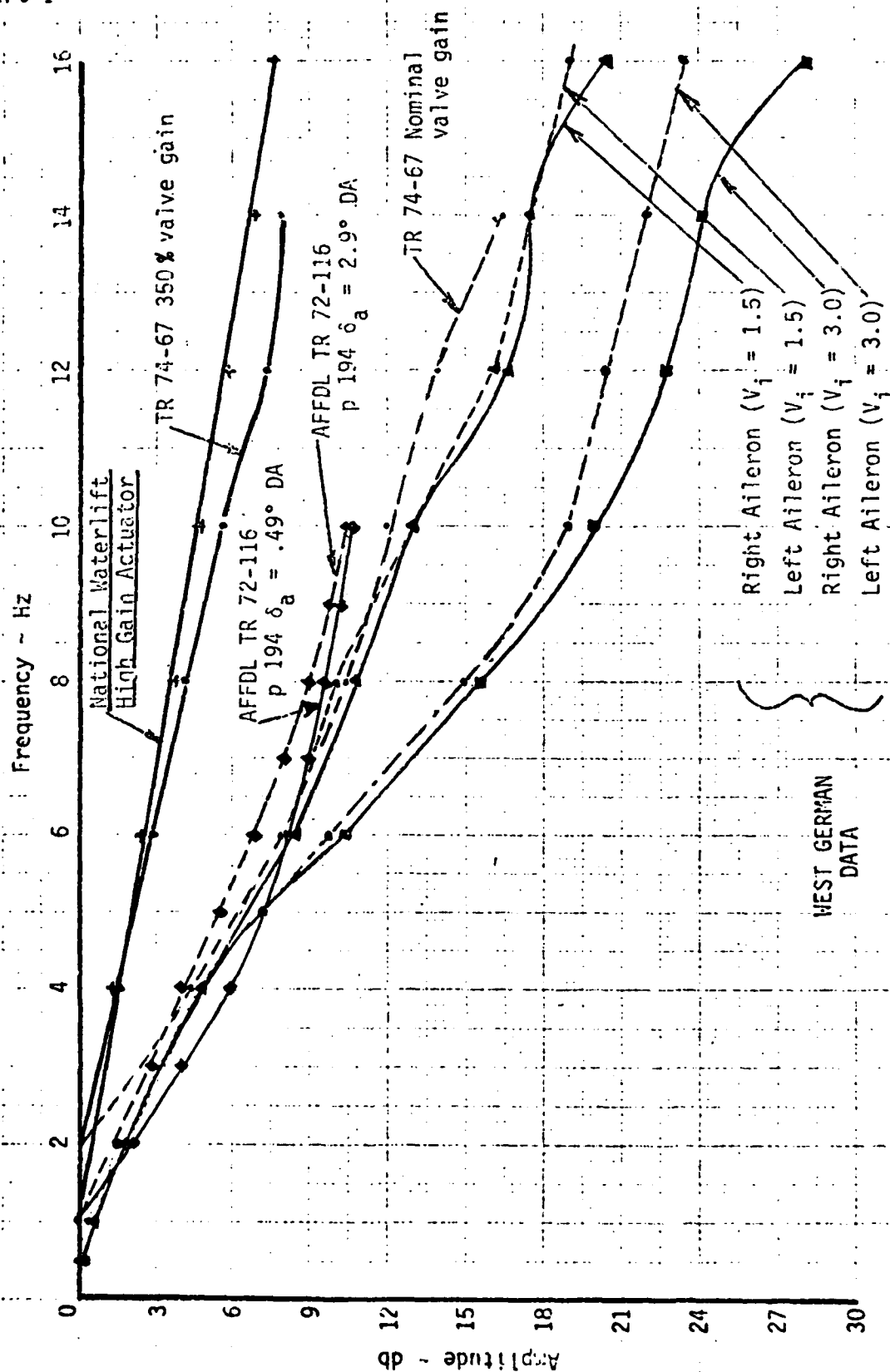


Figure 21. Transfer Function (Amplitude) of the Standard Power Actuator Compared with the NW High Gain Actuator

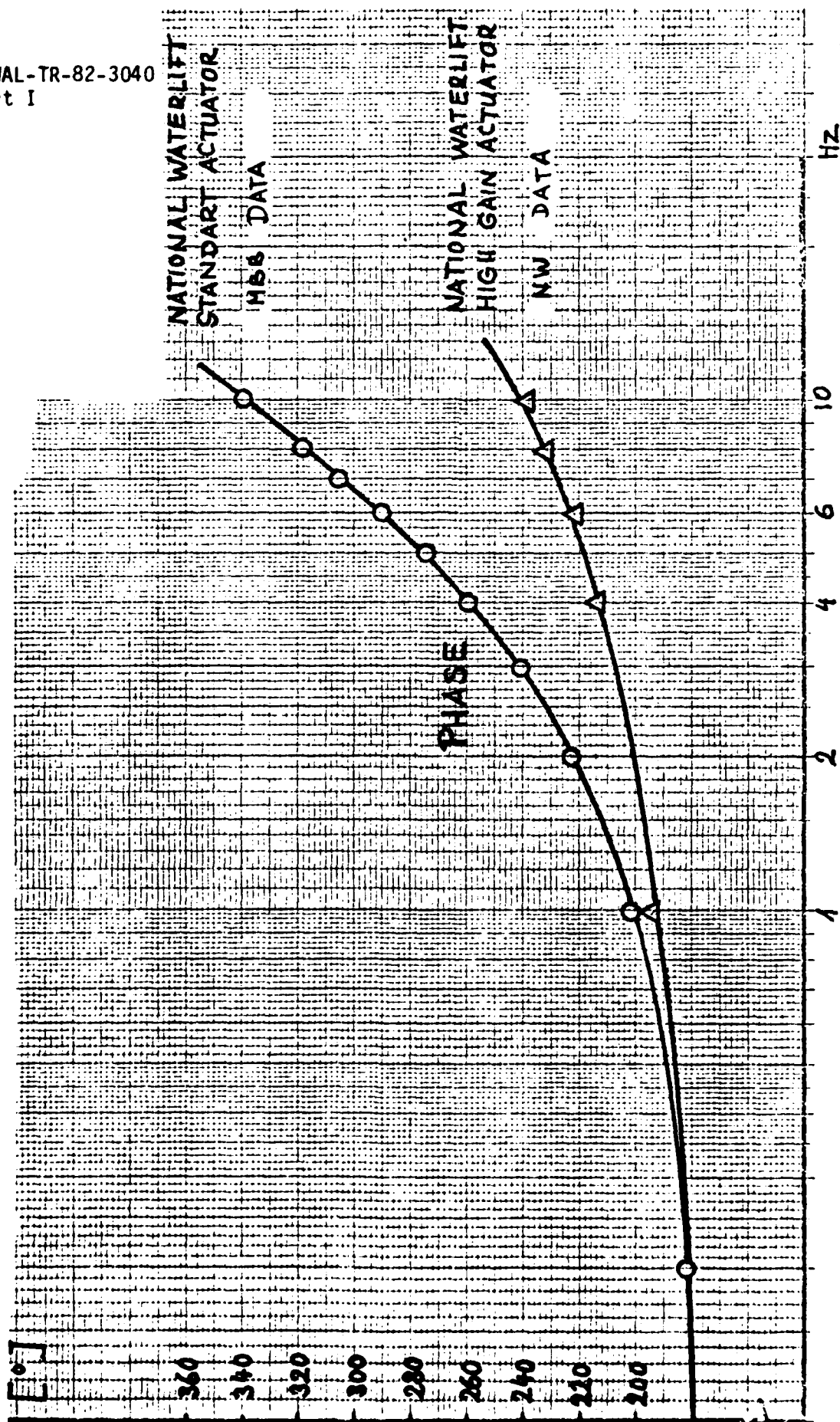


Figure 22. Comparison of the Phases of NW Standard and NW High Gain Actuator

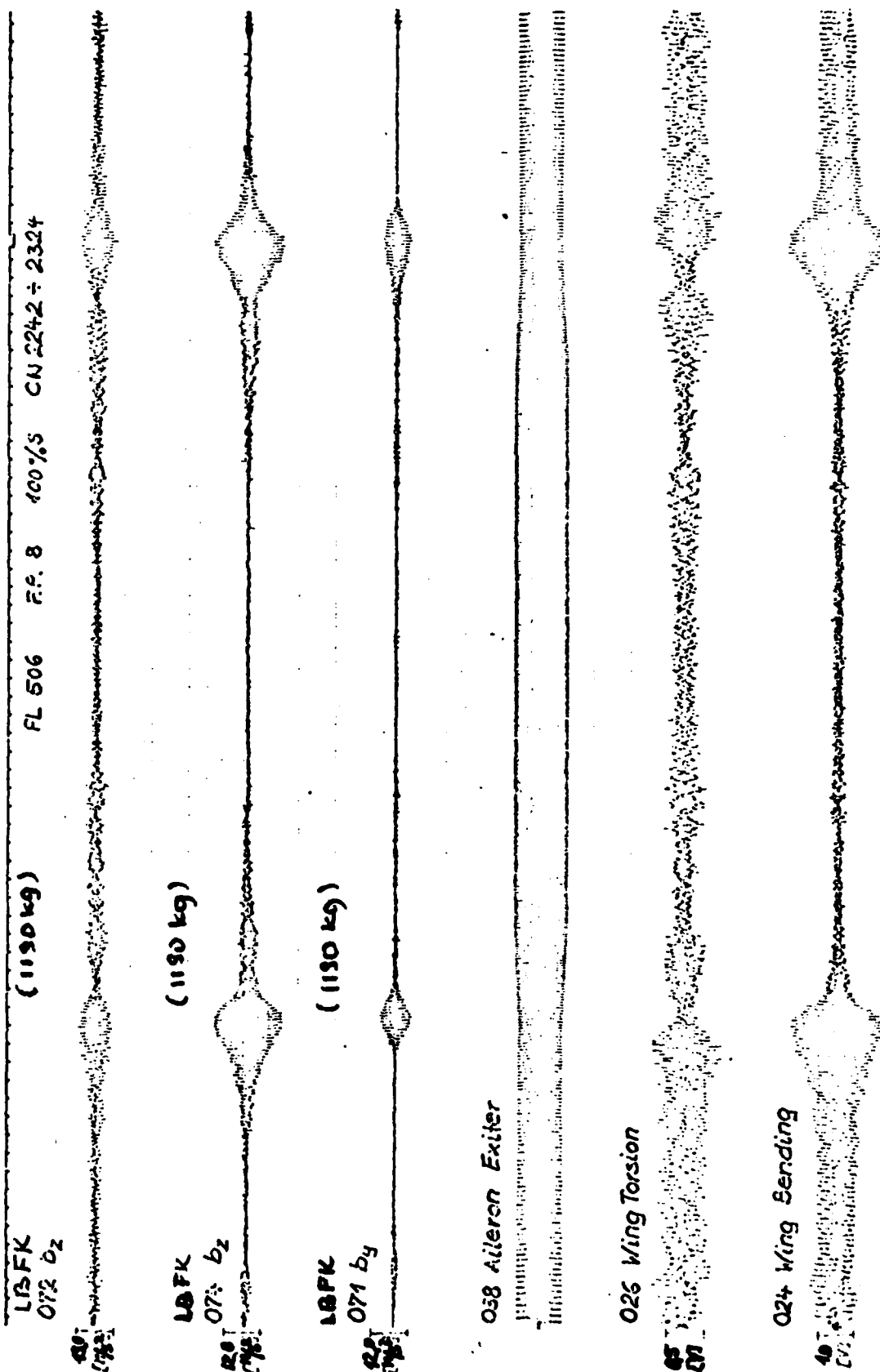


Figure 23. F-4F with Normal Store (1190 kg), In-Flight Measured Accelerations and Deformations due to Aileron Excitation

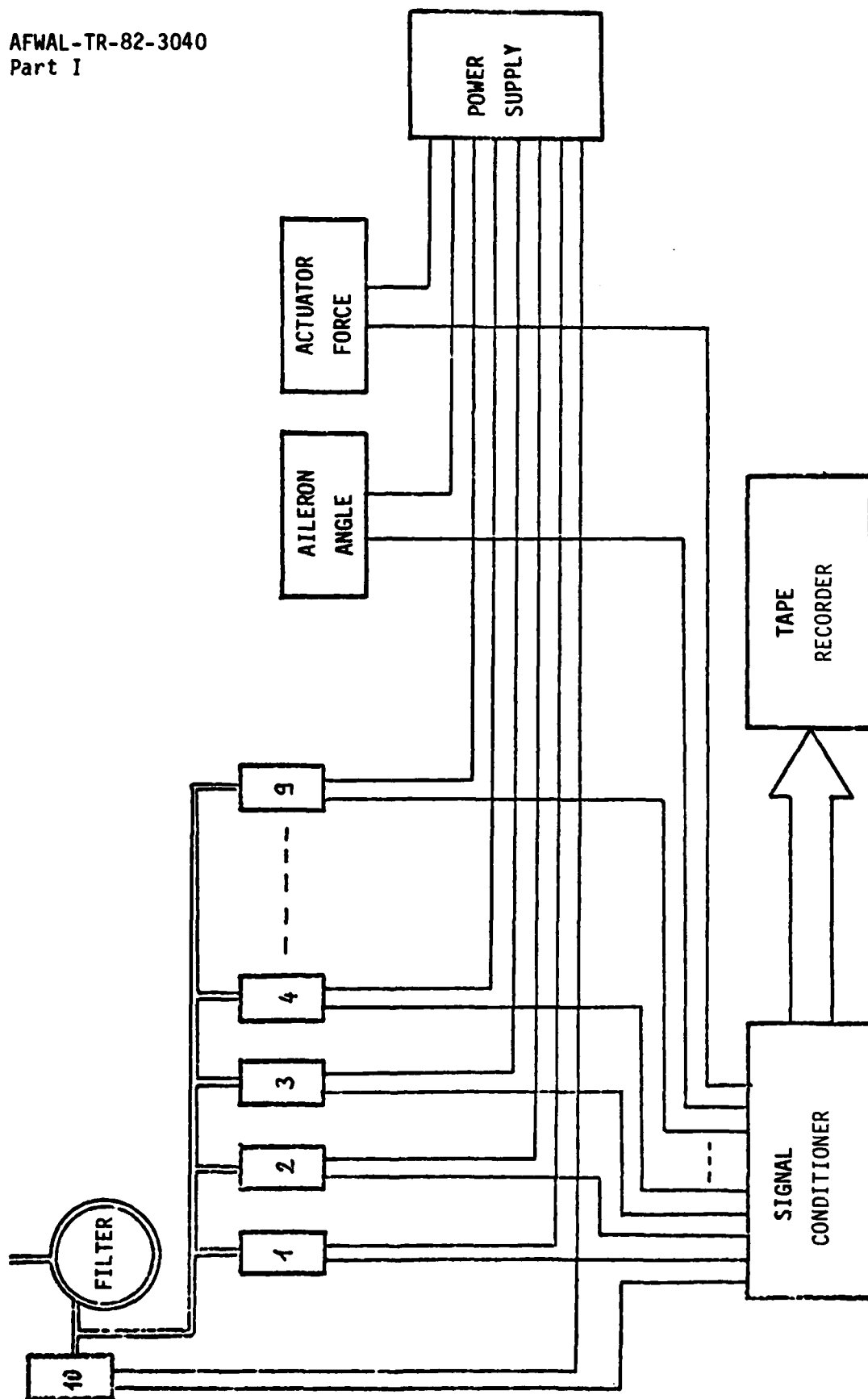


Figure 25. Block Diagram of the System to Measure the Unsteady Pressure Distribution on the Aileron

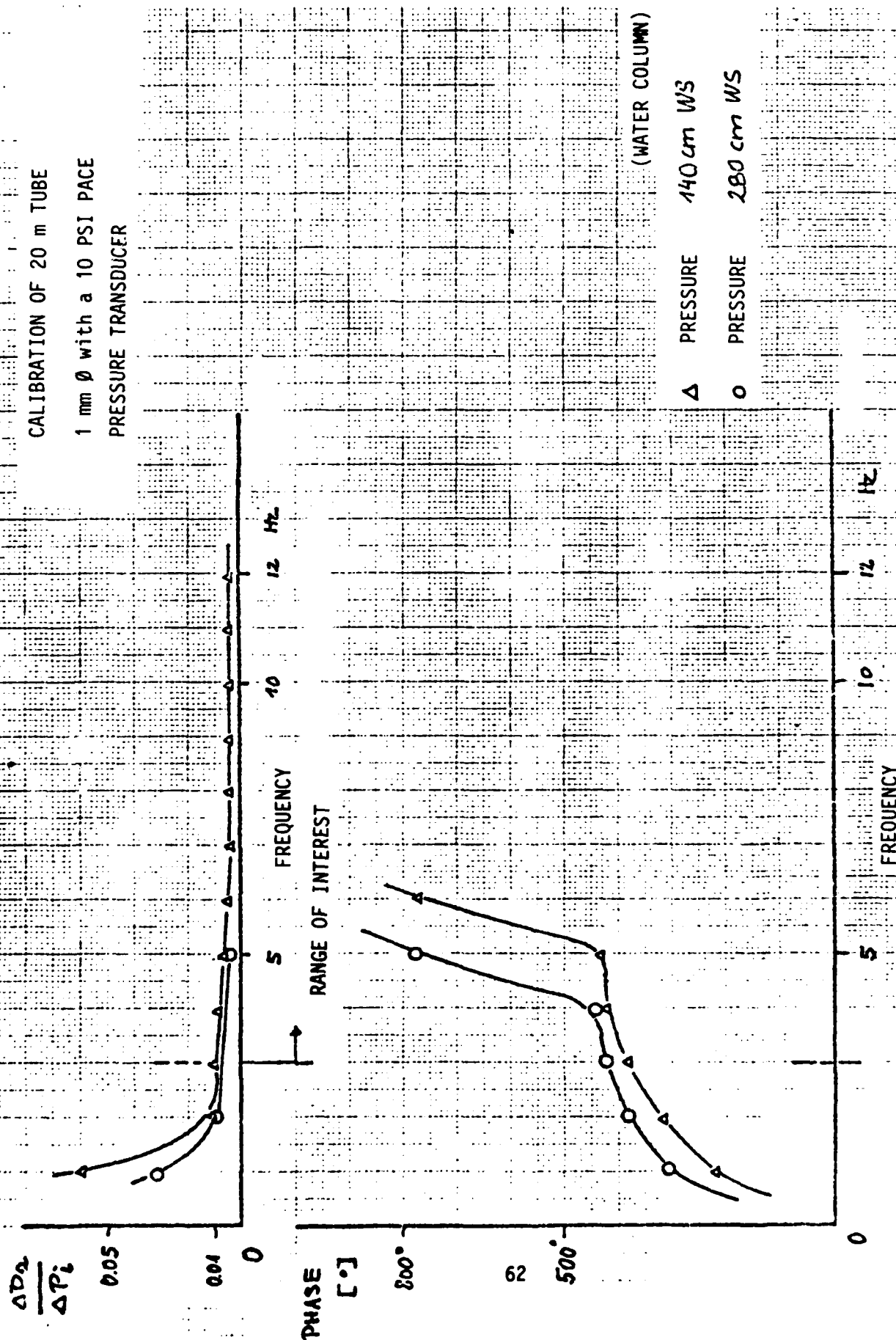


Figure 26. Calibration of the Filter Used for the Measurement of the
Steady Reference Pressure



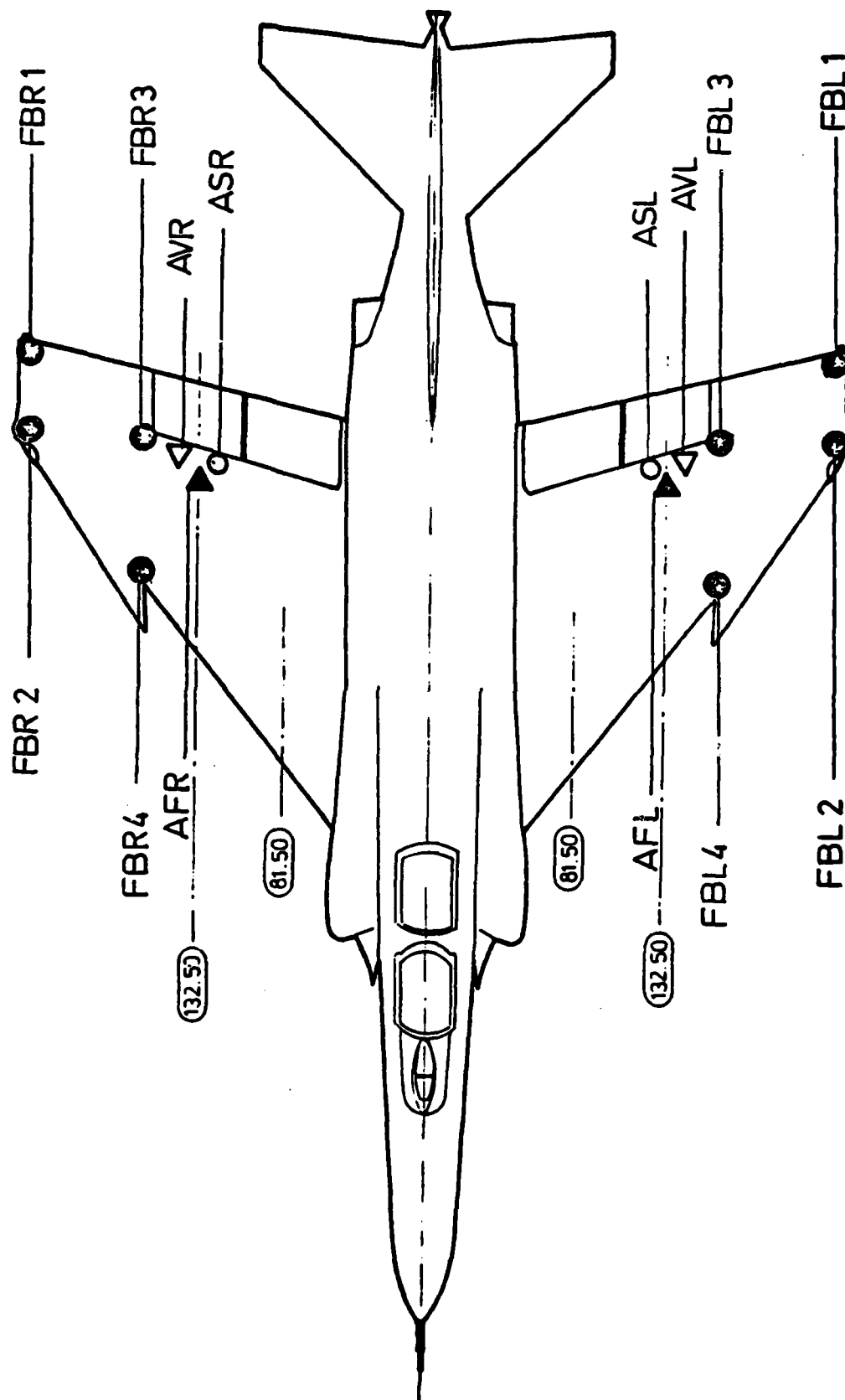
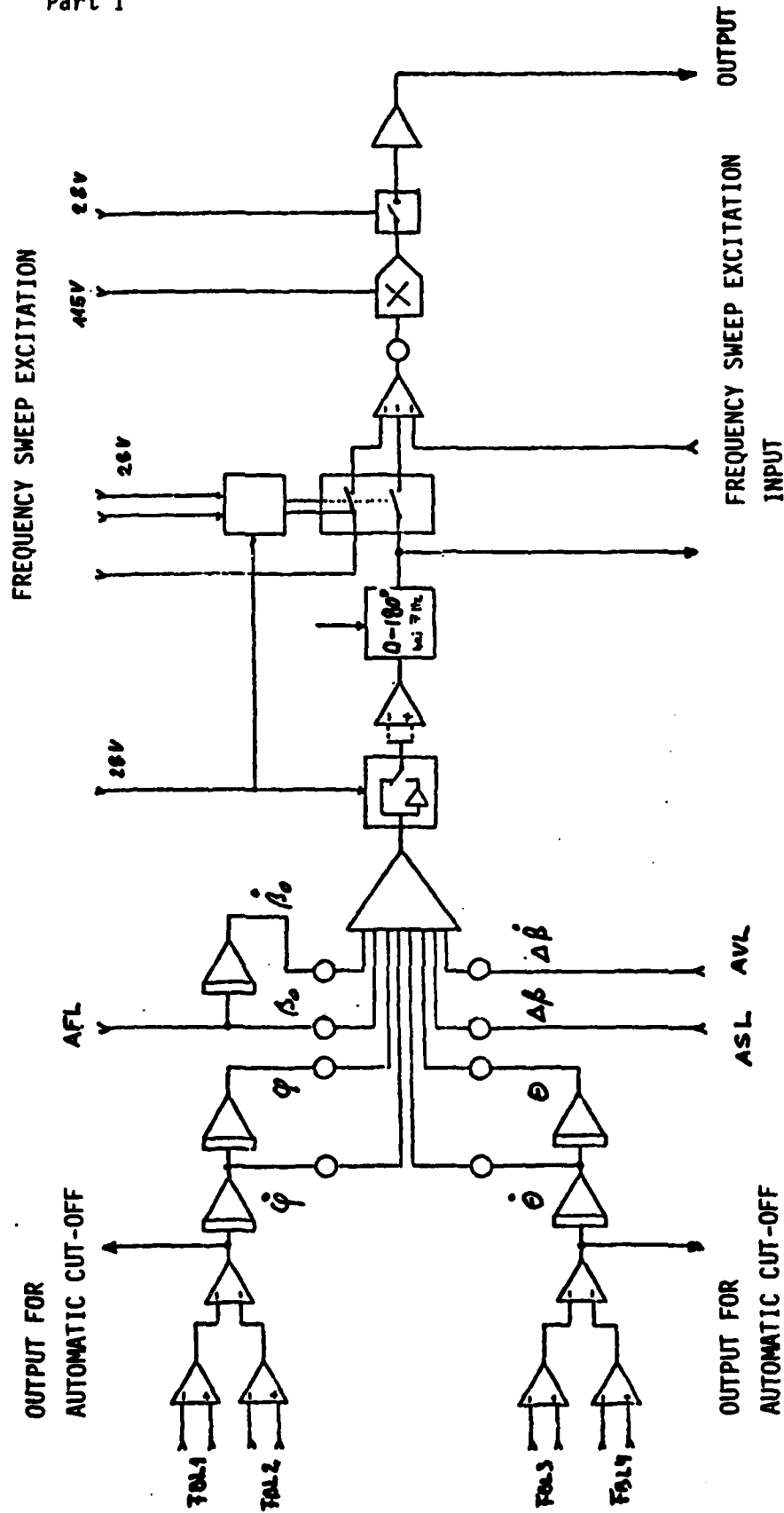


Figure 28. Position of the Sensors Installed for the Flutter Suppression System



POSITION OF SENSORS SEE FIGURE 28

Figure 29. Block Diagram of the Control Electronics for One Wing

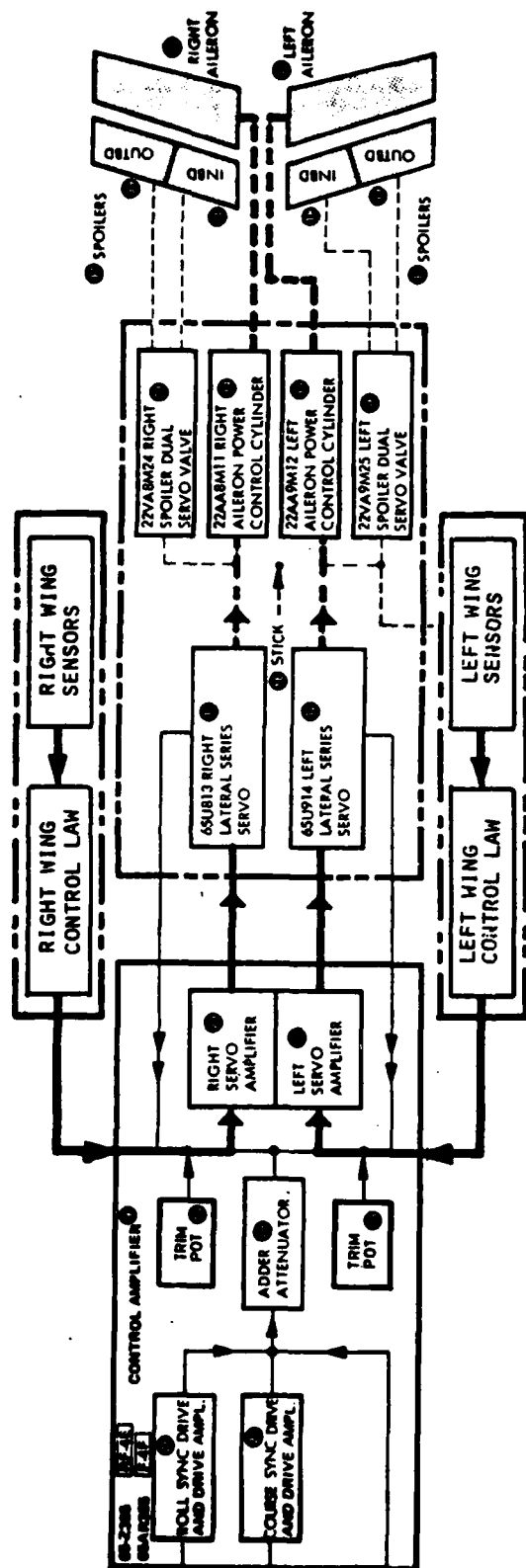


Figure 30. Integration of the Flutter Suppression System into the AFCS

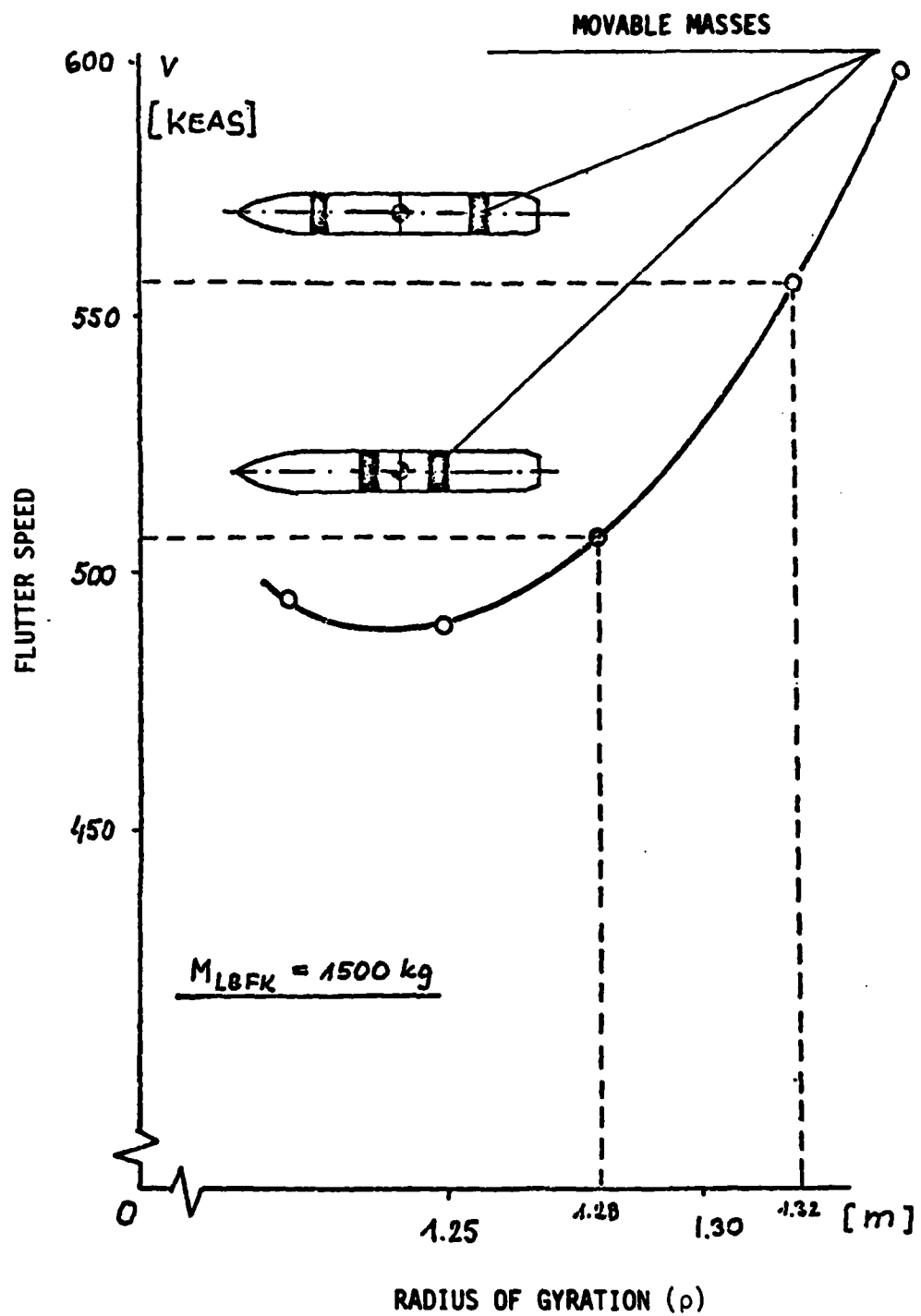
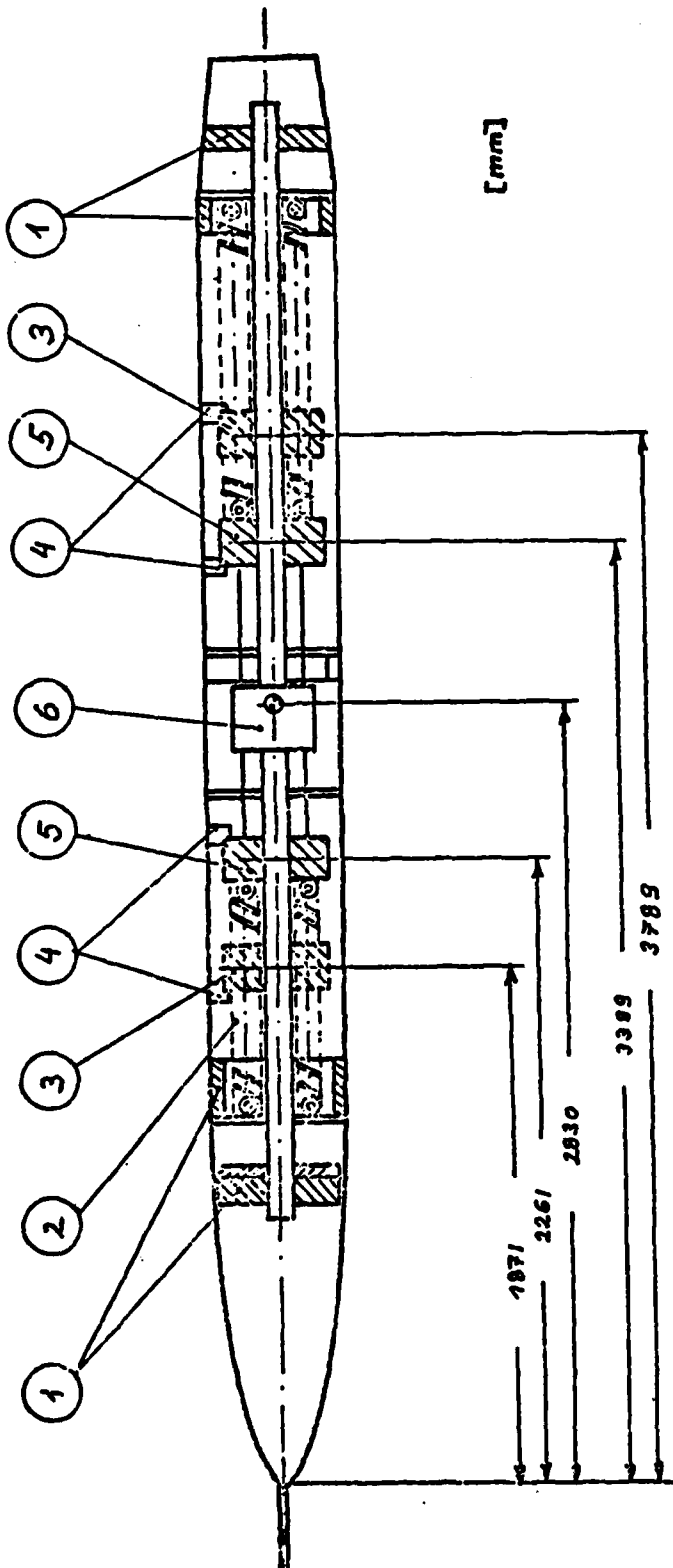


Figure 31. Efficiency of the Flutter Stopper



1. Fixed Trimm Weights
2. Springs for movable Trimm Weights
3. "Safe" Position of the movable Trimm Weights
4. Extreme Positions of the Trimm Weights
5. "Critical" Position of the movable Trimm Weights
6. System to move the Trimm Weights for preloading the Springs and electrical Release Unit

Figure 32. Sketch of the Flutter Stopper

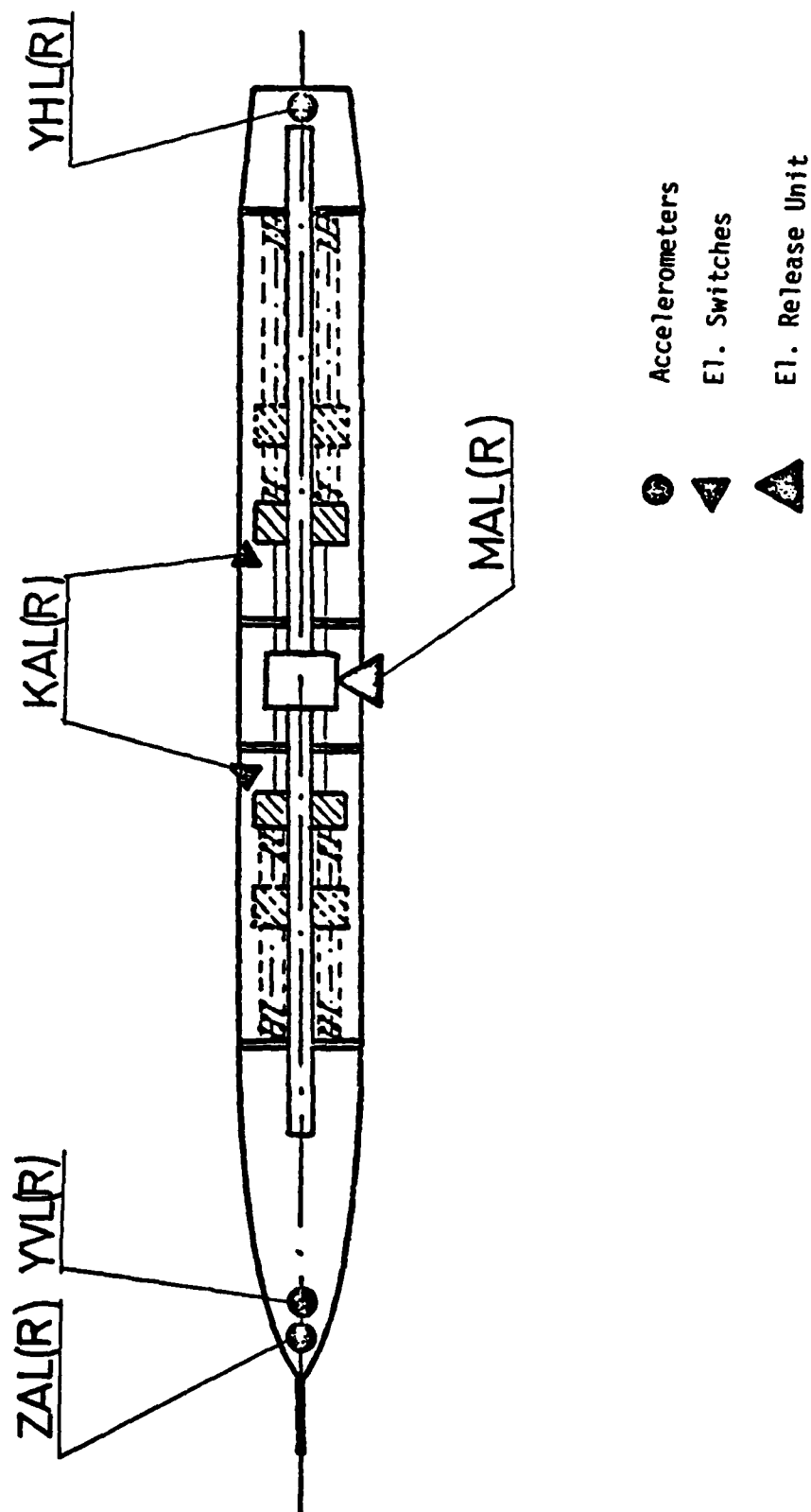


Figure 33. Sensor Installation in the Flutter Stopper

NO.	TEST PROGRAM		CUT OFF MODE			R/H CONTR. SYST.				L/H CONTR. SYST.			
	FUNCTION		TRIG OFF	AUTO OFF	EM. OFF	PROGR. OP.	SWEEP OFF	OPEN LOOP	CONTR. SYST. OFF	PROGR. OP.	SWEEP OFF	OPEN LOOP	CONTR. SYST. OFF
	R/H WING	L/H WING											
1	OPEN LOOP + FREQU. SWEEP	OPEN LOOP + FREQU. SWEEP	X	X			X	X	X		X	X	X
2	FREQU. SWEEP	DAMPING	X	X	X		X		X	X			X
3	DAMPING	FREQU. SWEEP	X	X	X	X			X		X		X
4	AUTOMATIC EXCITATION	AUTOMATIC EXCITATION	X	X	X			X	X			X	X
5	DAMPING	AUTOMATIC EXCITATION	X	X	X	X			X			X	X
6	AUTOMATIC EXCITATION	DAMPING	X	X	X			X	X	X			X
7	CLOSED LOOP + FREQU. SWEEP	CLOSED LOOP + FREQU. SWEEP	X	X	X	X	X		X	X	X		X
8	DAMPING	DAMPING		X	X				X				X

Figure 34. F-4F Flutter Suppression System, Switch-Off Modes of the Test Programs

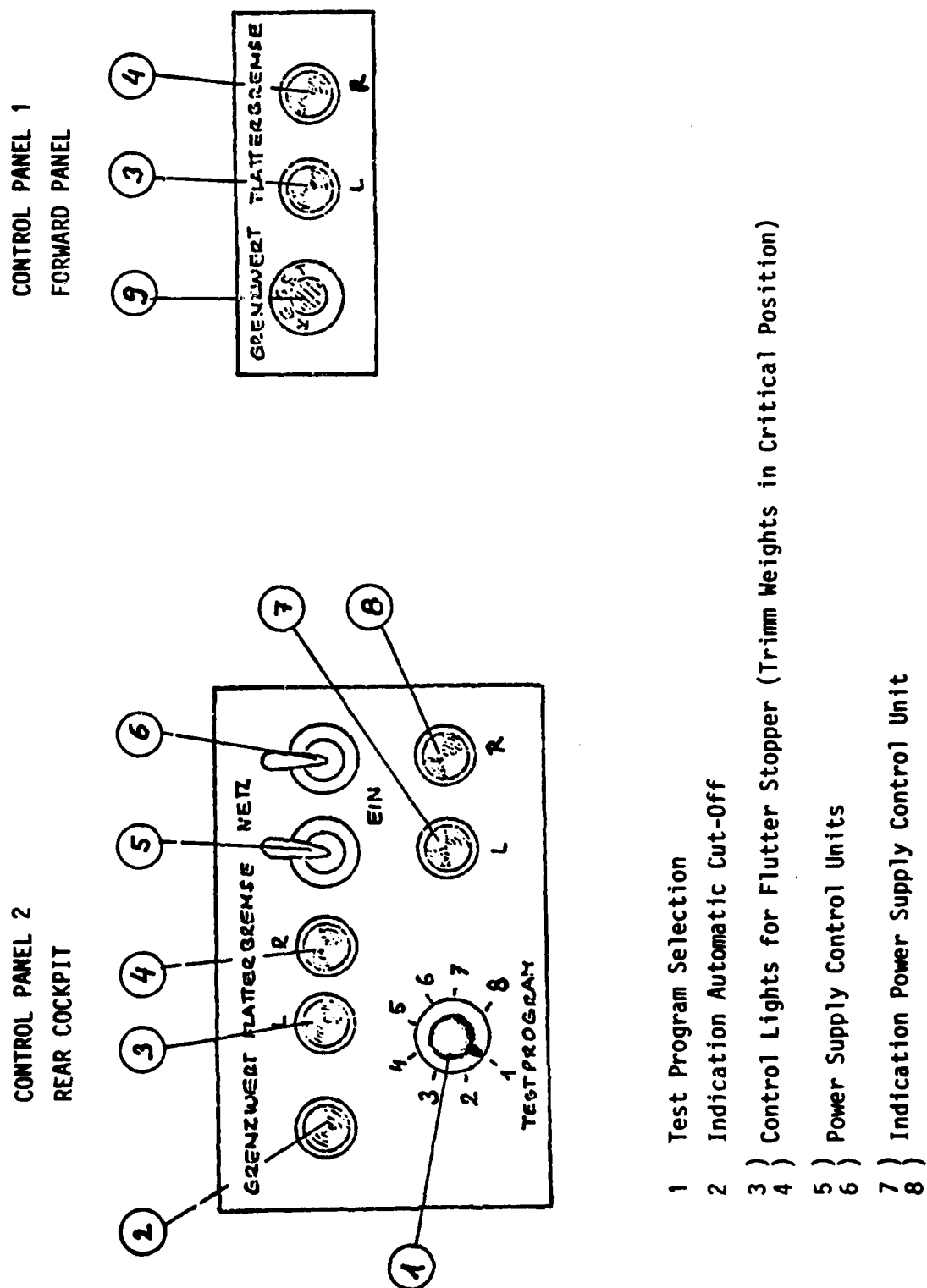


Figure 35. Control Panels for the Active Flutter Suppression System

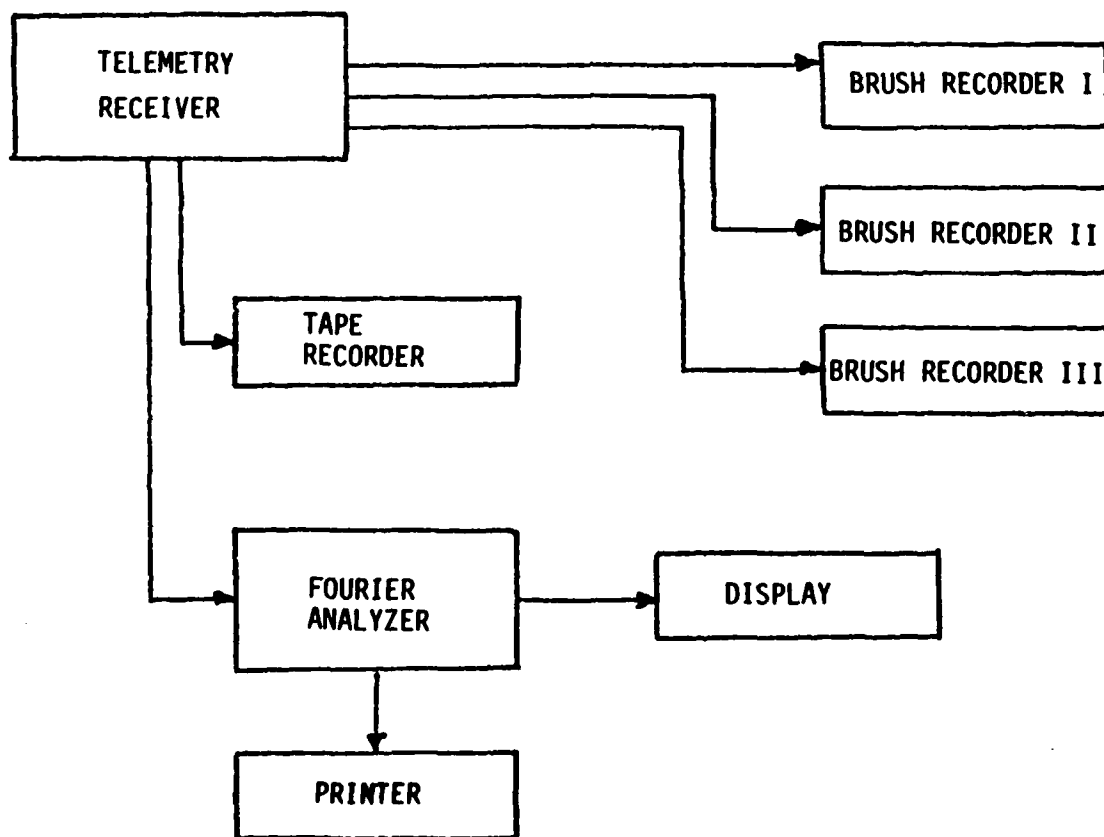


Figure 36. Block Diagram of Flight Data Processing

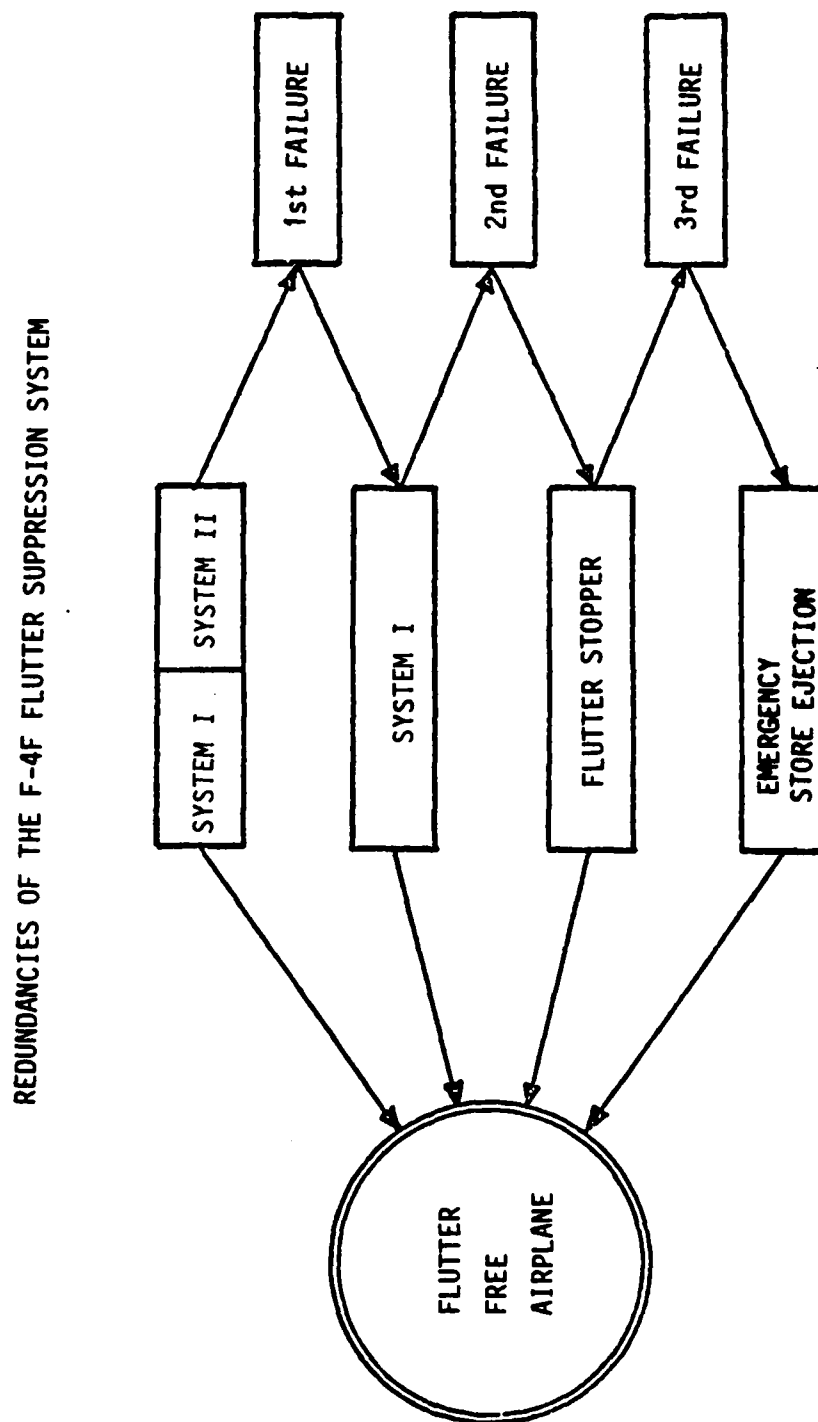


Figure 37. Safety Concept for Flight Tests with Flutter Suppression System

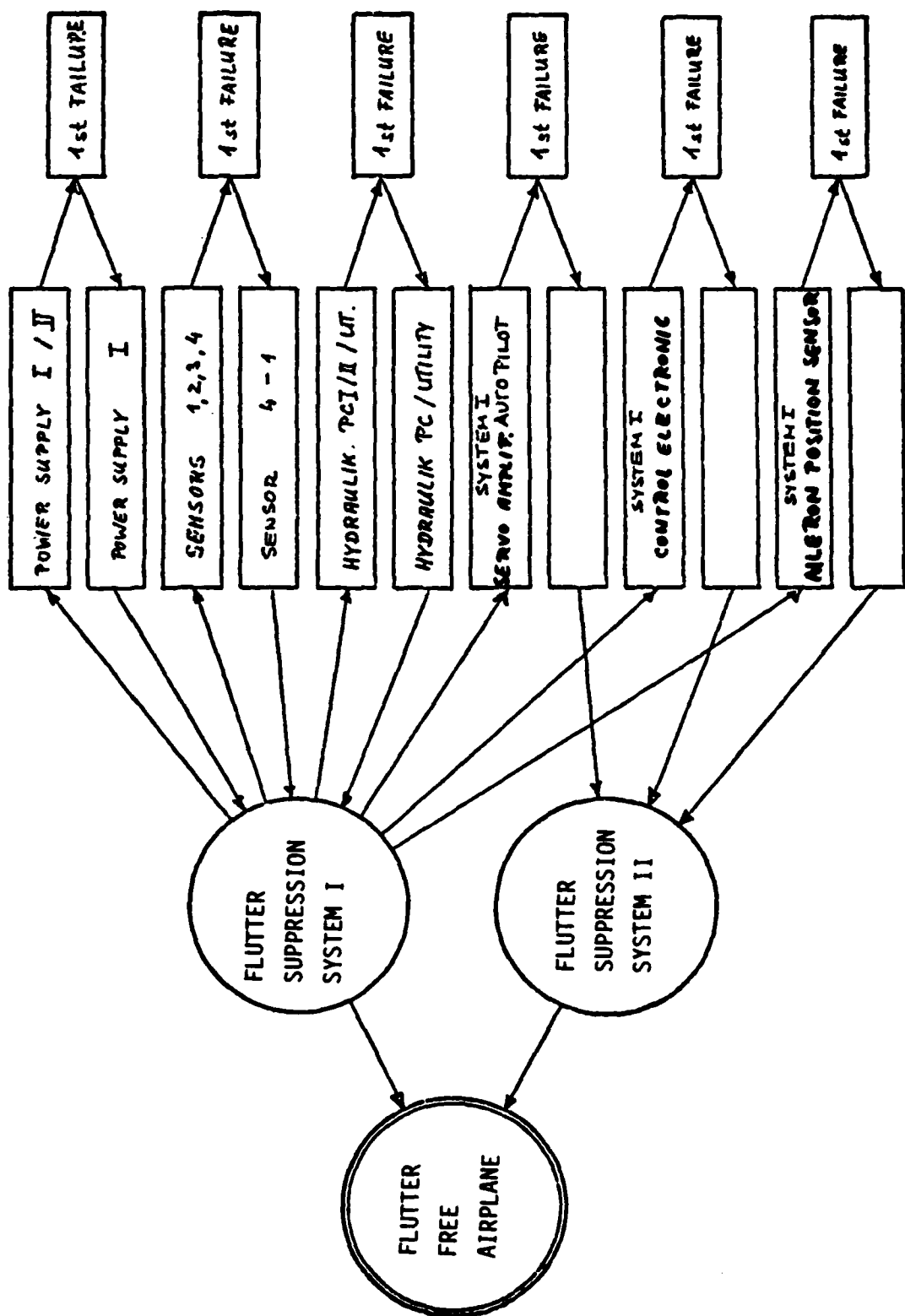


Figure 38. Block Diagram of Failure Mode Analysis for the Flutter Suppression System

F-4F FLUTTER STOPPER

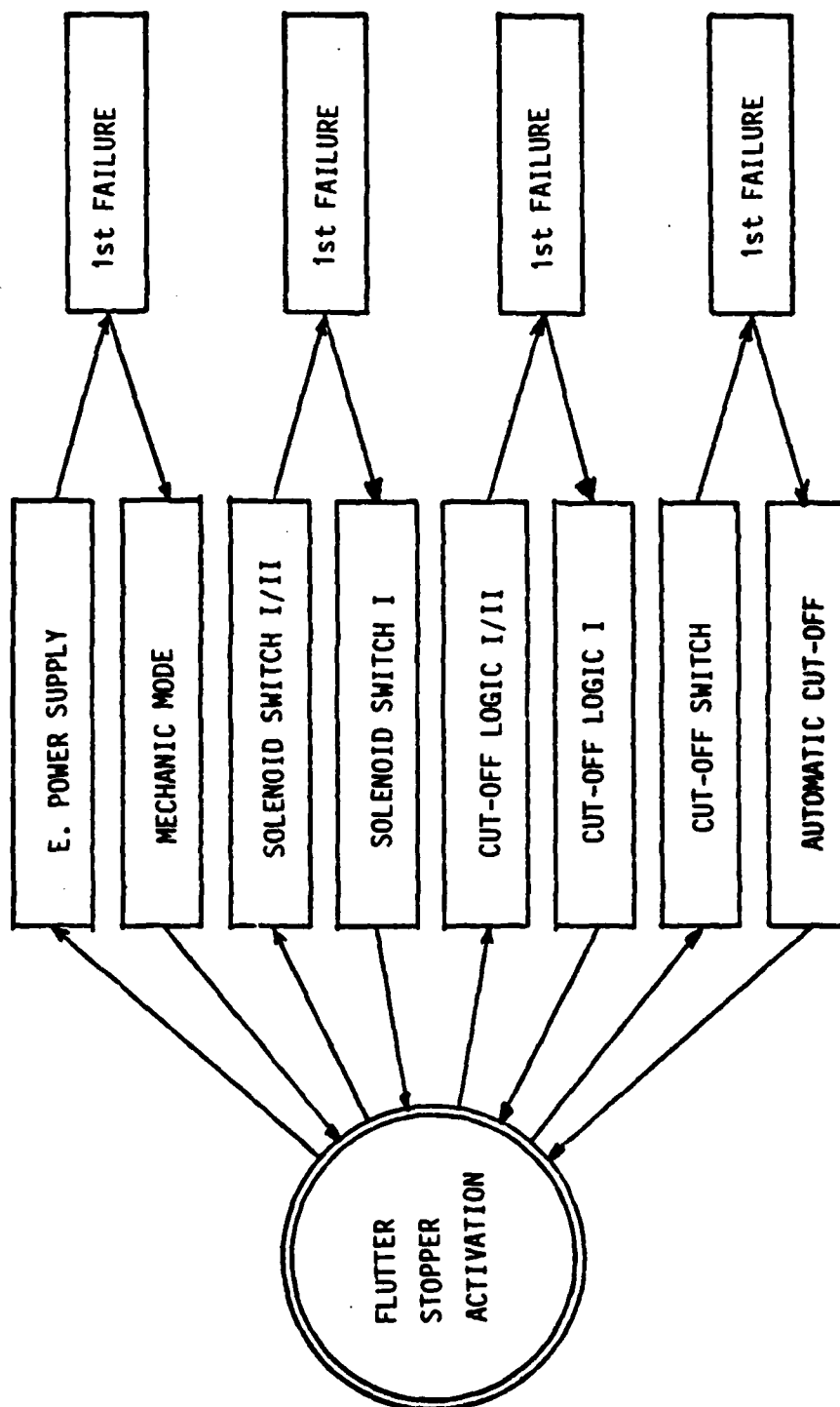


Figure 39. Block Diagram of Failure Mode Analysis of the Flutter-Stopper

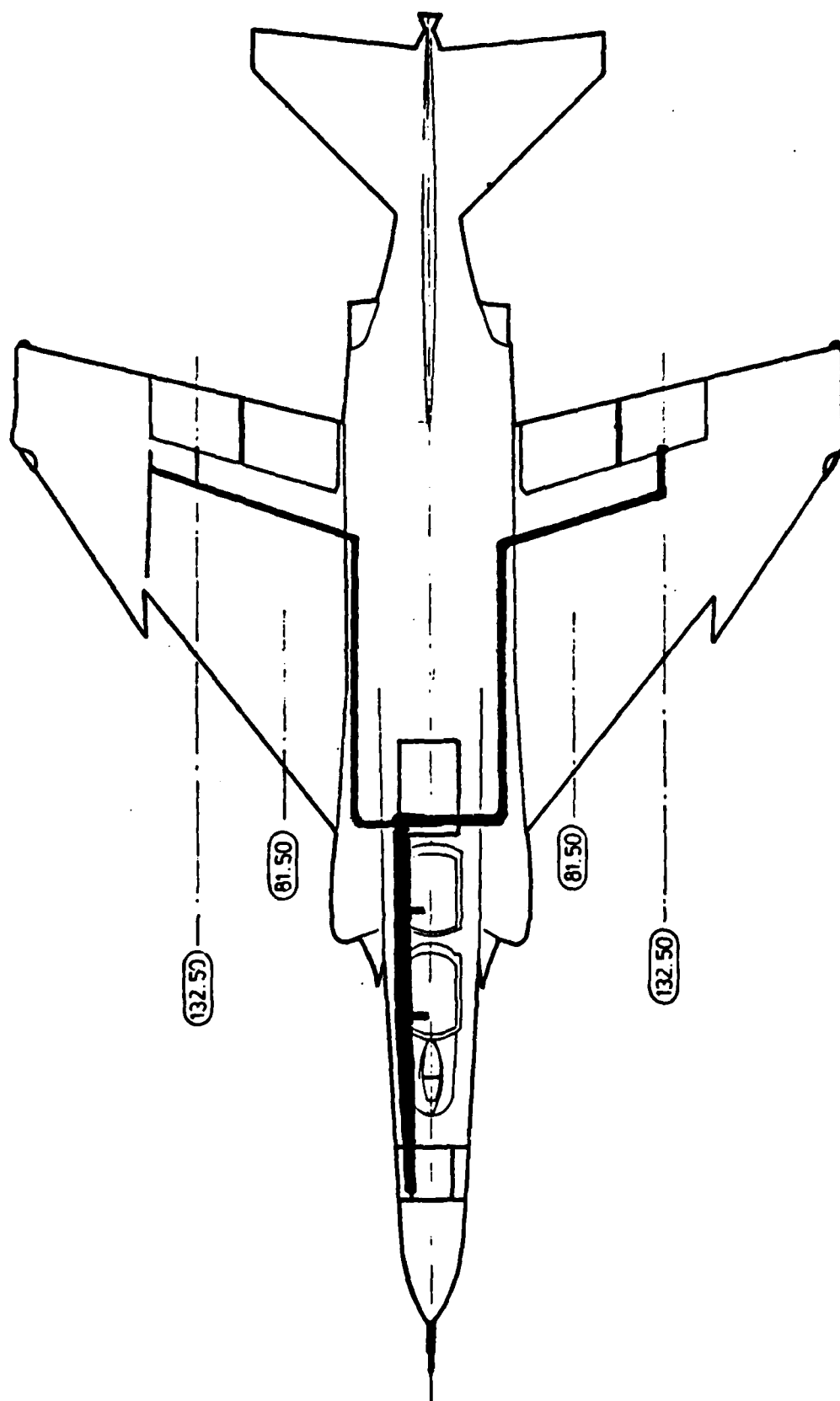


Figure 40. Additional Wiring in the F-4F for the Flutter Suppression System

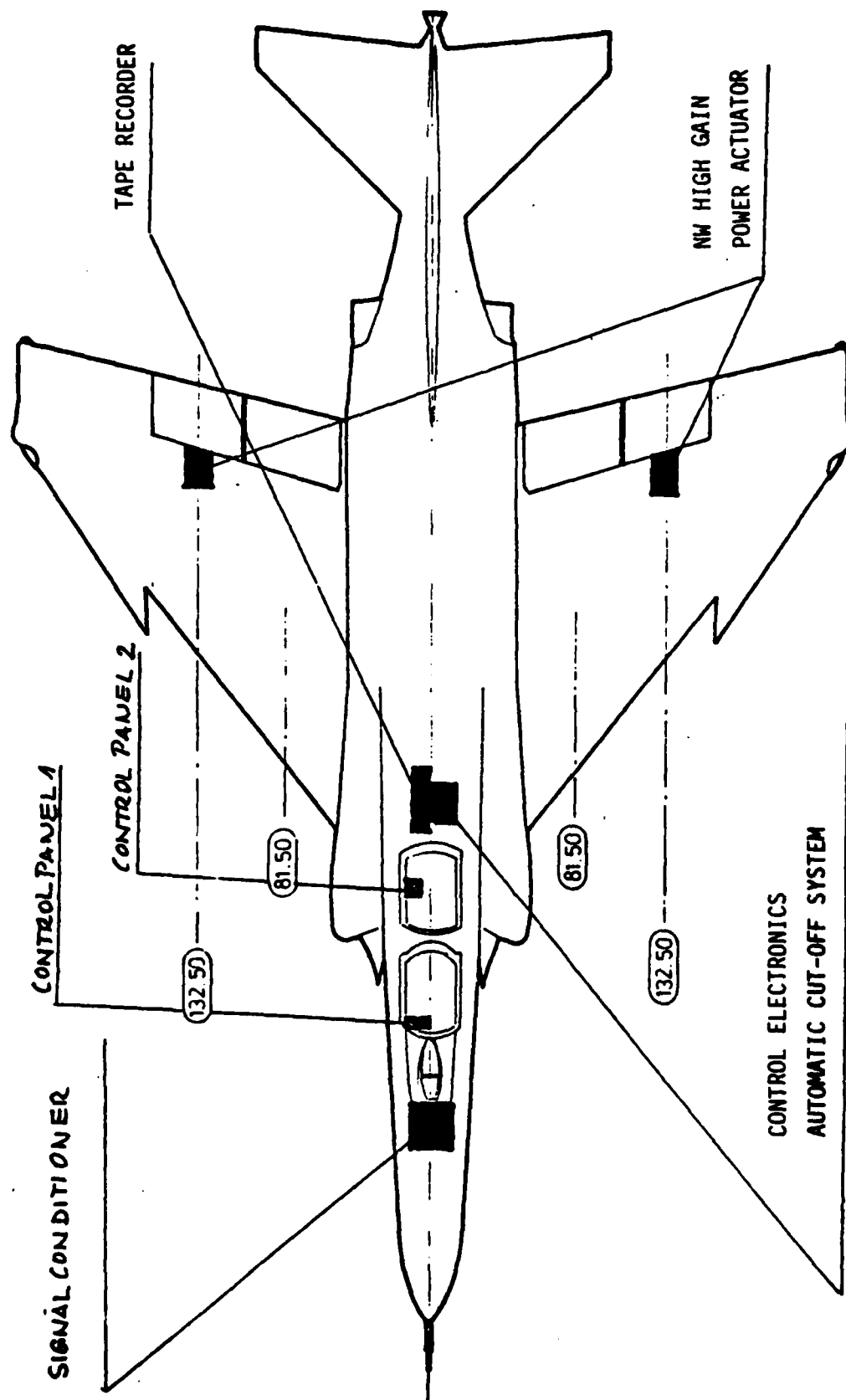


Figure 41. Additional Installations for the Flutter Suppression System and Flight Test Equipment.

Table 1. Modal Sensitivity Study

TEST NO.	NORMAL MODE	RIGID BODY MODE	FLUTTER SPEED KEAS
1	1, 3	0	427
2	1, 2, 3	0	424
3	1, 2, 3	1, 2, 3	412
4	1, 2, 3, 4	1, 2, 3	447
5	1, 2, 3, 4, 5	1, 2, 3	479
6	1, 2, 3, 4, 5, 6	1, 2, 3	501
7	1 - 9	1, 2, 3	553
See Figure 4 through 9 for Normal Modes.			

Table 2. Control Law Gains

	Control Law I	Control Law II
State - quantity	K_I	K_{II}
ϕ	-304.9	- 0.61
θ	-221.3	0.36
$\dot{\phi}$	1.71	0.013
$\dot{\theta}$	2.56	0.058
$\Delta\beta$	0	0
$\dot{\Delta\beta}$	0	0
β_o	0	0
$\dot{\beta}_o$	0	0

Table 3. Comparison of MDC and MBB Data for Fatigue Life Assessment

	MDC	MBB
Aileron BIAS	-3.5°	-2.0°
Max. amplitudes	-2 to -5°	-0.5 to -3.5°
Mean aileron frequency	10 Hz	6 Hz
Anticipated load cycles	$7 \cdot 10^5$	$7 \cdot 10^4$
Number of flights	25	20